Generalized Osteosclerotic Condition in the Skeleton of Nanophoca vitulinoides, a Dwarf Seal from the Miocene of Belgium

Leonard Dewaele, Olivier Lambert, Michel Laurin, Tim de Kock, Stephen Louwye, Vivian de Buffrénil

Journal of Mammalian Evolution

Generalized osteosclerotic condition in the skeleton of Nanophoca vitulinoides, a dwarf seal from the Miocene of Belgium

--Manuscript Draft--

Manuscript Number:	JOMM-D-17-00063R2
Full Title:	Generalized osteosclerotic condition in the skeleton of Nanophoca vitulinoides, a dwarf seal from the Miocene of Belgium
Article Type:	Original Article
Keywords:	Neogene; Phocidae; Nanophoca vitulinoides; osteohistology; microanatomy; osteosclerosis
Corresponding Author:	Leonard Dewaele Universiteit Gent Ghent, BELGIUM
Corresponding Author Secondary Information:	
Corresponding Author's Institution:	Universiteit Gent
Corresponding Author's Secondary Institution:	
First Author:	Leonard Dewaele
First Author Secondary Information:	
Order of Authors:	Leonard Dewaele
	Olivier Lambert
	Michel Laurin
	Tim De Kock
	Louwye Stephen
	Vivian de Buffrénil
Order of Authors Secondary Information:	
Funding Information:	Fonds Wetenschappelijk Onderzoek (11V9117N) — Mr. Leonard Dewaele
	Society of Vertebrate Paleontology (2016 Steven Cohen award for excellent student research) — Mr. Leonard Dewaele
	Fonds Wetenschappelijk Onderzoek — dr. Tim De Kock
Abstract:	In the fossil record, it has been shown that various clades of secondarily aquatic tetrapods experienced an initial densification of their bones in the early stages of their evolution, and developed spongier and lighter bones only later in their evolution, with the acquisition of more efficient swimming modes. Although the inner bone structure of most secondarily aquatic tetrapods has already been studied, no research hitherto focused on true seals, or Phocidae. However, preliminary observations previously made on a Miocene species, Nanophoca vitulinoides, suggested that this taxon showed pronounced specialization of bone structure as compared to other seals. This feature justifies a specific comparative study, which is the purpose of this article. Microanatomical analysis of bones of N. vitulinoides shows compactness values nearing 100%, which is much higher than in other semi-aquatic mammals, pinnipeds included. Osteohistological analyses show virtually complete remodeling of the medullary territory by Haversian substitution. Extreme bone compactness locally resulted from an imbalance, towards reconstruction, of this process. Cortical regions were less intensely remodeled. In a number of specimens, the cortex shows clear growth marks as seasonal lines of arrested growth. The results suggest that, despite the extreme compactness of long bones of N. vitulinoides and the small size of this

	taxon, the growth rate of the cortex, and that of the bones in general, did not differ strongly from that of other, larger phocids. Extreme skeletal compaction and densification must have increased body density in Nanophoca. Consequently, speed, acceleration, and maneuverability must have been low, and this taxon was most likely a near-shore bottom-dwelling seal. Consequently, dietary preferences were most likely oriented towards benthic food sources.

Leonard Dewaele
Department Geology
281 Krijgslaan
Ghent 9000
Belgium

Ghent, 2018/03/28

Dear Editor,

Please find attached the revised version of our manuscript "Generalized osteosclerotic condition in the skeleton of *Nanophoca vitulinoides*, a dwarf seal from the Miocene of Belgium." After minor revisions, we would like to resubmit the final manuscript to the *Journal of Mammalian Evolution*. We would also like to thank you for your helpful comments.

We implemented all grammar and spelling suggestions and comments.
Although few in number, we made a limited number of changes that have not been requested by the Editor:

1) On two occasions, we wrote "*Phocanella* ***pumilla.***" This has been changed to *"Phocanella* ***pumila***" with one "l".
2) We changed the position of Canoville and Laurin (2010) and Canoville et al. (2016) in the reference list in order to make it alphabetical.
3) The Editor did not explicitly request that "annuli" should not be in italics in the caption of Fig. 10. However, we adjusted this in order to be consistent with the other comments in the manuscript.

We added the paragraph "Data Availability" where the Editor requested it, and we hope that it fulfils the requirements for publication.

Although we adhere to the comments of the Editor, we wish to draw the attention to the abbreviations of genus names. For instance, in some instances, *Nanophoca vitulinoides* is abbreviated in some paragraphs before it is spelled out. This is the case in all paragraphs of the microanatomical part of the results. On other occasions, the Editor requests to spell out names after the first mention in a paragraph. This applies for instance to *Callophoca obscura* and *Phocanella pumila* in the caption for Fig. 12, and for *Phocanella pumila* on l.442, 447, and 449 of the returned manuscript, in the "Comparative data" section.
Although we follow the instructions of the Editor in the revised manuscript, we feel that this contradicts with the guidelines to spell out names only the first time they are mentioned in each paragraph.

We hope that the revised manuscript is in fulfillment for publication in *Journal of Mammalian Evolution*.

Sincerely,

Leonard Dewaele and co-authors

Generalized osteosclerotic condition in the skeleton of *Nanophoca vitulinoides*, a dwarf seal from the Miocene of Belgium

Leonard Dewaele[1,2*], Olivier Lambert[2], Michel Laurin[3], Tim De Kock[4], Stephen Louwye[1],Vivian de Buffrénil[3]

[1]Vakgroep Geologie, Universiteit Gent, Ghent, Belgium

[2]Directorate "Earth and History of Life", Institut Royal des Sciences Naturelles de Belgique, Brussels, Belgium

[3]Département Origines et Evolution, Muséum National d'Histoire Naturelle, Paris, France

[4]PProGRess, Vakgroep Geologie, Universiteit Gent, Ghent, Belgium

*Corresponding author: leonard.dewaele@ugent.be

ABSTRACT

In the fossil record, it has been shown that various clades of secondarily aquatic tetrapods experienced an initial densification of their bones in the early stages of their evolution, and developed spongier and lighter bones only later in their evolution, with the acquisition of more efficient swimming modes. Although the inner bone structure of most secondarily aquatic tetrapods has already been studied, no research hitherto focused on true seals, or Phocidae. However, preliminary observations previously made on a Miocene species, *Nanophoca vitulinoides*, suggested that this taxon showed pronounced specialization of bone structure as compared to other seals. This feature justifies a specific comparative study, which is the purpose of this article. Microanatomical analysis of bones of *N. vitulinoides* shows

compactness values nearing 100%, which is much higher than in other semi-aquatic mammals, pinnipeds included. Osteohistological analyses show virtually complete remodeling of the medullary territory by Haversian substitution. Extreme bone compactness locally resulted from an imbalance, towards reconstruction, of this process. Cortical regions were less intensely remodeled. In a number of specimens, the cortex shows clear growth marks as seasonal lines of arrested growth. The results suggest that, despite the extreme compactness of long bones of *N. vitulinoides* and the small size of this taxon, the growth rate of the cortex, and that of the bones in general, did not differ strongly from that of other, larger phocids. Extreme skeletal compaction and densification must have increased body density in *Nanophoca*. Consequently, speed, acceleration, and maneuverability must have been low, and this taxon was most likely a near-shore bottom-dwelling seal. Consequently, dietary preferences were most likely oriented towards benthic food sources.

Keywords: Neogene, Phocidae, *Nanophoca vitulinoides*, osteohistology, microanatomy, osteosclerosis

INTRODUCTION

Numerous studies have shown the existence of a general relationship between the bone microanatomy and the ecology of tetrapods (e.g., Wall 1983; Stein 1989; Fish and Stein, 1991; Turner 1998; Ricqlès and Buffrénil 2001; Germain and Laurin 2005; Liu et al. 2009; Amson et al. 2014). Several lineages of tetrapods returned to the aquatic environment (e.g., Uhen 2007; Pyenson et al. 2014; and references therein), and data available hitherto suggest that, in such forms, fast and agile swimming amniotes have lighter and spongier bones than slow bottom-dwellers, which generally have heavy and compact (osteosclerotic) bones (Buffrénil et al. 1988, 1989; Webb and Buffrénil 1990; Taylor 2000; Laurin et al. 2011; Houssaye et al. 2013). In slow secondarily aquatic tetrapods, such as sirenians, the heavy bones passively compensate the buoyancy generated by lung volume and help conserve energy during swimming at shallow depth (Domning and Buffrénil 1991; Ricqlès and Buffrénil 2001; Houssaye 2009; see also Taylor 2000). Two mechanisms may increase skeletal mass: thickening of the cortex (pachyostosis), or increased inner compactness of the bones (osteosclerosis); both can also occur simultaneously to form pachyosteosclerosis (e.g., Buffrénil et al. 2010; Houssaye et al. 2016). However, most marine tetrapod clades show an initial evolutionary stage of pachyosteosclerosis prior to the regression of this feature in pace with the development of more efficient swimming modes (Ricqlès 1989).

Although pinnipeds are "marine mammals," they retain some terrestrial mobility, which makes them an interesting model for studying the modification of bone structure in the course of an evolutionary adaptation to marine life. However, bone histology and microanatomy in these animals has received little attention in the past, with few exceptions (e.g., Stein 1989). Indeed, while the osteohistology and microanatomy of other marine mammal clades was specifically studied from an evolutionary point of view, pinnipeds were considered only in the context of broad comparative datasets including extensive taxonomic

sampling, at the scale of Mammalia or marine tetrapods (e.g., Laurin et al. 2011; Dumont et al. 2013; Canoville et al. 2016; Houssaye and Fish 2016; Houssaye et al. 2016). Two contributions specifically dealing with pinnipeds can be mentioned: the preliminary study of the extinct walrus *Valenictus*, showing pachyosteosclerosis in this taxon (Deméré 1994a, b), and the publication on pachyosteosclerosis in the seal *Pachyphoca*, from the middle Miocene of the Ukraine (Eastern Paratethys), by Koretsky and Rahmat (2017). Unfortunately, this study gives only a very brief microanatomical description, without histological, quantitative data or informative figures relevant to this topic. Existing information suggests that bone structure of the pinnipeds differs little from that of most other mammals, because they display none of the conspicuous specializations of bone inner architecture often encountered in marine tetrapods. Indeed, their appendicular long bones , though not strictly tubular (tubularity sensu stricto is a peculiar adaptation of the diaphyseal region of some limb bones to a terrestrial locomotion), have compact periosteal cortices framing a nearly open medullary cavity with only few slender trabeculae (see e.g., Quemeneur et al. 2013 for the femur; Canoville and Laurin 2010 for the humerus; Germain and Laurin 2005 for the radius; see also Nakajima and Endo 2013). Moreover, the structure of their ribs (comparative data in Canoville et al. 2016) and vertebrae (Dumont et al. 2013; Houssaye et al. 2014) merely reflects the common condition observed in most mammals. This situation may seem paradoxical considering the intermediate habitat and mode of locomotion that characterizes this taxon. Miscellaneous observations nevertheless suggest that the question may be more complex and that in the pinnipeds, and more generally within a given clade and a general habitat (e.g. coastal, pelagic, etc.), bone structure may differ between taxa according to the detailed characteristics of their ecological adaptations (see also on this topic Houssaye et al. 2016). Such is the case, for example, of the bones of *Nanophoca vitulinoides*, a small phocid from the middle Miocene (late Langhian–late Serravallian; ca. 14.2–11.6 Ma) of Antwerp

region, in Belgium. From broken and fractured specimens, the internal structure of bones in this taxon appears extremely compact and lacks a differentiated medullary cavity. These intriguing preliminary observations call for further analysis.

The aim of the present study is to describe and interpret the osseous structure of *Nanophoca* at both the microanatomical and histological levels, and compare it with similar data from other phocids and more distantly related taxa. *Nanophoca vitulinoides* is the best-known extinct seal from the Neogene (Miocene + Pliocene, 23.03 – 2.58 Ma) of the North Sea Basin, and represents more than half the fossil seal specimens at the Royal Belgian Institute of Natural Sciences, or RBINS (Dewaele et al. 2017a). Its postcranial skeleton is the most complete described hitherto (Fig. 1); however, cranial elements are still lacking. *Nanophoca vitulinoides* is remarkable in two respects: first, with a total estimated length of approximately one meter, it is one of the smallest known Phocidae (Dewaele et al. 2017a); in this family, only *Batavipusa neerlandica* from the early to middle Tortonian (8–11.5 Ma) of the Netherlands, *Monachopsis* from the early to middle Tortonian (c. 8.4–11.4 Ma) of Moldova, and *Pachyphoca chapskii* from the late Serravallian to early Tortonian (11.2–12.3 Ma) of Ukraine are about as small or smaller, based on humeral length (Koretsky 2001; Koretsky and Peters 2008; Koretsky and Rahmat 2013; Dewaele et al. 2017a). Second, most late Neogene seal taxa found in Belgium also occur in the Lee Creek Mine of the Yorktown Formation, Aurora, North Carolina, USA; *N. vitulinoides* is the only one restricted to Belgian strata (Koretsky and Ray 2008; Dewaele et al. 2017a). Studying bone structure in this taxon, and comparing it with other seals could, on the one hand, bring basic data (still missing hitherto) on bone histology in phocids and, on the other hand, show the nature of the structural specialization of the *Nanophoca* skeleton, which would help in inferring its development and possible functional/ecological significance.

MATERIAL AND METHODS

BIOLOGICAL SAMPLE

This study rests on two main methodological approaches: A) gross (macro-anatomic) morphometry for assessing the presence or absence of pachyostosis in *Nanophoca*; B) microanatomy and histology for describing the inner structure of the bones.

For the morphometric part, 29 humeri from 13 phocid species and 25 femora from 12 species were measured by one of us (LD), roughly following the procedure used by Buffrénil et al. (2010) for sirenian ribs. Similar data from the literature were also considered (Tables 1, 2).The new morphometric data presented below include three extant taxa: the grey seal *Halichoerus grypus* from the cold temperate and subarctic zones of the North Atlantic, the harbor seal *Phoca vitulina* from the temperate to arctic zones of the North Atlantic and North Pacific, and the Baikal seal *Pusa sibirica* from Lake Baikal. All bones included in the study were from adult or subadult individuals, judging from the degree of epiphyseal fusion in associated long bones (see Storå 2000). The comparative sample of extinct phocids is largely dependent on the published fossil record; this is why some taxa are represented in the dataset by both humeri and femora, while others are only represented by measurements of either humeri or femora.

Because the dataset used for the morphometric study depends on the literature, the dataset employed for the microanatomical and histological studies is necessarily different as it is based on first-hand analyses of actual specimens available for scanning and/or sectioning. (see Tables 1, 2 versus Table 3). The microanatomical dataset includes measurements on the extant phocine *Phoca vitulina*, the extinct phocids *Nanophoca vitulinoides*, including the neotype specimen IRSNB M2276, *Callophoca obscura* from the Tortonian to Zanclean (late Miocene – early Pliocene) of Belgium and North Carolina (LD pers. obs.), *Leptophoca proxima* from the late Aquitanian to late Serravallian (late early Miocene – late middle

Miocene) of Belgium and the North American Chesapeake Bay area (Koretsky 2001; Dewaele et al. 2017b), and *Phocanella pumila* from the Tortonian to Zanclean (late Miocene – early Pliocene) of Belgium and North Carolina (LD pers. obs.). Two additional small extinct Neogene phocids from the southern North Sea Basin are also considered: *Batavipusa neerlandica*, from the early to middle Tortonian (8 – 11.5 Ma) of the Netherlands, and *Praepusa boeska*, from the late Miocene to late Pliocene of Belgium and the Netherlands (Koretsky and Peters 2008; Koretsky et al. 2015). However, the fossil record of these taxa is extremely scarce and the attribution of the various specimens to each taxon is questionable (e.g., Koretsky and Peters 2008, Koretsky et al. 2015, Dewaele et al. 2017a). Tomographic (CT) data for *B. neerlandica* and *Pr. boeska* are of moderate quality. Distinction between the internal structures of the bone and the sediment infill proved unpractical, and both taxa are only considered qualitatively. Additional data (from either classical thin sections or micro-CT scans) already published by Buffrénil and Schoevaert (1989), Buffénil et al. (2010), Canoville and Laurin (2010), Canoville et al. (2016), and Amson et al. (2014) about the inner structure of long bones in various extant and extinct aquatic mammals (otters, marine sloths, polar bear, and sirenians) were also considered for the comparisons (Table 3). In extinct phocid taxa, the osteohistological dataset is limited to three species, in addition to *N. vitulinoides*: the monachine *Callophoca obscura*, and the phocines *Leptophoca proxima* and *Phocanella pumila* (Table 3). The bone samples for these taxa include femora, humeri, radii, ribs, tibiae, and lumbar vertebrae with both transverse and longitudinal sections. These bones are also known in the fossil record of *N. vitulinoides* and can therefore allow detailed comparisons.

PROCESSING OF THE SPECIMENS

Morphometric features. Buffrénil et al.'s (2010) study focused on the discrimination of pachyostosis sensu stricto (cortical hyperplasy) in ribs and used, among other measurements,

rib length. Unfortunately, very few entire ribs are available for fossil seals, and the so-called Cortical Development index used by these authors (the calculation of this index requires measurements of total length, chord, and mean circumference of the ribs) could not be applied to the ribs of *N. vitulinoides*; conversely, this index, called here "bulkiness index," or BI, could be used for the humeri and femora in the same conditions as for the other phocid specimens (Fig. 2). For the humerus, two measurements were taken: A) absolute sagittal length of the bone between the most proximal point and most distal point, or BL, and B) transverse width at mid-shaft, or TW. For the femur, three measurements were taken: A) absolute sagittal length (BL), B) transverse width at the narrowest portion of the diaphysis (TW), and C) anteroposterior width of the diaphysis in the same portion (APW), which is perpendicular to transverse width. For the humerus, the calculated ratio is BI = TW/BL. A low BI value indicates a relatively narrow diaphysis, and a high value indicates a relatively thick diaphysis. For the femur, the ratio is BI = [0.5(TW+APW)]/BL. Similarly, a low value of BI indicates a relatively narrow diaphysis, and a high value indicates a relatively thick diaphysis.

Thin section analysis (microanatomy and histology). Thin section preparation was carried out according to the classical procedures used for this kind of preparations (Lamm 2013). All the sections made for this study are now part of the Histothèque (i.e., thin section collection) housed in the Muséum national d'Histoire naturelle in Paris, where they are recorded under various numbers within the Histos database. These sections include transverse mid-diaphyseal and metaphyseal sections, with additional longitudinal sections through the epiphyses. Microscopy was performed using a Zeiss Axioskop microscope, with ordinary and polarized transmitted light at low (x25) to medium (x400) magnifications. All measurements of sectional dimensions were performed with the software ImageJ (National Institute of Health, USA) on microphotographs. For microanatomy, only mid-diaphyseal transverse sections were

considered. The terminology used in microanatomical and histological descriptions refers to Francillon-Vieillot et al. (1990) and Prondvai et al. (2014).

X-ray computed microtomography (micro-CT). A part of the biological sample (see Table 4–8) consists of specimens scanned at the Ghent University Centre for X-ray Tomography (www.ugct.ugent.be) with a custom-built microtomograph HECTOR (Masschaele et al. 2013). Depending on the sample, the tube was operated at 140 to 160 kV and 40 to 45 W. A 1 mm Al filter was applied to reduce beam hardening, which was then further filtered during the reconstruction process. The reconstruction was performed with OCTOPUS RECONSTRUCTION (XRE Belgium). Resulting images had a voxel size of approximately 30 µm, 46 µm, or 84 µm, depending on the magnification (see Table 4–8).

Cross-section analysis using *BONE PROFILER*—All cross-sections (be they material thin sections or virtual micro-CT Scan sections) were analyzed using BONE PROFILER Version 4.5.8 (Girondot and Laurin 2003). BONE PROFILER is a freeware dedicated to the analysis of bone compactness in sections, i.e., the area actually occupied by mineralized bone tissue divided by total sectional area, and designed to calculate relevant parameters describing the compactness profile. To do so, the entire cross-section is divided in 3060 cells created by the intersection of 60 sectors (360°/60 = 6° per sector) and 51 concentric rings parallel to the section outline (Laurin et al. 2004: fig. 3). Compactness distribution and variation from the ontogenetic center of the sections to cortical surface are presented as the ‘compactness profile’. The compactness profile is characterized by four parameters S, P, Min, and Max. S is the reciprocal of the slope at the curve inflection point, and it is proportional to the relative width of the transition zone between the medulla and the cortical regions. P is the position of the curve inflection point on the x-axis, and it represents the position of the transition area between the medulla and the cortical region. Min and Max are the minimum and maximum asymptotes, respectively, representing the minimum and maximum values of bone

compactness in a section. Other parameters can be calculated using BONE PROFILER (Laurin et al. 2004; Quemeneur et al. 2013), but these were not used in the current study. More elaborate analyses with BONE PROFILER including parameters Minrad, Maxrad, Srad, and Prad are not used in the present study, but are provided as Supporting Information (Appendix 1). These are similar to the abovementioned parameters, but are the radial versions, i.e., the average values of the measurements for the 60 sectors. Hence, standard deviations (SD) are also calculated for these values.

PHYLOGENETIC FRAMEWORK

For the phylogenetic position of *N. vitulinoides* in the current study, we follow the phylogenetic analysis by Dewaele et al. (2017a), which is, to date, the only published analysis including this species (Fig. 3). According to Dewaele et al. (2017a: fig. 25; Fig 3. in the current study), *N. vitulinoides* is a relatively late-branching stem-phocine; it is the closest known relative of crown Phocinae. Evidently, it should be noted that this phylogenetic position is only relative to the other Operational Taxonomic Units (OTUs) included in this analysis. The phylogenetic relationships of other small phocids, such as *Batavipusa neerlandica*, *Pontophoca sarmatica*, *Praepusa boeska*, or –most notably– *Monachopsis pontica* has been studied by Koretsky (2001) and Koretsky and Rahmat (2013). However, their fossil record is too scarce (e.g., *B. neerlandica* is only known from one isolated humerus, an isolated ilium, and an isolated partial femur tentatively assigned to it; *M. pontica* is only known from multiple isolated humeri and femora) to be confident about their phylogenetic position. Not surprisingly, previous phylogenetic analyses including those taxa show little consensus and confidence on their phylogenetic position (Koretsky 2001; Koretsky and Rahmat 2013). For the phylogeny of other, extant Pinnipedia included in this study, we refer to Higdon et al. (2007). The extinct *Callophoca obscura*, *Leptophoca proxima*, and

Phocanella pumila have all been considered in phylogenetic analyses. There is little consensus about the phylogenetic position of the monachine *C. obscura*. Some researchers consider *C. obscura* most closely related to the extant elephant seal *Mirounga*, while others group it with the late Pliocene *Pliophoca etrusca* from Italy, or consider it as a stem monachine (compare Muizon 1981; Koretsky and Ray 2008; Koretsky and Rahmat 2013; Amson and Muizon 2014; Berta et al. 2015). Therefore, we consider *C. obscura* a monachine phocid, but we do not make genus-level phylogenetic inferences for this taxon. The phylogenetic position of *L. proxima* (or as *Leptophoca lenis*) has been first analyzed by Koretsky (2001) and Koretsky and Rahmat (2013), but without consensus. Cozzuol (2001) interpreted *L. lenis* as an early-branching phocine, while Berta et al. (2015) suggested that the taxon was an early-branching stem monachine. However, the latter expressed doubt over their phylogenetic results for *Leptophoca*. More recent studies by Dewaele et al. (2017a, b) placed *L. proxima* as a stem phocine with strong statistical support. The phylogenetic position of *P. pumila* has only been analyzed once, by Koretsky and Rahmat (2013). However, they neither present the character matrix nor a list of synapomorphies to support their analysis. In addition, this analysis differs on key nodes from other, widely-accepted phylogenetic analyses (e.g. Bininda-Emonds and Russell 1996), inhibiting us of considering this analysis to elucidate the phylogenetic position of *Phocanella pumila.* The phylogenetic position of the latter remains unclear, pending future discoveries of more complete material and new analyses. This information is provided only as contextual information; we did not perform any phylogeny-informed statistical tests in this study given that the focus is on only three early pinniped taxa.

INSTITUTIONAL ABBREVIATIONS

IRSNB/RBINS, Institut royal des Sciences naturelles de Belgique, Brussels, Belgium; **MAB**, Oertijdmuseum Groene Poort, Boxtel, the Netherlands; **MNHN**, Muséum national d'Histoire

naturelle, Paris, France; **MSC**, Smithsonian Institution Museum Support Center, Suitland, Maryland, USA; **USNM**, National Museum of Natural History, Washington, DC, USA.

DATA AVAILABILITY

All data used in this study is presented within the main text. Additional results from the radial analysis with BONE PROFILER are provided as Supporting Information (Appendix 1). Thin sections that are used in this study are housed at the MNHN. Specimens that have been CT-scanned are housed at the IRSNB. Specimens are available for consultation and access should be requested at the respective institutions.

RESULTS

MORPHOMETRIC DATA

Although no complete ribs of *N. vitulinoides* are preserved to perform morphometric measurements, the sub-circular morphology of the cross-section from these bones differs from that of related taxa (Fig. 5A versus Fig. 5B, C). For a similar rib length (a parameter that unfortunately is lacking), it could possibly be indicative of some incipient tendency toward pachyostosis. Morphometric results for the humerus and femur are listed as Tables 1 and 2. The diaphysis of the humerus of *Nanophoca* is relatively slender, as compared to other extant and extinct Phocidae. BI ratio for the humerus of two specimens of *N. vitulinoides* is 0.121 and 0.135, which is at the lower half of the range of the 29 calculated values (0.109 – 0.210) (Table 1). Apart from the extinct *Batavipusa neerlandica* (0.182), *Monachopsis pontica* (0.169), and *Pachyphoca ukrainica* (0.210), extinct Phocidae in our sample tend to have a

relatively slender humeral diaphysis, as compared to extant forms. This rules out the eventual occurrence of pachyostosis in the humerus of *N. vitulinoides*.

Bulkiness index values indicate that the femoral diaphysis of *N. vitulinoides* (0.200, 0.207, and 0.208) and other extinct Phocidae (0.173 – 0.240) is overall relatively thick, as compared to extant Phocidae (0.158 – 0.187) (Table 2). This contrasts with the measurements of the humeri. As for the humerus, the taxon with the bulkiest femur is *Pachyphoca*, returning a value of 0.240 for *Pachyphoca ukrainica*, based on the average of three specimens presented by Koretsky and Rahmat (2013), and a value of 0.229 for one specimen of *Pachyphoca chapskii*. Given that the femora of the extinct taxa in our sample have consistently higher values, i.e., suggestive of pachyostosis, it remains difficult to find conclusive evidence on the presence or absence of pachyostosis in the femur of *N. vitulinoides* in comparison to contemporaneous taxa.

MICROANATOMY

Vertebrae

[Table 4]

[Figure 4]

Bone compactness in the centra of the two lumbar vertebrae of *N. vitulinoides*, ranges from 93.8% for the adult, to 63.6% for the juvenile. (Table 4; Fig. 4). These values are much higher than those observed in the other pinnipeds and semi-aquatic mammals included in this study (Table 4): compactness values indeed range for these taxa from 22.3% (hooded seal, *Cystophora cristata*) to 44.3% (sea otter, *Enhydra lutris*). Apart from *N. vitulinoides*, the compactness values for the vertebrae of the Phocinae (22.3% for *C. cristata* and 29.3% for the

harp seal, *Pagophilus groenlandicus*) are lower than the values calculated for Monachinae and Otariidae.

Rib

[Table 5]

[Figure 5]

With an overall compactness of 99.8%, the rib of *N. vitulinoides* is almost completely ossified, and much more compact than that of other semi-aquatic mammals (Table 5; Fig. 5). The Cape fur seal *Arctocephalus pusillus* and the Californian sea lion *Zalophus californianus* have the second and third most compact ribs in the biological sample, with compactnesses of 78.4% and 78.2%, respectively. While there is no differentiated medullary cavity in the rib of *N. vitulinoides* (Fig. 5A), the medullary cavity in the ribs of other taxa in the biological sample is occupied by loose spongiosa and surrounded by a compact cortex (Fig. 5B, C).

Humerus

[Table 6]

[Figure 6]

[Figure 7]

With an overall compactness of 99.7% for one specimen and 99.9% for the other, the humerus of *N. vitulinoides* is almost completely solid (Table 6; Fig. 6). Only the humerus of *Phocanella pumila* has a comparably (though somewhat lesser) high compactness (95.9%); but unlike *Phocanella pumila*, there is no discernable medullary cavity in the two specimens

of *N. vitulinoides* (Fig. 6A, B versus Fig. 6C). Given the poor density differentiation between the mineralized bone tissue and the sediment infill in *Batavipusa neerlandica* and *Praepusa boeska*, quantitative microanatomical analysis using BONE PROFILER was precluded. A qualitative analysis reveals the presence of a porous medullary cavity framed by compact cortices in both taxa (Fig. 7A, B).

Femur

[Table 7]

[Figure 8]

Compactness values for the two femora of *N. vitulinoides*, i.e., 97.1% and 99.4%, are much higher than those of all extant and most extinct semi-aquatic taxa considered in this study (Table 7; Fig. 8A, B versus Fig. 8C, D, F-I). Only the femur of *Phocanella pumila* shows a compactness approaching the condition in *N. vitulinoides* (Table 7; Fig. 8A, B versus Fig. 8E).

Other bones

[Table 8]

[Figure 9]

Other long bones of *N. vitulinoides*, i.e., the radius and the tibia, have been studied as well and show very high compactness ratios, similar to the condition observed in the rib, humerus, and femur (Table 8; Fig. 9). There is no discernable medullary cavity present, unlike, for example, the extant *Phoca vitulina* (Table 8; Fig. 9A, C versus Fig. 9B, D).

BONE HISTOLOGY

In cross and sagittal sections, all bones of *N. vitulinoides* examined in this study share the same basic histological features (in addition to their microanatomical similarity), with only few differences most likely related to ontogenetic age. In most of the bones, except one of the radii (Histos 2142) and one of the vertebral centra (Histos 2150), Haversian remodeling is mild in the cortex; the characteristics of primary periosteal deposits thus remain visible (Fig.10A, B). They consist in layers of woven-parallel tissue (according to Prondvai et al.'s 2014 terminology) with longitudinal primary osteons, separated by very birefringent annuli made of parallel-fibered or lamellar bone (Fig.10C). Short Sharpey's fibers (60-80 µm long) colonize the basal parts of the woven-parallel layers (Fig.10C). The annuli are wide (up to 180 µm) in the cortical depth, and thinner (some 60-70 µm) towards the cortical periphery. The bone displaying the greatest number of visible growth marks is the humerus, with five sharp annuli (Fig.10A) associated with lines of arrested growth. Of course, in this specimen, several annuli were erased by remodeling in the depth of the cortex. In the long bones where they occur, the annuli tend to be more tightly spaced towards the cortical periphery, but they nevertheless maintain a significant spacing, e.g., 320 µm between the fourth and fifth annuli in the humerus (Fig.10A). In the femur and the humerus, in which cortical structure is perfectly preserved up to the outer margin of the diaphysis, the last growth mark is an annulus (Fig.10A). The nature of the last growth mark is less evident in the other long bones, due to the impregnation of superficial layers by a dark substance during fossilization. However, there is no clear indication of the presence of an external fundamental system (EFS) that could have shown that the growth of the bones, at least in diameter, had dropped to a very low level and that skeletal growth was ending by the time the animals died. In the two specimens (radius Histos 2142 and centrum of the vertebra Histos 2150) where the structure of primary

periosteal deposits is no longer visible, bone cortices are entirely occupied by a particularly dense Haversian tissue (Fig.10E) that extends continuously towards the central (medullary) region of the bones.

The medullary territory of all bones is entirely compact, with the exception of some scarce, vaguely circular cavities measuring generally less than 300-400 µm in diameter. The dense Haversian tissue occupying this region (Fig.10F) has three basic characteristics: A) Its secondary osteons are roughly longitudinal, but their orientation can be locally variable; moreover, their central canals (Havers' canals) develop numerous transversal anastomoses (Wolkman's canals), suggesting high BMU (Bone Multicellular Units, i.e., the populations of cells responsible for the formation of secondary osteons; Frost 1969) activation frequency, i.e., parameter *Ac.f* in classical histomorphometric nomenclature (cf. Dempster 2013). B) Most of the secondary osteons show evidence of particularly intense remodeling (Fig.10G, H), with the presence of two to four cycles of resorption and reconstruction centered on the Haversian canal. By this process, several generations of osteons with decreasing diameters were formed inside ontogenetically older secondary osteons. This situation is general in *N. vitulinoides*; it occurs in all secondary bone deposits, be they localized in the medullary or cortical regions of the bones. C) Such a process resulted in extreme thinning of the lumens of Havers' canals, which are very seldom wider than 10 µm, and most often less than 5 µm. Havers' canals in numerous osteons are so drastically reduced that they seem to be completely occluded (Fig.10H).

This special Haversian tissue, characteristic of the medullary (and occasionally cortical) region, can be observed in all parts of the long bones: in the mid-diaphyseal region as well as in metaphyses, from which it extends continuously into the whole epiphyseal regions, up to the proximal and distal extremities of the bones, where it merges into the thin layers of calcified cartilage covering articular surfaces (Fig.11A-C). None of the longitudinal sections

(which were made in all specimens) reveal the presence of a functional growth plate or a lack of fusion of primary and secondary centers of ossification (Fig.11A, B). We thus conclude that the growth in length of long bone specimens in our sample was complete.

With the exception of the vertebral centra (considered below), there is only one variation to this general pattern. In the radius Histos 2174, the medullary territory (51% of the total area in cross section) is occupied by a compacted spongiosa whose former trabeculae, still clearly distinguishable, show numerous reversion lines (created by a strong resorption – reconstruction activity), but no secondary osteons (Fig.11D, E). Conversely, inter-trabecular spaces are entirely filled by endosteal lamellar tissue showing evidence of intense Haversian substitution. This process resulted in several generations of concentric secondary osteons (Fig.10E). Such a detailed topographical difference in remodeling patterns, through which the initial architecture of the medullary spongiosa was preserved, is unknown in all other specimens studied here.

The femur, humerus, and ulna examined here display a strong off-centering of growth (Fig.11F) that provoked, on the one hand, the development of a thick primary cortex on the lateral side of these bones and, on the other hand, the superficial outcropping of remodeled medullary regions, due to extensive resorption on their medial side. The result of this double process was a lateral drift of growth. Moreover, several of the long bones show, on cross sections, variably oriented fissures 120 to 200 µm long (Fig.11E). These cracks are observed only in deep cortical regions and in the medullary territory; they never reach the peripheral margins of the bones. Their possible nature and the causes of their occurrence are discussed below (see Discussion).

The trabeculae occupying the centrum of the largest vertebra (specimen IRSNB prov. 16), as well as the lamellar bone that partly fills inter-trabecular spaces, have a histological structure similar to that observed in the medullary region of long bones: they are formed of

intensively-remodeled tissue (Fig.11G). Remodeling is less intensive in the smaller vertebra; therefore, the growth pattern of this bone remains legible. It was a normal endochondral osteogenesis, with complete resorption of epiphyseal calcified cartilages and active remodeling of primary trabeculae, at a small distance away from the zone of cartilage hypertrophy. In general, none of the bones examined in this study displays the slightest residue of calcified cartilage outside a narrow band (200 to 400 µm) localized just under the epiphyseal surface (Fig.11C). The largest centrum retains only a thin layer of primary periosteal bone tissue spared by remodeling on the walls of the neural arch (Fig.11I). Six tightly spaced growth marks (mean spacing < 50 µm) forming an external fundamental system are visible in this layer: the bone was thus reaching the end of its growth.

Comparative data

The vertebrae of pinniped taxa other than *N. vitulinoides* show relatively little microanatomical or histological differences from other mammals. Moreover, the diaphyses of their long bones, though presenting some few, slender medullary trabeculae, do not display typical microanatomical or histological peculiarities (very high or very low global compactness, lack of a medullary cavity, cortical hyperplasy, diaphyseal persistence of calcified cartilage, etc.) likely to distinguish these taxa unambiguously from other mammals (see also the Introduction). The only exception is the small development of the medullary cavity in the femur of *Phocanella pumila* (Fig.12A). When primary periosteal cortices in long bones, are partly spared by Haversian substitution (as observed in the femur of *Phocanella pumila* and a rib from *Monachus monachus*), they are composed, like those of *N. vitulinoides*, of a woven-parallel complex containing longitudinal primary osteons, annuli and lines of arrested growth (Fig.12B–D). Otherwise, remodeling is intense and spreads to the totality of bone cortices; however, extreme remodeling resulting in the closure of vascular canals does

not occur (Fig.12D, E). In all taxa, except *Phocanella pumila*, the thin trabeculae occurring in the medullary cavity are made of remodeled lamellar bone, framing wide inter-trabecular spaces (Fig.12E, F). In *Phocanella pumila*, medullary trabeculae are also intensely remodeled, but they are much thicker than in other pinnipeds (compare Fig.12A and 12F). As a consequence, they divide the medullary cavity into small lacunae and strongly increase its compactness (on cross sections).

DISCUSSION

MORPHOMETRICS AND MICROANATOMY

Based on the sample of specimens used for the morphometric analysis, the diaphysis of the humerus of extinct Phocidae is generally more slender than in extant specimens, apart from the late Miocene *Pachyphoca ukrainica*, which shows pachyostotic 'swelling' of the humeral diaphysis. However, the femoral diaphysis of the sampled extinct Phocidae is generally a little thicker than that of extant Phocidae. The femoral diaphysis in *Pachyphoca* and, to a lesser extent, *N. vitulinoides* is also relatively bulky, without appearing swollen. Thus, we detected no clear pachyostotic trend in our sample.

Despite the absence of pachyostosis in the humerus and the femur of *N. vitulinoides*, osteosclerosis appears to be extreme in this taxon, and occurs also in *Phocanella pumila*. For the studied specimens of *N. vitulinoides*, namely one rib, two humeri, one radius, two femora, and one tibia, actual bone compactness (0.971 – 0.999) approaches 1 (100%). Similarly, although slightly lower (0.959 – 0.977), compactness values in the humerus and femur of *Phocanella pumila* are much above the common situation of other specimens. The relatively high compactness of the lumbar vertebrae of both the juvenile and the adult specimens of *N. vitulinoides* shows that osteosclerosis in the taxon extends to the entire postcranial skeleton.

Moreover, differences in compactness between the adult (93.8%) and the juvenile (63.6%) suggest that the increase in compactness is an ongoing process during the growth of the animal. In addition to that, it is noteworthy that the compactness observed in the vertebrae of Phocinae (excluding *N. vitulinoides*) is noticeably lower than the compactness observed in Monachinae and Otariidae. This may hypothetically be related to differences in locomotion (Pierce et al. 2011; Kühn and Prey 2012) or differences in maternal care (Boness and Bowen 1996). However, this is beyond the scope of the current study and should be treated in a future studies.

Considering the entire set of microanatomical observations made on the bones of *Nanophoca*, it seems obvious that osteosclerosis touches most (and perhaps all) of the appendicular elements. This contrasts with the situation prevailing in the sirenian *Dugong dugon*, in which there is a gradual decrease in compactness from the more proximal portion of the forelimb towards its distal portion (Buffrénil and Schoevaert 1989). A similar condition has been described in the marine sloth *Thalassocnus* (Amson et al. 2014) in which the radius is noticeably less compact than the humerus.

GROWTH PATTERN OF THE BONES AND MECHANISM OF THEIR COMPACTION

***Growth pattern of bone cortices*.** According to the experimental data presently available about the relationship between the structure of periosteal bone deposits and their accretion rate, the so-called Amprino's (1947) rule, the growth in thickness of *N. vitulinoides* bone cortices proceeded at relatively moderate speed. The woven-parallel bone with longitudinal primary osteons that compose them is generally associated, in extant mammals and birds, with apposition rates ranging between 4 and 8 µm per day (Castanet et al. 1996, 2000). All other forms of woven-parallel bone, i.e., reticular, plexiform, laminar, or radial tissues, correspond to higher growth rates. This question is nevertheless complex; it remains incompletely settled

and contrasting results have been presented by Margerie et al. (2002). To our knowledge, there are neither experimental data on bone apposition rate in pinnipeds nor precise histological descriptions of the structure of periosteal cortices in their bones. The comparative observations made in the present study suggest that, despite its modest size, *N. vitulinoides* did not grow at a rate very different from that of larger species.

The growth of primary bone cortices was cyclic in *Nanophoca* with, as in most mammals for which accurate data exist, the yearly alternation of a fast growth phase (accretion of the woven-parallel layers) when food was abundant, and a slow growth phase, corresponding to unfavorable environmental conditions, during which the annuli were formed. In one specimen at least, the humerus Histos 2139, a total arrest of growth occurred each year, resulting in the formation of lines of arrested growth. The comparative sample reveals that *Nanophoca* did not differ from other pinnipeds for these characteristics. More generally, several recent studies (e.g., Castanet 2006; Köhler et al. 2012) show that the presence of growth cycles of annual periodicity (supposed so in fossils) is a general, plesiomorphic feature in vertebrates (it primarily depends on endogenous rhythms), whatever their phylogenetic position, physiological characteristics, or ecological adaptations, as shown by the occurrence of cyclic growth marks in Silurian placoderms (Giles et al. 2013).

The ontogenetic transformation of primary cortices in *Nanophoca* was basically due to intense Haversian remodeling, a situation also observed in other pinnipeds and otherwise common to most mammals. Cortical remodeling presented some delay as compared to that occurring in the medullary region, which explains that non-remodeled primary cortices co-existed with a densely remodeled medulla in most bones.

***Mechanism of medullary compaction*.** Our histological observations suggest that the fundamental process of endochondral osteogenesis was not significantly modified in *N. vitulinoides*. Contrary to the situation prevailing in numerous secondarily aquatic tetrapods

(reviewed in e.g., Ricqlès and Buffrénil 2001), the calcified cartilage formed in growth plates was entirely eroded and the formation of primary trabeculae was apparently normal. Compaction of the medullary region basically resulted from the mode of remodeling of these trabeculae. The erosion and reconstruction process involved in bone remodeling is generally balanced, the amount of bone resorbed by osteoclasts being approximately compensated by an equivalent amount of reconstructive (secondary) osseous tissue (Parfitt 1981, 1982). In *N. vitulinoides*, imbalance visibly existed in favor of the reconstructive stage: the amount of secondary deposits produced by endosteal osteoblasts exceeded the volume of tissue previously eroded by the osteoclasts. The detailed histogenetical mechanism controlling this peculiar functioning of the osteoblasts is, of course, beyond reach of this study. The regulation of osteoblast activity during Haversian remodeling is a complex, still poorly elucidated question (e.g., Martin 2000; Burr and Allen 2014). It nevertheless remains that the cause responsible for osteosclerosis in *N. vitulinoides* obviously resided in a modification of this regulation mechanism. Occlusion of intra-osseous cavities due to this process was extremely pronounced because several, successive peri-vascular remodeling cycles occurred locally (over-remodeling), up to a quasi-total closure of vascular canals. Vascular canals reduced to diameters less than 10 µm, and a fortiori the thinner capillaries housed in them, are unlikely to have remained functional, as the mean diameter of mammalian erythrocytes (not to speak of other blood cells) is 7 to 8 µm (e.g., Fawcett and Jensh 1997). In humans, the lumen of the Haversian canal of a normal, fully developed, secondary osteon is 20 – 50 µm in diameter (Jaworski 1993; Fiala 1980; see also Polig and Jee 1990). For example, in the ribs of male humans aged 20 – 25 years, mean Haversian canal perimeter (variable *Hc.Pm* in classical nomenclature) is 0.165 mm, and Haversian canal area (*Hc.Ar*) is 0.002 mm² (Qiu et al. 2003); these parameters indeed correspond to a diameter of some 50 µm.

The compaction process described here in *N. vitulinoides* is known also from other marine tetrapods; it was observed in the femur and humerus of *Clausiosaurus germaini* (Buffrénil and Mazin 1989), the rostral region of the skull of several ziphiid whales (Buffrénil and Casinos 1995; Zylberberg et al. 1998; Lambert et al. 2011; Dumont et al. 2016), and the five species of the xenarthran genus *Thalassocnus* (Amson et al. 2014). Conversely, it was not observed in other pinnipeds, albeit our data suggest that *Phocanella pumila* might have displayed a similar specialization, though far less pronounced than in *N. vitulinoides*.

Remark on the timing of somatic growth in Nanophoca vitulinoides—The results of the present study reveal a paradoxical situation in which two conditions, which can be considered contradictory, coexist. A) In several long bones (humerus, femur, ulna), primary periosteal cortices display rather broadly spaced annuli up to bone periphery and, although the outer margins of the bones are bordered by an annulus, there is no clearly characterized external fundamental system. This situation should normally indicate that, on the one hand, the growth of the bones was still actively progressing when the animals died and that, on the other hand, death occurred during the unfavorable season, when annuli were formed. B) However, in all long bones, growth plates are entirely erased by remodeling; therefore, no further growth in length could occur. A possible explanation for these contrasted data is that the growth in diameter of the bones remained active by the time their growth in length was already stopped. This hypothesis is not convincing because such a process would have created a great diversity in the shape of the bones of *N. vitulinoides*, a situation that does not exist (see Dewaele et al. 2017a). Another hypothesis is to consider that growth ceased abruptly, with both the destruction of growth plates and a sudden stop in periosteal apposition, when a certain size was reached. In this situation, peripheral annuli should be viewed as functional equivalents of EFS. For each individual, this double process of growth cessation is likely to have occurred during the unfavorable season, when annuli were deposited. Depending on the age when this

process normally occurred (this age cannot be determined because early growth marks were erased by remodeling) it could explain the small size of *N. vitulinoides*. This issue requires the examination of a larger sample of *Nanophoca* bones and cannot be settled for the present. Moreover, slight local differences in the timing of the growth dynamics are not to be excluded, as suggested by the occurrence of an EFS in the largest vertebra.

Possible consequence of compaction on bone biomechanics—The unusual frequency of the short fissures observed in several specimens of *N. vitulinoides* cannot be readily explained by the effect of taphonomic constraints because *N. vitulinoides* fossils do not show traces of crushing or deformation (although they can be broken). Moreover, the cracks are restricted to the central region of the bones, and never extend towards their peripheral margins; such extensions should nevertheless have occurred if an external constraint had been exerted on the bones. The aspect of the fissures observed here is strongly reminiscent of the fatigue micro-fractures, as they are classically described and illustrated in the skeleton of *Homo* (e.g., Schaffer et al. 1995; Lee et al. 2003; Landrigan et al. 2011) and numerous domestic and wild animals such as, e.g., dogs (Burr et al. 1985), rats (Voide et al. 2011), sheep (Mohsin et al. 2006), etc. In the absence of another plausible interpretation, the fissures observed in bones of *N. vitulinoides* are considered as genuine fatigue micro-fractures. The accumulation and coalescence of these small lesions, caused by long-lasting, repetitive mechanical stress, constitute the major processes responsible for the degradation of bone mechanical properties (Danova et al. 2003). Their relative abundance in *N. vitulinoides* could have been indirectly induced by the compaction of bone tissue that occurred in this taxon. It is indeed possible that the pronounced reduction, or even the total occlusion, of the lumen of vascular canals by excessive secondary deposits resulted in a local cessation of Haversian remodeling, as the precursors of the osteoclasts (monocytes), cells of the blood lineage, arrive in situ via vascular networks (syntheses in Marks and Popoff 1988; Charles and Aliprantis 2014; see also Lafage-

Proust et al. 2015). It is therefore likely that the extreme and imbalanced remodeling in bones of *N. vitulinoides* was a self-blocking process, a hypothesis that could additionally explain why open resorption cavities are so scarce in the bones of *N. vitulinoides* observed in this study. One of the functions most commonly attributed to remodeling, be it of the Haversian type or not, is precisely to operate a local replacement of the osseous tissue damaged by the proliferation of fatigue micro-fractures (Burr 1993; Burr et al. 1995; Lieberman et al. 2003). In *N. vitulinoides*, this process might have been hampered by local restriction to blood supply. If a strong increase in bone compactness in this taxon was positively selected for the functional benefit that it could provide, the "price to pay" was a decrease in the mechanical resistance of the bones. This result is maladaptive because a total closure of vascular canals actually provided negligible gain in mass (which was not the case for the closure of larger bone cavities). This situation suggests that such an extreme degree of bone compaction might have resulted from developmental constraints that could have prevented compaction of the skeleton to be optimal throughout. Several, relatively common, disorders of the skeleton likely to have a genetic origin provoke increased and imbalanced remodeling, e.g., Paget's disease, osseous mastocytosis, etc. (Ralston 2008; Michou and Brown 2011; see also Evans et al. 1983), and can produce symptoms reminiscent of, though not strictly identical to, the situation observed in *N. vitulinoides*. It seems possible that the peculiarities of bone structure in *Nanophoca* could have initially resulted from a process akin to such pathological processes. Pending an actual genetic causality, the latter could have been selected and subsequently increased during evolution for its adaptive consequences, if the resulting general compactness increase of the skeleton of *N. vitulinoides* was advantageous. Such a process might have occurred also in other aquatic tetrapods showing the same bone structural peculiarities as *Nanophoca*. Future studies should address this issue and point out the frequency of this putative process.

FUNCTIONAL CONSIDERATIONS

One of the obvious consequences of the osteosclerotic-like process described here was to increase the overall mass of the *N. vitulinoides* skeleton. In the absence of pachyostosis, this increase was relatively moderate, as compared to the extreme situations encountered in the Sirenia (Kaiser 1974; Buffrénil et al. 2010) or the marine squamates (the so-called limbed snakes) from the Cenomanian of Europe and North Africa (Buffrénil and Rage 1993; Houssaye, 2013). Nevertheless, it necessarily provoked an increase in the density and inertia of the body, and proportionally reduced its buoyancy and maneuverability in the water as well as on land (Taylor 2009; Domning and Buffrénil 1991). It is thus likely that, as compared to the other pinnipeds devoid of osteosclerosis, (e.g., *Arctocephalus*, *Phocarctos*, and *Zalophus*: Godfrey 1985; Beentjes 1990; Fish et al. 2003), the locomotor capabilities of *N. vitulinoides* were characterized by a lower swimming speed and a poor aptitude for steep accelerations or sudden direction changes (maneuverability). Until now, no skull of this taxon has been discovered; thus, its feeding strategy and food preferences cannot be determined. The extreme compactness of postcranial elements strongly suggests that *N. vitulinoides* was not adapted to the capture of fast and mobile prey in open seas. Rather, it must have fed upon benthic or fixed animals in coastal shallow waters. One well-known extant benthic feeder is the walrus, *Odobenus rosmarus* (e.g., Fay 1982; Gjertz and Wiig 1992; Dehn et al. 2006). However, bone densification in the walrus is limited to pachyostosis in certain cranial regions (Kaiser 1967), while the postcranial skeleton is largely untouched by pachyosteosclerosis (e.g., Canoville et al. 2016: fig. 7O). In addition, Deméré (1994a, b) showed that the skeleton of the extinct walrus *Valenictus* was pachyosteosclerotic and that this taxon most likely had an even more pronounced benthic foraging lifestyle than the extant *Odobenus*. Moreover, the interpretation of *N. vitulinoides* as a benthic feeder closely fits the conclusions drawn by Dewaele et al.

(2017a) from extensive anatomical clues and reconstructions of the appendicular musculature: pectoral and pelvic girdles were used by *N. vitulinoides* in a different way than in other Phocidae, presumably for grasping and crawling on the substrate. For instance, the strong development of the greater tubercle of the humerus, the weak development of the lesser tubercle of the latter, and the strong development of the olecranon process on the ulna point toward powerful extension and abduction of the foreflippers, contrasting with the conditions displayed by extant phocids. In this functional context, even a limited buoyancy decrease (as compared to other taxa such as the sirenians or some Cenomanian aquatic squamates; the bone ballast of *Nanophoca* is moderate) must have facilitated a passive control, with little energy expense, of body position and trim in the water column. The same may apply to the contemporaneous late Miocene–early Pliocene *Phocanella pumila*, given the similar trend toward density increase in the humerus and femur. Hence, a comparable feeding pattern might have existed in these two taxa. Unfortunately, no dental remains are known from *Phocanella pumila*, which precludes elucidating the feeding habits of this species and, indirectly, that of *N. vitulinoides*. Both are nevertheless found in the same geological context, and might therefore have shared close ecological adaptations. Although our analysis includes only two specimens of the latter taxon (the extent of bone compaction in the rest of the skeleton cannot be assessed), a similar ecology to that of *N. vitulinoides* can be expected. The presence of a (thick) spongy trabecular network in the medullary cavity of *Batavipusa neerlandica* and *Praepusa boeska*, two small, roughly contemporaneous (late Miocene–early Pliocene) species from the southern margin of the North Sea Basin, shows that the extreme compactness of the long bones of *N. vitulinoides* is not strictly correlated with the small body size of the taxon.

CONCLUSIONS

Nanophoca vitulinoides from the middle Miocene of the North Sea Basin is the first extinct phocid taxon to undergo a detailed microanatomical and osteohistological description. Its long bones are extremely compact, lacking a differentiated medullary cavity and exhibiting compactness values close to 100%. Apart from the extinct phocine seal *Phocanella pumila*, such structural peculiarities are unknown among pinnipeds. The spine of *Nanophoca* was also touched by this process, which is a unique case among mammals. The high compactness is not observed in any other semi-aquatic mammal. The high compactness observed in the skeleton of *Nanophoca* resulted from an imbalanced remodeling process located in the medullary region. Positively selected during evolution, this process might have been rooted in an initial genetic condition akin to one form of the so-called "metabolic bone diseases." It increased body density, thus reducing buoyancy and facilitating long-lasting underwater stays. Conversely, it limited speed and maneuverability. Although more complete fossils, and especially cranial remains, are needed to draw definite conclusions on *Nanophoca* ecology, the results of this study strongly suggest that *N. vitulinoides* was a bottom-dwelling seal, living in shallow waters close to the shore in the Miocene North Sea Basin, and feeding on benthic prey.

ACKNOWLEDGEMENTS

The research presented in this study is in partial fulfillment of the PhD research of LD, conducted at Ghent University, Ghent, Belgium, and in collaboration with the Royal Belgian Institute of Natural Sciences, Brussels, Belgium. This PhD research is funded by the Research Foundation – Flanders (FWO) through an FWO PhD Fellowship to LD. This research is also partly funded by the Society of Vertebrate Paleontology's 2016 Steven Cohen Award for Excellent Student Research, awarded to LD. TDK holds a postdoctoral Fellowship at the FWO.

We also want to thank S Bruaux, C Cousin, and A Folie from the RBINS for providing access to the collections. We thank R Fraaije and N Peters from the Oertijdmuseum Groene Poort, Boxtel, Netherlands, for allowing access to the holotypes of *Batavipusa neerlandica* and *Praepusa boeska*. We are grateful to M Bosselaers for donating specimens from his private collection for the elaboration of thin sections. Special thanks to JR Wible (editor-in-chief), A Houssaye (reviewer), and a second anonymous reviewer for helpful comments that improved the quality of this work.

REFERENCES CITED

Amprino R (1947) La structure du tissu osseux envisagée comme expression de différences dans la vitesse de l'accroissement. Arch Biol 58:315–330

Amson E, Muizon C de (2014) A new durophagous phocid (Mammalia: Carnivora) from the late Neogene of Peru and considerations on monachine seal phylogeny. J Syst Paleontol 12:523–548. doi: 10.1080/14772019.2013.799610

Amson E, Muizon C de, Laurin M, Argot C, Buffrénil V de (2014) Gradual adaptation of bone structure to aquatic lifestyle in extinct sloths from Peru. Proc Biol Soc 281:20140192. doi: 10.1098/rspb.2014.0192

Beentjes MP (1990) Comparative terrestrial locomotion of the Hooker's sea lion (*Phocarctos hookeri*) and the New Zealand fur seal (*Arctocephalus forsteri*): evolutionary and ecological implications. Zool J Linn Soc 98:307–325. doi: 10.1111/j.1096-3642.1990.tb01204.x

Berta A, Kienle S, Bianucci G, Sorbi S (2015) A reevaluation of *Pliphoca etrusca* (Pinnipedia, Phocidae) from the Pliocene of Italy: phylogenetic and biogeographic implications. J Vertebr Paleontol 35:e88944. doi: 10.1080/02724634.2014.889144

Bininda-Emonds ORP, Russell AP (1996) A morphological perspective on the phylogenetic relationships of the extant phocid seals (Mammalia: Carnivora: Phocidae). Bonn Zool Monogr 41:1–256

Boness DJ, Bowen WD (1996) The evolution of maternal care in pinnipeds. Bioscience 46:645–654

Buffrénil V de, Canoville A, D'Anastasio R, Domning DP (2010) Evolution of sirenian pachyosteosclerosis, a model-case for the study of bone structure in aquatic tetrapods. J Mammal Evol 17:101–120.doi: 10.1007/s10914-010-9130-1

Buffrénil V de, Casinos A (1995) Observations histologiques sur le rostre de *Mesoplodon densirostris* (Mammalia, Cetacea, Ziphiidae): le tissu osseux le plus dense connu. Ann Sci Nat Zool 13ème Ser 16:21–32

Buffrénil V de, Mazin J-M (1989) Bone histology of *Claudiosaurus germaini* (Reptilia, Claudiosauridae) and the problem of pachyostosis in aquatic tetrapods. Hist Biol 2:311–322.doi: 10/1080/08912968909386509

Buffrénil V de, Rage J-C (1993) La 'pachyostose' vertébrale de *Simoliophis* (Reptilia, Squamata): données comparatives et considérations fonctionnelles. Ann Paleontol (Vertebr) 79:315–335

Buffrénil V de, Ricqlès A de, Ray CE, Domning, DP (1990) Bone histology of the ribs of the archaeocetes (Mammalia: Cetacea). J Vertebr Paleontol 10:455–466.doi: 10/1080/02724634.1990.10011828

Buffrénil V de, Schoevaert D (1989) Données quantitatives et observations histologiques sur la pachyostose du squelette du dugong, *Dugong dugon* (Müller) (Sirenia, Dugongidae). Can J Zool 67:2107-2119. doi: 10.1139/z89-300

Burr DB (1993) Remodeling and the repair of fatigue damage. Calcif Tissue Internatl 53 (suppl 1):S75–S81. doi: 10.1007/BF01673407

Burr DB, Allen MR (eds) (2014) Basic and Applied Bone Biology. Elsevier/Academic Press, London

Burr DB, Martin RB, Schaffler MB, Radin EL (1985) Bone remodeling in response to *in vivo* fatigue microdamage. J Biomech 18:189–200. doi:10.1016/0021-9290(85)90204-0

Canoville A, Buffrénil V de, Laurin M (2016) Microanatomical diversity of amniote ribs: an exploratory quantitative study. Biol J Linn Soc 118:706–733. doi: 10.1111/bij.12779

Canoville A, Laurin M (2010) Evolution of humeral microanatomy and lifestyle in amniotes, and some comments on palaeobiological inferences. Biol J Linn Soc 100:384–406. doi: 10.1111/j.1095-8312.2010.01431.x

Castanet J (2006) Time recording in bone microstructures of endothermic animals; functional relationships. CR Palevol 5:629–636. doi: 10.1016/j.crpv.2005.10.006

Castanet J, Grandin A, Abourachid A, Ricqlès A de (1996) Expression de la dynamique de croissance dans la structure de l'os périostique chez *Anas platyrhynchos*. CR Acad Sci Paris, Sci Vie 319:301–308

Castanet J, Curry Rogers C, Cubo J, Boisard J (2000) Periosteal bone growth rates in extant ratites (ostrich and emu). Implications for assessing growth in dinosaurs. CR Acad Sci Paris, Sci Vie 323:543–550. doi: 10.1016/S0764-4469(00)00181-5

Charles JF, Aliprantis AO (2014) Osteoclasts: more than 'bone eaters'. Trends Mol Med 20:449–459. doi: 10.1016/j.molmed.2014.06.001

Cozzuol MA (2001) A "northern" seal from the Miocene of Argentina: implications for phocid phylogeny and biogeography. J Vertebr Paleontol 21:415–421. doi: 10.1671/0272-4634(2001)021[0415:ANSFTM]2.0.CO;2

Danova NA, Colopy SA, Radtke CL, Kalscheur VL, Markel MD, Vanderby R Jr, McCabe RP, Escarcega AJ, Muir P (2003) Degradation of bone structural properties by accumulation and coalescence of microcracks. Bone 33:197–205. doi: 10.1016/S8756-3282(03)00155-8

Dehn L-A, Sheffield GG, Follmann EH, Duffy LK, Thomas DL, O'Hara TM (2006) Feeding ecology of phocid seals and some walrus in the Alaskan and Canadian Arctic as determined by stomach contents and stable isotope analysis. Polar Biol 30:167–181. doi: 10.1007/s00300-006-0171-0

Deméré TA (1994a) Two new species of fossil walruses (Pinnipedia: Odobenidae) from the upper Pliocene San Diego Formation. Proc San Diego Soc Nat Hist 29:77–98

Deméré TA (1994b) The family Odobenidae: a phylogenetic analysis of fossil and living taxa. Proc San Diego Soc Nat Hist 29:99–123

Dempster, DW, Compston JE, Drezner MK, Glorieux FH, Kanis JA, Malluche H, Meunier PJ, Ott SM, Recker RR, Parfitt AM (2013) Standardized nomenclature, symbols, and units for bone histomorphometry: a 2012 update of the report of the ASBMR Histomorphometry Nomenclature Committee. J Bone Miner Res 28:1–16. doi: 10.1002/jbmr.1805

Dewaele L, Amson E, Lambert O, Louwye S (2017a) Reappraisal of the extinct seal "*Phoca*" *vitulinoides* from the Neogene of the North Sea Basin, with bearing on its geological age, phylogenetic affinities, and locomotion. PeerJ 5:e3316. doi: 10.7717/peerj.3316

Dewaele L, Lambert O, Louwye S (2017b) On *Prophoca* and *Leptophoca* (Pinnipedia, Phocidae) from the Miocene of the North Atlantic realm: redescription, phylogenetic affinities and paleobiogeographic implications. PeerJ 5:e3024. doi: 10.7717/peerj.3024

Domning D, Buffrénil V de (1991) Hydrostasis in the Sirenia: quantitative data and functional interpretation. Mar Mammal Sci 7:331–368. doi: 10.1111/j.1748-7692.1991.tb00111.x

Dumont M, Buffrénil V de, Mijan I, Lambert O (2016) Structure and growth pattern of the bizarre hemispheric prominence of the rostrum of the fossil beaked whale *Globicetus huberus* (Mammalia, Cetacea, Ziphiidae). J Morphol 277:1292–1308. doi: 10.1002/jmor.20575

Dumont M, Laurin M, Jacques F, Pellé E, Dabin W, Buffrénil V de (2013) Inner architecture of vertebral centra in terrestrial and aquatic mammals: a two-dimensional comparative study. J Morphol 274:570–584. doi: 10.1002/jmor.20122

Evans RA, Hughes WG, Dunstan CR, Lennon WP, Kohan L, Hills E, Wong SYP(1983) Adult osteosclerosis. Metab Bone Dis Relat 5:111–117. doi: 10.1016/0221-8747(83)90011-5

Fawcett DW, Jensh RP (1997) Bloom and Fawcett: Concise Histology. Chapman and Hall, New York

Fay FH (1982) Ecology and biology of the Pacific walrus, *Odobenus rosmarus divergens* Illiger. N Am Fauna 74:1–279. doi: 10.3996/nafa.74.0001

Fiala P (1980) Structure of the long limb bones and its significance in determining age in man. Folia Morphol 28:259–263

Fish FE, Stein BR (1991) Functional correlates of differences in bone density among terrestrial and aquatic genera in the family Mustelidae (Mammalia). Zoomorphology 110:339–345. doi: 10.1007/BF01668024

Fish FE, Hurley J, Costa DP (2003) Maneuverability by the sea lion *Zalophus californianus*: turning performance of an unstable body design. J Exp Biol 206:667–674. doi: 10.1242/jeb.00144

Francillon-Vieillot H, de Buffrénil V, Castanet J, Geraudie J, Meunier JF, Sire JY, Zylberberg L, Ricqlès A de (1990) Microstructure and mineralization of vertebrate skeletal tissues.In: Carter JG (ed) Skeletal Biomineralizations: Patterns, Processes and Evolutionary Trends, Vol. 1. Van Nostrand Reinhold, New York, pp 471–530.

Frost HM (1969) Tetracycline-based histological analysis of bone remodeling. Calc Tiss Res 33:211–237. doi: 10.1007/BF02058664

Fulton TL, Strobeck C (2010) Multiple markers and multiple individuals refine true seal phylogeny and bring molecules and morphology back in line. Proc Roy Soc B–Biol Sci 277:1065–1070. doi: 10.1098/rspb.2009.1783

Germain D, Laurin M (2005) Microanatomy of the radius and lifestyle in amniotes (Vertebrata, Tetrapoda). Zool Scr 34:335–350. doi: 10.1111/j.1463-6409.2005.00198.x

Giles S, Rücklin M, Donoghue PCJ (2013) Histology of "placoderm" dermal skeletons: implications for the nature of the ancestral gnathostomes. J Morphol 274:627–644. doi: 10.1002/jmor.20119

Girondot M, Laurin M (2003) Bone Profiler: a tool to quantify, model and statistically compare bone section compactness profiles. J Vertebr Paleontol 23:458-461. doi: 10.1671/0272-4634(2003)023[0458:BPATTQ]2.0.CO;2

Gjertz I, Wiig Ø (1992) Feeding of walrus *Odobenus rosmarus* in Svalbard. Polar Record 28:57–59. doi: 10.1017/S0032247400020283

Godfrey SJ (1985) Additional observations of subaqueous locomotion in the California Sea Lion (*Zalophus californianus*). Aquat Mammal 11:53–57

Gray N-M, Kainec K, Madar SI, Tomko L, Wolfe S (2007) Sink or swim? Bone density as a mechanism for buoyancy control in early cetaceans. Anat Rec 290:638–653. doi: 10.1002/ar.20533

Higdon JW, Bininda-Emonds ORP, Beck RMD, Ferguson SH (2007) Phylogeny and divergence of the pinnipeds (Carnivora: Mammalia) assessed using a multigene dataset. BMC Evol Biol 7 :216. doi: 10.1186/1471-2148-7-216.

Houssaye A (2009) "Pachyostosis" in aquatic amniotes: a review. Integr Zool 4:325–340. doi: 10.1111/j.1749-4877.2009.00146.x

Houssaye A (2013) Palaeoecological and morphofunctional interpretation of bone mass increase: an example in Late Cretaceous shallow marine squamates. Biol Rev 88:117–139.

Houssaye A, Fish FE (2016) Functional (secondary) adaptation to an aquatic life in vertebrates: an introduction to the symposium. Integr Comp Biol 56:1266–1270. doi: 10.1093/icb.icw129

Houssaye A, Lindgren J, Pellegrini R, Lee AH, Germain D, Polcyn MJ (2013) Microanatomical and histological features in the long bones of mosasaurine mosasaurs (Reptilia, Squamata)–implications for aquatic adaptation and growth rates. PLoS One 8:e76741. doi: 10.1371/journal.pone.0076741

Houssaye A, Sander PM, Klein N (2016) Adaptive patterns in aquatic amniote bone microanatomy—more complex than previously thought. Integr Comp Biol 56:1349–1369. doi: 10.1093/icb/icw120

Houssaye A, Tafforeau P, Muizon C de, Gingerich PD (2015). Transition of Eocene whales from land to sea: evidence from bone microstructure. PLoS One 10:e0118409. doi: 10.1371/journal.pone.0118409

Jaworski ZFG (1992) Haversian system and Haversian bone. In: Hall BK (ed) Bone Metabolism and Mineralization. CRC Press, Boca Raton, pp 21–45.

Jefferson TA, Webber MA, Pitman RL (2008) Marine Mammals of the World: A Comprehensive Guide to their Identification. Elsevier/Academic Press, Amsterdam

Kaiser HE (1974) Morphology of the Sirenians. A Macroscopic X-Ray Atlas of the Morphology of Recent Species. S. Karger, Basel

Köhler M, Marin-Moratalla N, Jordana X, Aanes R (2012) Seasonal bone growth and physiology in endotherms shed light on dinosaur physiology. Nature 487:358–361. doi: 10.1038/nature11264

Koretsky IA (2001) Morphology and systematics of the Miocene Phocinae (Mammalia: Carnivora) from Paratethys and the North Atlantic Region. Geol Hung Ser Palaeontol 54:1–109

Koretsky IA, Grigorescu D (2002) The fossil monk seal *Pontophoca sarmatica* (Alekseev) (Mammalia: Phocidae: Monachinae) from the Miocene of eastern Europe. Smithson Contrib Paleobiol 93:149–162

Koretsky IA, Peters N (2008) *Batavipusa* (Carnivora, Phocidae, Phocinae): a new genus from the eastern shore of the North Atlantic Ocean (Miocene seals of the Netherlands, part II). Deinsea 12:53–62

Koretsky IA, Peters N, Rahmat SJ (2015) New species of *Praepusa* (Carnivora, Phocidae, Phocinae) from the Netherlands supports east to west Neogene dispersal of true seals.

Vestn Zool 49:57–66

Koretsky IA, Rahmat SJ (2013) First record of fossil Cystophorinae (Carnivora, Phocidae): middle Miocene seals from the northern Paratethys. Riv Ital Paleontol S 119:325–350. doi: 10.13130/2039-4942/6043

Koretsky IA, Rahmat SJ (2017). Preliminary report of pachyosteosclerotic bones in seals. Open Acc Res Anat 1:1–3

Koretsky IA, Ray CE (2008) Phocidae of the Pliocene of Eastern North America. Virginia Mus Nat Hist Spec Pub 14:81–140

Kriloff A, Germain D, Canoville A, Vincent P, Sache M, Laurin M (2008) Evolution of bone microanatomy of the tetrapod tibia and its use in palaeobiological inference. J Evol Biol 21:807–826. doi: 10.1111/j.1420-9101.2008.01512.x

Kühn C, Frey E (2012) Walking like caterpillars, flying like bats—pinniped locomotion. Palaeobio Palaeoenv 92:197–210. doi: 10.1007/s12549-012-0077-5

Lafage-Proust M-H, Roche B, Langer M, Cleret D, Vanden Bossche A, Olivier T, Vico L (2015) Assessment of bone vascularization and its role in bone remodeling. BoneKEy Rep 4, art. no. 662:1–8. doi: 10.1038/bonekey.2015.29

Lambert O, Muizon C de, Buffrénil V de (2011) Hyperdense rostral bones of ziphiid whales: diverse processes for a similar pattern. CR Palevol 10:453–468. doi: 10.1016/j.crpv.2011.03.012

Lamm ET (2013) Preparation and sectioning of specimens. In: Padian K, Lamm ET (eds) Bone Histology of Fossil Tetrapods: Advancing Methods, Analysis, and Interpretation. University of California Press, Berkeley, pp 55–160

Landrigan MD, Li J, Turnbull TL, Burr DB, Niebur GL, Roeder RK (2011) Contrast-enhanced micro-computed tomography of fatigue microdamage accumulation in human cortical bone. Bone 48:443–450. doi: 10.1016/j.bone.2010.10.160

Laurin M, Canoville A, Germain D (2011) Bone microanatomy and lifestyle: a descriptive approach. CR Palevol 10:381–402. doi: 10.1016/j.crpv.2011.02.003

Laurin M, Girondot M, Loth M-M (2004) The evolution of long bone microanatomy and lifestyle in lissamphibians. Paleobiology 30:589–613. doi: 10.1666/0094-8373(2004)030<0589:TEOLBM>2.0.CO;2

Lee TC, Mohsin S, Taylor D, Parkesh R, Gunnlaugsson T, O'Brien FJ, Giehl M, Gowin W (2003) Detecting microdamage in bone. J Anat 203:161–172. doi: 10.1046/j.1469-7580.2003.00211.x

Lieberman DE, Pearson OM, Polk JD, Demes B, Crompton AW (2003) Optimization of bone growth and remodeling in response to loading in tapered mammalian limbs. J Exp Biol 206:3125–3138. doi: 10.1242/jeb.00514

Liu XS, Bevill G, Keaveny TM, Sajda P, Guo XE (2009) Micromechanical analyses of vertebral trabecular bone based on individual trabeculae segmentation of plates and rods. J Biomech 42:249–256. doi: 10.1016/j.biomech.2008.10.035

Margerie E de, Cubo J, Castanet J (2002) Bone typology and growth rate: testing and quantifying "Amprino's rule" in the mallard (*Anas platyrhynchos*). CR Biol 325:221–230. doi: 10.1016/S1631-0691(02)01429-4

Marks SC, Popoff SN (1988) Bone cell biology: the regulation of development, structure and function of the skeleton. Am J Anat 183:1–44. doi: 10.1002/aja.1001830102

Martin RB (2000) Toward a unifying theory of bone remodeling. Bone 26:1–6. doi: 10.1016/S8756-3282(99)00241-0

Masschaele B, Dierick M, Loo DV, Boone MN, Brabant L, Pauwels E, Cnudde V, Hoorebeke LV (2013) HECTOR: A 240kV micro-CT setup optimized for research. J Phys Conf Ser 463:012012. doi: 10.1088/1742-6596/463/1/012012.

Michou L, Brown JP (2011) Genetics of bone diseases: Paget's disease, fibrous dysplasia, osteopetrosis and osteogenesis imperfecta. Joint Bone Spine 78: 252–258. doi: 10.1016/j.bspin.2010.07.010

Mohsin S, O'Brien FJ, Lee TC (2006) Osteonal crack barriers in ovine compact bone. J Anat 208: 81-89

Muizon C de (1981) Les vertébrés fossiles de la Formation Pisco (Pérou). Première partie: deux nouveaux Monachinae du Pliocène de Sud Sacaco. Inst Franc Etud Andines Mem 6 20–161

Nakajima Y, Endo H (2013). Comparative humeral microanatomy of terrestrial, semiaquatic, and aquatic carnivorans using micro-focus CT scan. Mammal Study 38:1–8

Parfitt AM (1981) Bone effect of spaceflight: analysis by quantum concept of bone remodeling. Acta Astronaut 8:1083–1090. doi: 10.1016/0094-5765(81)90082-5

Parfitt AM (1982) The coupling of bone formation to bone resorption: a critical analysis of the concept and of its relevance to the pathogenesis of osteoporosis. Metab Bone Dis Relat 4:1–6. doi: 10.1016/022-8747(82)90002-9

Pierce SE, Clack JA, Hutchinson JR (2011) Comparative axial morphology in pinnipeds and its correlation with aquatic locomotory behaviour. J Anat 219:502–514. doi: 10.1111/j.1469-7580.2011.01406.x

Polig E, Jee WSS (1990) A model of osteon closure in cortical bone. Calcif Tissue Internatl 47:261–269. doi: 10.1007/BF02555907

Prondvai E, Stein KHW, Ricqlès A de, Cubo J (2014) Development-based revision of bone tissue classification: the importance of semantics for science. Biol J Linn Soc 112:799–816. doi: 10.1111/bio.12323

Pyenson, ND, Kelley NP, Parham JF (2014) Marine tetrapod macroevolution: physical and biological drivers on 250 Ma of invasions and evolution in ocean ecosystems. Palaeogeogr Palaeoclimatol Palaeoecol 400:1–8. doi:10.1016/j.palaeo.2014.02.18

Qiu S, Fyhrie DP, Palnitkar S, Sudhaker Rao D (2003) Histomorphometric assessment of Haversian canal and osteocyte lacunae in different-sized osteons in human ribs. Anat Rec 272A:520–525. doi: 10.1002/ar.a.10058

Quemeneur S, Buffrénil V de, Laurin M (2013) Microanatomy of the amniote femur and inference of lifestyle in limbed vertebrates. Biol J Linn Soc 109:644–655. doi: 10.1111/bij.12066

Ralston SH (2008) Pathogenesis of Paget's disease of Bone. Bone 43: 819–825.doi: 10.1016/j.bone.2008.06.015

Ricqlès A de (1989). Les mécanismes hétérochroniques dans le retour des tétrapodes au milieu aquatique. Geobios Mem Spec 12:337–348. doi: 10.1016/S0016-6995(89)80034-8

Ricqlès A de, Buffrénil V de (1995) Sur la présence de pachyostéosclérose chez la rhytine de Steller [*Rhytina (Hydrodamalis) gigas*], sirénien récent éteint. Ann Sci Nat Zool Paris, 13e Ser 16:47–53

Ricqlès A de, Buffrénil V de (2001) Bone histology, heterochronies and the return of Tetrapods to life in water: w[h]ere are we? In: Mazin J-M, Buffrénil V de (eds)Secondary Adaptation of Tetrapods to Life in Water. Verlag Dr. Friedrich Pfeil, München, pp 289–310

Schaffler MB, Choi K, Milgrom C (1995) Aging and matrix microdamage accumulation in human compact bone. Bone 17:521–527. doi: 10.1016/8756-3282(95)00370-3

Stein BR (1989) Bone density and adaptation in semiaquatic mammals. J Mammal 70:467–476. doi: 10.2307/1381418

Storå J (2000) Skeletal development in the Grey seal *Halichoerus grypus*, the Ringed seal *Phoca hispida botnica*, the Harbour seal *Phoca vitulina vitulina* and the Harp seal *Phoca groenlandica*. Epiphyseal fusion and life History. Archaeozoologia 11:199–222.

Taylor MA (2009) Functional significance of bone ballast in the evolution of buoyancy control strategies by aquatic tetrapods. Hist Biol 14:15–31. doi: 10.1080/10292380009380550

Thompson DW (1961) On Growth and Form. Cambridge University Press, Cambridge

Turner CH (1998) Three rules for bone adaptation to mechanical stimuli. Bone 23:399–407. doi: 10.1016/S8756-3282(98)00118-5

Uhen MD (2007) Evolution of marine mammals: back to the sea after 300 million years. Anat Rec 290:514–522. doi:10.1002/ar.20545

Van Beneden P-J (1871) Les phoques de la mer scaldisienne. Bul Acad R Sci Let b-Arts Belg 2ième Ser 32:5–19

Van Beneden P-J (1877) Description des ossements fossiles des environs d'Anvers, première partie. Pinnipèdes ou amphithériens. Ann Mus R Hist Nat Belg 1:1–88.

Voide R, Schneider P, Stauber M, van Lenthe GH, Stampanoni M, Müller R (2011) The importance of murine cortical bone microstructure for microcrack initiation and propagation. Bone 49:1186–1193. doi: 10.1016/j.bone.2011.08.011

Wall WP (1983) The correlation between high limb-bone density and aquatic habits in recent mammals. J Paleontol 57:197–207

Webb P, Buffrénil V de (1990) Locomotion in the biology of large aquatic vertebrates. Trans Am Fish Soc 119:629–641. doi: 10.1577/1548-8659(1990)119<0629:LITBOL>2.3.CO;2

Zylberberg L, Traub W, Buffrénil V de, Alizard F, Arad T, Weiner S (1998) Rostrum of a toothed whale: ultrastructural study of a very dense bone. Bone 23:241–247. doi: 10.1016/S8756-3282(98)00101-X

LEGENDS OF THE FIGURES

Fig. 1 – Reconstruction of the skeleton of the phocid *Nanophoca vitulinoides* from the middle Miocene of the southern North Sea, with the partial skeleton of specimen IRSNB M2276 superimposed. Light gray indicates bone types that have been subjected to micro-CT scanning exclusively; dark gray indicates bone types that have been subjected to thin sectioning exclusively; and intermediate gray indicates bones that have been subjected to both micro-CT scanning and thin sectioning. Thin sectioning includes transverse sections and longitudinal sections. Note: thin sectioning has been performed on other specimens than IRSNB M2276. Modified from Dewaele et al. (2017a: fig. 1).

Fig. 2 – Line drawing of a humerus and femur of the *Nanophoca vitulinoides* neotype specimen IRSNB M2276 showing the measurements taken for the basic morphometric analysis. Gray lines on the humerus show total length of the humerus and least transverse width of the humeral diaphysis. Gray lines on the femur show total length of the femur and least transverse width across the diaphysis. Anteroposterior width is shown as an arrow perpendicular to the field of view (circle with diagonal cross).

Fig. 3 – Phylogeny of *Nanophoca vitulinoides*, as presented by Dewaele et al. (2017a). Both *Leptophoca proxima* and *N. vitulinoides* are shown as stem phocines. Based on the literature, the phylogenetic position of *Callophoca obscura* is difficult to ascertain. The phylogenetic position of *Batavipusa neerlandica*, *Phocanella pumila*, and *Praepusa boeska* remains unclear, in part due to the incompleteness of their respective fossil records.

Fig.4 – Microanatomy of the vertebra of *Nanophoca vitulinoides*. Longitudinal microanatomical drawings of an **A**) adult (Histos 2150, thin section) and **B**) juvenile (Histos

2147, thin section) lumbar vertebra. The compactness in the adult specimen is clearly much higher than in the juvenile specimen. Scale bars equal 5 mm.

Fig. 5 – Microanatomy of the rib of *Nanophoca vitulinoides*. Microanatomical drawings of the transverse sections through the ribs of **A**) *N. vitulinoides* (Histos 2152, thin section), **B**) *Callophoca obscura* (Histos 168, thin section), and **C**) *Phoca vitulina* (specimen from Canoville et al. 2016, thin section), and the corresponding compactness profiles. Scale bars equal 5 mm.

Fig.6 – Microanatomy of the humerus of *Nanophoca vitulinoides*. Microanatomical drawings of the transverse sections through the humerus of **A**) *N. vitulinoides* (IRSNB M2276c, micro-CT), **B**) *N. vitulinoides* (Histos 2136, thin section), **C**) *Phocanella pumila* (Histos 163, thin section), **D**) *Phoca vitulina* (IRSNB 1157E, micro-CT), **E**) *Mirounga leonina* (specimen from Canoville and Laurin 2010, thin section), **F**) *Otaria byronia* (specimen from Canoville and Laurin 2010, thin section), and **G**) *Lutra lutra* (specimen from Canoville and Laurin 2010, thin section), and the corresponding compactness profiles. Scale bars equal 5 mm.

Fig.7 – Micro-CT scans of the holotype humeri of *Batavipusa neerlandica* and *Praepusa boeska* from the middle Miocene of the southern North Sea basin. Scans show the diaphyseal cross sections of holotype humeri of **A**) *B. neerlandica* (MAB 3798) and **B**) *P. boeska* (MAB 4686). Anterior end up. White arrows point toward different concentric cortical layers. A spongy medullary region is clearly visible in *B. neerlandica*, but less conspicuous in *P. boeska*. Scale bars equal 5 mm.

Fig.8 – Microanatomy of the femur of *Nanophoca vitulinoides*. Microanatomical drawings of the transverse sections through the femur of **A**) *N. vitulinoides* (Histos 1935, thin section), **B**) *N. vitulinoides* (IRSNB M2276d, micro-CT), **C**) *Leptophoca proxima* (Histos 166, thin

section), **D**) *Callophoca obscura* (Histos 170, thin section), **E**) *Phocanella pumila* (Histos 160, thin section), **F**) *Phoca vitulina* (IRSNB 1157E, micro-CT), **G**) *Otaria byronia* (specimen from Quemeneur et al. 2013, thin section), and **H**) and **I**) *Lutra lutra* (specimen from Quemeneur et al. 2013, thin section), and the corresponding compactness profiles. Scale bars equal 5 mm.

Fig.9 – Microanatomy of the radius and tibia of *Nanophoca vitulinoides*. Microanatomical drawings of the transverse sections through the radius of **A**) *N. vitulinoides* (Histos 2142, thin section), and **B**) *Phoca vitulina* (IRSNB 1157E, micro-CT), and through the tibia **C**) *N. vitulinoides*(IRSNB M2276g, micro-CT), and **D**) *P. vitulina* (IRSNB 1157E, micro-CT), and the corresponding compactness profiles. Scale bars equal 5 mm.

Fig.10 – Bone structure in the cortex and medulla of *Nanophoca vitulinoides*. **A**) The cortex of the humeral diaphysis (cross section) is composed of a woven-parallel complex with longitudinal primary osteons and conspicuous, broadly spaced annuli (arrows). Left half: ordinary transmitted light, right half: polarized light. **B**) Longitudinal section in the same bone in the metaphyseal region. The primary osteons appear brightly birefringent. **C**) Closer view at the diaphyseal cortex between annuli 2 and 4. The arrows point to short Sharpey's fibers. **D**) Lines of arrested growth (arrows) in the humeral cortex. **E**) Cross-section in the larger radius (Histos 2174). The whole bone area is occupied by a dense Haversian tissue, and no medullary cavity is visible. **F**) Closer view at the remodeled medullary of the radius shown in Fig.10E. **G**) Detail of the structure of the dense Haversian tissue in the medulla of the radius. Remark that vascular canals are extremely thin or occluded. **H**) Close view at over-remodeled bone in the medulla of the radius. The two arrows point at occluded Haversian canals. Scale bars equal 5 μm, except E) 5 mm, and H) 50 μm.

Fig.11 – Inner bone remodeling in long bones and vertebrae. **A**) Longitudinal section in the proximal metaphyseal and epiphyseal regions of the femur. The whole bone is compact and

composed of densely remodeled osseous tissue. **B**) Longitudinal section in the proximal metaphysis and epiphysis of a rib. Same comment as for the femur. **C**) Longitudinal section in the epiphysis of the larger radius (Histos 2174). Epiphyseal surface is covered by a thin layer of calcified cartilage. Under it, the metaphyseal medulla is already compact and densely remodeled (right half: polarized light). **D**) Cross section in the diaphysis of the smaller radius (Histos 2142). The architecture of the spongiosa that once occupied the medulla is still visible, though inter-trabecular spaces are filled. **E**) Detail of the medullar of the smaller radius. The endosteal deposits filling inter-trabecular spaces are densely remodeled and vascular canals (arrows) tend to be occluded. The asterisks indicate micro-cracks. **F**) Off-centered growth of Humeral diaphysis. One face of the bone is under resorption (hollow arrow) while accretion occurs on the other (solid arrow). **G**) Cross section in the centrum of the larger vertebra. Polarized light reveals that the thick trabeculae filling the centrum are densely remodeled. **H**) Longitudinal section in the same specimen (polarized light) showing densely remodeled osseous tissue. **I**) External fundamental system on the outer wall of the neural arch (cross section) in polarized light. Scale bars equal 5 mm for A) and B); 1 mm for D), F), G), H), and I); and 500µm for C), and E).

Fig.12 – Comparative data in extant and extinct pinnipeds. **A**) Cross section in the femur of *Phocanella pumila*. Remark the relatively high compactness of this bone, and its non-remodeled cortex. White rectangle: field shown in Fig.11B. **B**) Detail of the cortex showing a woven-parallel tissue with longitudinal primary osteons and annuli. Right half: polarized light. **C**) lines of arrested growth in the femoral cortex of *Phocanella pumila*. **D**) Non-remodeled part of the cortex of a rib in *Monachus monachus* (polarized light). Histology of primary cortices is comparable to that prevailing in *Phocanella pumila* and *Nanophoca vitulinoides*. **E**) Remodeling in the deep femoral cortex of *Callophoca obscura*. Remodeling is intense, but Havers' canals remain widely open. **F)** Normal (most frequent) bone

architecture in extant and some extinct pinnipeds (here: femur of *Callophoca obscura*). The medullary region is hollow, and contains only a loose spongiosa with thin trabeculae. Scale bars equal 10 mm for A) and F); 1 mm for the inset of F); and 500 μm for B), C), D), and E).

Generalized osteosclerotic condition in the skeleton of *Nanophoca vitulinoides*, a dwarf seal from the Miocene of Belgium

Leonard Dewaele[1,2*], Olivier Lambert[2], Michel Laurin[3], Tim De Kock[4], Stephen Louwye[1],Vivian de Buffrénil[3]

[1]Vakgroep Geologie, Universiteit Gent, Ghent, Belgium

[2]Directorate "Earth and History of Life", Institut Royal des Sciences Naturelles de Belgique, Brussels, Belgium

[3]Département Origines et Evolution, Muséum National d'Histoire Naturelle, Paris, France

[4]PProGRess, Vakgroep Geologie, Universiteit Gent, Ghent, Belgium

*Corresponding author: leonard.dewaele@ugent.be

ABSTRACT

In the fossil record, it has been shown that various clades of secondarily aquatic tetrapods experienced an initial densification of their bones in the early stages of their evolution, and developed spongier and lighter bones only later in their evolution, with the acquisition of more efficient swimming modes. Although the inner bone structure of most secondarily aquatic tetrapods has already been studied, no research hitherto focused on true seals, or Phocidae. However, preliminary observations previously made on a Miocene species, *Nanophoca vitulinoides*, suggested that this taxon showed pronounced specialization of bone structure as compared to other seals. This feature justifies a specific comparative study, which is the purpose of this article. Microanatomical analysis of bones of *N. vitulinoides* ~~bones~~

shows compactness values nearing 100%, which is much higher than in other semi-aquatic mammals, pinnipeds included. Osteohistological analyses show virtually complete remodeling of the medullary territory by Haversian substitution. Extreme bone compactness locally resulted from an imbalance, towards reconstruction, of this process. Cortical regions were less intensely remodeled. In a number of specimens, the cortex shows clear growth marks as seasonal lines of arrested growth. The results suggest that, despite the extreme compactness of long bones of *N. vitulinoides* ~~long bones~~ and the small size of this taxon, the growth rate of the cortex, and that of the bones in general, did not differ strongly from that of other, larger phocids. Extreme skeletal compaction and densification must have increased body density in *Nanophoca*. Consequently, speed, acceleration, and manc~~e~~uverability must have been low, and this taxon was most likely a near-shore bottom-dwelling seal. Consequently, dietary preferences were most likely oriented towards benthic food sources.

Keywords: Neogene, Phocidae, *Nanophoca vitulinoides*, osteohistology, microanatomy, osteosclerosis

INTRODUCTION

Numerous studies have shown the existence of a general relationship between the bone microanatomy and the ecology of tetrapods (e.g., Wall 1983; Stein 1989; Fish and Stein, 1991; Turner 1998; Ricqlès and Buffrénil 2001; Germain and Laurin 2005; Liu et al. 2009; Amson et al. 2014). Several lineages of tetrapods returned to the aquatic environment (e.g., Uhen 2007; Pyenson et al. 2014; and references therein), and data available hitherto suggest that, in such forms, fast and agile swimming amniotes have lighter and spongier bones than slow bottom-dwellers, which generally have heavy and compact (osteosclerotic) bones (Buffrénil et al. 1988, 1989; Webb and Buffrénil 1990; Taylor 2000; Laurin et al. 2011; Houssaye et al. 2013). In slow secondarily aquatic tetrapods, such as sirenians, the heavy bones passively compensate the buoyancy generated by lung volume and help conserve energy during swimming at shallow depth (Domning and Buffrénil 1991; Ricqlès and Buffrénil 2001; Houssaye 2009; see also Taylor 2000). Two mechanisms may increase skeletal mass: thickening of the cortex (pachyostosis), or increased inner compactness of the bones (osteosclerosis); both can also occur simultaneously to form pachyosteosclerosis (e.g., Buffrénil et al. 2010; Houssaye et al. 2016). However, most marine tetrapod clades show an initial evolutionary stage of pachyosteosclerosis prior to the regression of this feature in pace with the development of more efficient swimming modes (Ricqlès 1989).

Formatted: Space After: 0 pt

Although pinnipeds are "marine mammals," they retain some terrestrial mobility, which makes them an interesting model for studying the modification of bone structure in the course of an evolutionary adaptation to marine life. However, bone histology and microanatomy in these animals has received little attention in the past, with few exceptions (e.g., Stein 1989). Indeed, while the osteohistology and microanatomy of other marine mammal clades was specifically studied from an evolutionary point of view, pinnipeds were considered only in the context of broad comparative datasets including extensive taxonomic

Formatted: Indent: First line: 0.5", Space After: 0 pt

sampling, at the scale of Mammalia or marine tetrapods (e.g., Laurin et al. 2011; Dumont et al. 2013; Canoville et al. 2016; Houssaye and Fish~~,~~ 2016; Houssaye et al. 2016). Two contributions specifically dealing with pinnipeds can be mentioned: the preliminary study of the extinct walrus *Valenictus*, showing pachyosteosclerosis in this taxon (Deméré~~,~~ 1994a, b), and the publication on pachyosteosclerosis in the seal *Pachyphoca*, from the middle Miocene of the Ukraine (Eastern Paratethys), by Koretsky and Rahmat (2017). Unfortunately, this study gives only a very brief microanatomical description, without histological, quantitative data or informative figures relevant to this topic. Existing information suggests that bone structure of the pinnipeds differs little from that of most other mammals, ~~since~~ because they display none of the conspicuous specializations of bone inner architecture often encountered in marine tetrapods. Indeed, their appendicular long bones , though not strictly tubular (tubularity sensu stricto is a peculiar adaptation of the diaphyseal region of some limb bones to a terrestrial locomotion), have compact periosteal cortices framing a nearly open medullary cavity with only few slender trabeculae (see e.g., Quemeneur et al. 2013 for the femur; Canoville and Laurin 2010 for the humerus; Germain and Laurin 2005 for the radius; see also Nakajima and Endo 2013). Moreover, the structure of their ribs (comparative data in Canoville et al. 2016) and vertebrae (Dumont et al. 2013; Houssaye et al. 2014) merely reflects the common condition observed in most mammals. This situation may seem paradoxical considering the intermediate habitat and mode of locomotion that characterizes this taxon. Miscellaneous observations nevertheless suggest that the question may be more complex and that in the pinnipeds, and more generally within a given clade and a general habitat (e.g. coastal, pelagic, etc.), bone structure may differ between taxa according to the detailed characteristics of their ecological adaptations (see also on this topic Houssaye et al. 2016). Such is the case, for example, of the bones of *Nanophoca vitulinoides*, a small phocid from the middle Miocene (late Langhian–late Serravallian; ~~c.~~ca. 14.2–11.6 Ma) of Antwerp

Formatted: Font: Not Italic

Formatted: Font: Not Italic

Formatted: Font: Not Italic

region, in Belgium. From broken and fractured specimens, the internal structure of bones in this taxon appears extremely compact and lacks a differentiated medullary cavity. These intriguing preliminary observations call for further analysis.

The aim of the present study is to describe and interpret the osseous structure of *Nanophoca* at both the microanatomical and histological levels, and compare it with similar data from other phocids and more distantly related taxa. *Nanophoca vitulinoides* is the best-known extinct seal from the Neogene (Miocene + Pliocene, 23.03 – 2.58 Ma) of the North Sea Basin, and represents more than half the fossil seal specimens at the Royal Belgian Institute of Natural Sciences, or RBINS (Dewaele et al. 2017a). Its postcranial skeleton is the most complete described hitherto (Fig. 1); however, cranial elements are still lacking. *Nanophoca~~N.~~ vitulinoides* is remarkable in two respects: first, with a total estimated length of approximately one meter, it is one of the smallest known Phocidae (Dewaele et al. 2017a); in this family, only *Batavipusa neerlandica* from the early to middle Tortonian (8–11.5 Ma) of the Netherlands, *Monachopsis* from the early to middle Tortonian (c. 8.4–11.4 Ma) of Moldova, and *Pachyphoca chapskii* from the late Serravallian to early Tortonian (11.2–12.3 Ma) of Ukraine are about as small or smaller, based on humeral length (Koretsky 2001; Koretsky and Peters 2008; Koretsky and Rahmat 2013; Dewaele et al. 2017a). Second, most late Neogene seal taxa found in Belgium also occur in the Lee Creek Mine of the Yorktown Formation, Aurora, North Carolina, USA; *N. vitulinoides* is the only one restricted to Belgian strata (Koretsky and Ray 2008; Dewaele et al. 2017a). Studying bone structure in this taxon, and comparing it with other seals could, on the one hand, bring basic data (still missing hitherto) on bone histology in phocids and, on the other hand, show the nature of the structural specialization of the *Nanophoca* skeleton, which would help in inferring its development and possible functional/ecological significance.

Formatted: Indent: First line: 0.5"

MATERIAL AND METHODS

BIOLOGICAL SAMPLE

This study rests on two main methodological approaches: A) gross (macro-anatomic) morphometry for assessing the presence or absence of pachyostosis in *Nanophoca*; B) microanatomy and histology for describing the inner structure of the bones.

For the morphometric part, 29 humeri from ~~thirteen~~ 13 phocid species and 25 femora from ~~twelve~~ 12 species were measured by one of us (LD), roughly following the procedure used by Buffrénil et al. (2010) for sirenian ribs. Similar data from the literature were also considered (Tables~~Tab.~~ 1, 2).The new morphometric data presented below include three extant taxa: the grey seal *Halichoerus grypus* ~~Fabricius 1791~~ from the cold temperate and subarctic zones of the North Atlantic, the harbor seal *Phoca vitulina* ~~Linnaeus 1758~~ from the temperate to arctic zones of the North Atlantic and North Pacific, and the Baikal seal *Pusa sibirica* ~~(Gmelin 1788)~~ from Lake Baikal. All bones included in the study were from adult or subadult individuals, judging from the degree of epiphyseal fusion in associated long bones (see Storå 2000). The comparative sample of extinct phocids is largely dependent on the published fossil record; this is why some taxa are represented in the dataset by both humeri and femora, while others are only represented by measurements of either humeri or femora.

Because the dataset used for the morphometric study depends on the literature, the dataset employed for the microanatomical and histological studies is necessarily different ~~since~~ as it is based on first-hand analyses of actual specimens available for scanning and/or sectioning. (see ~~Tab.~~Tables 1, 2 versus Table~~Tab.~~ 3). The microanatomical dataset includes measurements on the extant phocine *Phoca vitulina*, the extinct phocids *Nanophoca vitulinoides* ~~(Van Beneden 1871)~~, including the neotype specimen IRSNB M2276, *Callophoca obscura* ~~Van Beneden, 1876~~ from the Tortonian to Zanclean (late Miocene – early Pliocene) of Belgium and North Carolina (LD pers. obs.), *Leptophoca proxima* ~~(Van~~

Formatted: Space After: 0 pt

Formatted: Indent: First line: 0.5", Space After: 0 pt

Formatted: Indent: First line: 0.5"

Formatted: Font: Not Italic

~~Beneden 1877)~~ from the late Aquitanian to late Serravallian (late early Miocene – late middle Miocene) of Belgium and the North American Chesapeake Bay area (Koretsky 2001; Dewaele et al. 2017b), and *Phocanella pumila* from the Tortonian to Zanclean (late Miocene – early Pliocene) of Belgium and North Carolina (LD pers. obs.). Two additional small extinct Neogene phocids from the southern North Sea Bbasin are also considered: *Batavipusa neerlandica* ~~Koretsky and Peters, 2008~~, from the early to middle Tortonian (8 – 11.5 Ma) of the Netherlands, and *Praepusa boeska* ~~Koretsky, Peters and Rahmat, 2015~~, from the late Miocene to late Pliocene of Belgium and the Netherlands (Koretsky and Peters 2008; Koretsky et al. 2015). However, the fossil record of these taxa is extremely scarce and the attribution of the various specimens to each taxon is questionable (e.g., Koretsky and Peters 2008, Koretsky et al. 2015, Dewaele et al. 2017a). Tomographic (CT) data for *B. neerlandica* and *Pr. boeska* are of moderate quality. Distinction between the internal structures of the bone and the sediment infill proved unpractical, and both taxa are only considered qualitatively. Additional data (from either classical thin sections or micro-CT scans) already published by Buffrénil and Schoevaert (1989), Buffénil et al. (2010), Canoville and Laurin (2010), Canoville et al. (2016), and Amson et al. (2014) about the inner structure of long bones in various extant and extinct aquatic mammals (otters, marine sloths, polar bear, and sirenians) were also considered for the comparisons (~~Tab.~~Table 3). In extinct phocid taxa, the osteohistological dataset is limited to three species, in addition to ~~*Nanophoca*~~ *N. vitulinoides*: the monachine *Callophoca obscura*, and the phocines *Leptophoca proxima* and *Phocanella pumila* (~~Tab.~~Table 3). The bone samples for these taxa include femora, humeri, radii, ribs, tibiae, and lumbar vertebrae with both transverse and longitudinal sections. These bones are also known in the fossil record of *N. vitulinoides* and can therefore allow detailed comparisons.

PROCESSING OF THE SPECIMENS

Morphometric features. Buffrénil et al.'s (2010) study focused on the discrimination of pachyostosis sensu stricto (cortical hyperplasy) in ribs and used, among other measurements, rib length. Unfortunately, very few entire ribs are available for fossil seals, and the so-called Cortical Development index used by these authors (the calculation of this index requires measurements of total length, chord, and mean circumference of the ribs) could not be applied to the ribs of ~~*Nanophoca*~~ *N. vitulinoides* ~~ribs~~; conversely, this index, called here "bulkiness index," ~~,~~ or BI, could be used for the humeri and femora in the same conditions as for the other phocid specimens (Fig. 2). For the humerus, two measurements were taken: A) absolute sagittal length of the bone between the most proximal point and most distal point, or BL, and B) transverse width at mid-shaft, or TW. For the femur, three measurements were taken: A) absolute sagittal length (BL), B) transverse width at the narrowest portion of the diaphysis (TW), and C) anteroposterior width of the diaphysis in the same portion (APW), which is perpendicular to transverse width. For the humerus, the calculated ratio is BI = TW/BL. A low BI value indicates a relatively narrow diaphysis, and a high value indicates a relatively thick diaphysis. For the femur, the ratio is BI = [0.5(TW+APW)]/BL. Similarly, a low value of BI indicates a relatively narrow diaphysis, and a high value indicates a relatively thick diaphysis.

Thin section analysis (microanatomy and histology). Thin section preparation was carried out according to the classical procedures used for this kind of preparations (Lamm 2013). All the sections made for this study are now part of the Histothèque (i.e., thin section collection) housed in the Muséum national d'Histoire naturelle in Paris, where they are recorded under various numbers within the Histos database. These sections include transverse mid-diaphyseal and metaphyseal sections, with additional longitudinal sections through the epiphyses. Microscopy was performed using a Zeiss Axioskop microscope, with ordinary and polarized

Formatted: Font: Not Italic

Formatted: Font: Not Italic

Formatted: Font: Not Italic

Formatted: Font: Not Italic

transmitted light at low (x25) to medium (x400) magnifications. All measurements of sectional dimensions were performed with the software ImageJ (National Institute of Health, USA) on microphotographs. For microanatomy, only mid-diaphyseal transverse sections were considered. The terminology used in microanatomical and histological descriptions refers to Francillon-Vieillot et al. (1990) and Prondvai et al. (2014).

X-ray computed microtomography (micro-CT). A part of the biological sample (see ~~Tab.~~Table 4–8) consists of specimens scanned at the Ghent University Centre for X-ray Tomography (www.ugct.ugent.be) with a custom-built microtomograph HECTOR (Masschaele et al. 2013). Depending on the sample, the tube was operated at 140 to 160 kV and 40 to 45 W. A 1 mm Al filter was applied to reduce beam hardening, which was then further filtered during the reconstruction process. The reconstruction was performed with OCTOPUS RECONSTRUCTION (XRE Belgium). Resulting images had a voxel size of approximately 30 µm, 46 µm, or 84 µm, depending on the magnification (see ~~Tab.~~Table 4–8).

Cross-section analysis using *BONE PROFILER*—All cross-sections (be they material thin sections or virtual micro-CT Scan sections) were analyzed using BONE PROFILER Version 4.5.8 (Girondot and Laurin 2003). BONE PROFILER is a freeware dedicated to the analysis of bone compactness in sections, i.e., the area actually occupied by mineralized bone tissue divided by total sectional area, and designed to calculate relevant parameters describing the compactness profile. To do so, the entire cross-section is divided in 3060 cells created by the intersection of 60 sectors (360°/60 = 6° per sector) and 51 concentric rings parallel to the section outline (Laurin et al.~~,~~ 2004: fig. 3). Compactness distribution and variation from the ontogenetic center of the sections to cortical surface are presented as the ‘compactness profile’. The compactness profile is characterized by four parameters S, P, Min, and Max. S is the reciprocal of the slope at the curve inflection point, and it is proportional to the relative width of the transition zone between the medulla and the cortical regions. P is the position of

the curve inflection point on the x-axis, and it represents the position of the transition area between the medulla and the cortical region. Min and Max are the minimum and maximum asymptotes, respectively, representing the minimum and maximum values of bone compactness in a section. Other parameters can be calculated using BONE PROFILER (Laurin et al. 2004; Quemeneur et al. 2013), but these were not used in the current study. More elaborate analyses with BONE PROFILER including parameters Minrad, Maxrad, Srad, and Prad are not used in the present study, but are provided as Supporting Information (Appendix 1). These are similar to the abovementioned parameters, but are the radial versions, i.e., the average values of the measurements for the 60 sectors. Hence, standard deviations (SD) are also calculated for these values.

PHYLOGENETIC FRAMEWORK

For the phylogenetic position of ~~*Nanophoca*~~ *N. vitulinoides* in the current study, we follow the phylogenetic analysis by Dewaele et al. (2017a), which is, to date, the only published analysis including this species (Fig. 3). According to Dewaele et al. (2017a: fig. 25; Fig 3. in the current study), *N. vitulinoides* is a relatively late-branching stem-phocine; it is the closest known relative of crown Phocinae. Evidently, it should be noted that this phylogenetic position is only relative to the other Operational Taxonomic Units (OTUs) included in this analysis. The phylogenetic relationships of other small phocids, such as *Batavipusa neerlandica*, *Pontophoca sarmatica*, *Praepusa boeska*, or –most notably– *Monachopsis pontica* has been studied by Koretsky (2001) and Koretsky and Rahmat (2013). However, their fossil record is too scarce (e.g., *B. neerlandica* is only known from one isolated humerus, an isolated ilium, and an isolated partial femur tentatively assigned to it; *M. pontica* is only known from multiple isolated humeri and femora) to be confident about their phylogenetic position. Not surprisingly, previous phylogenetic analyses including those taxa show little

consensus and confidence on their phylogenetic position (Koretsky 2001; Koretsky and Rahmat 2013). For the phylogeny of other, extant Pinnipedia included in this study, we refer to Higdon et al. (2007). The extinct *Callophoca obscura*, *Leptophoca proxima*, and *Phocanella pumila* have all been considered in phylogenetic analyses. There is little consensus about the phylogenetic position of the monachine *C. obscura*. Some researchers consider *C. obscura* most closely related to the extant elephant seal *Mirounga*, while others group it with the late Pliocene *Pliophoca etrusca* from Italy, or consider it as a stem monachine (compare Muizon 1981; Koretsky and Ray 2008; Koretsky and Rahmat 2013; Amson and Muizon 2014; Berta et al. 2015). Therefore, we consider *C. obscura* a monachine phocid, but we do not make genus-level phylogenetic inferences for this taxon. The phylogenetic position of *L. proxima* (or as *Leptophoca lenis*) has been first analyzed by Koretsky (2001) and Koretsky and Rahmat (2013), but without consensus. Cozzuol (2001) interpreted *L. lenis* as an early-branching phocine, while Berta et al. (2015) suggested that the taxon was an early-branching stem monachine. However, the latter expressed doubt over their phylogenetic results for *Leptophoca*. More recent studies by Dewaele et al. (2017a, b) placed *L. proxima* as a stem phocine with strong statistical support. The phylogenetic position of *P. pumila* has only been analyzed once, by Koretsky and Rahmat (2013). However, they neither present the character matrix nor a list of synapomorphies to support their analysis. In addition, this analysis differs on key nodes from other, widely-accepted phylogenetic analyses (e.g. Bininda-Emonds and Russell 1996), inhibiting us of considering this analysis to elucidate the phylogenetic position of *Phocanella* ~~*P.*~~ *pumila.* The phylogenetic position of the latter remains unclear, pending future discoveries of more complete material and new analyses. This information is provided only as contextual information; we did not perform any phylogeny-informed statistical tests in this study given that the focus is on only three early pinniped taxa.

INSTITUTIONAL ABBREVIATIONS

IRSNB/RBINS, Institut royal des Sciences naturelles de Belgique, Brussels, Belgium; **MAB**, Oertijdmuseum Groene Poort, Boxtel, the Netherlands; **MNHN**, Muséum national d'Histoire naturelle, Paris, France; **MSC**, Smithsonian Institution Museum Support Center, Suitland, Maryland, USA; **USNM**, National Museum of Natural History, Washington, DC, USA.

DATA AVAILABILITY

All data used in this study is presented within the main text. Additional results from the radial analysis with BONE PROFILER are provided as Supporting Information (Appendix 1). Thin sections that are used in this study are housed at the MNHN. Specimens that have been CT-scanned are housed at the IRSNB. Specimens are available for consultation and access should be requested at the respective institutions.

RESULTS

MORPHOMETRIC DATA

Although no complete ribs of ~~*Nanophoca*~~ *N. vitulinoides* are preserved to perform morphometric measurements, the sub-circular morphology of the cross-section from these bones differs from that of related taxa (Fig. 5A versus Fig. 5B, C). For a similar rib length (a parameter that unfortunately ~~lacks~~is lacking), it could possibly be indicative of some incipient tendency toward pachyostosis. Morphometric results for the humerus and femur are listed as ~~Tab.~~Tables 1 and 2. The diaphysis of the humerus of *Nanophoca* ~~humerus~~ is relatively slender, as compared to other extant and extinct Phocidae. BI ratio for the humerus of two specimens of *N. vitulinoides* is 0.121 and 0.135, which is at the lower half of the range of the

Formatted: Space After: 0 pt

29 calculated values (0.109 – 0.210) (~~Tab.~~Table 1). Apart from the extinct *Batavipusa neerlandica* (0.182), *Monachopsis pontica* (0.169), and *Pachyphoca ukrainica* (0.210), extinct Phocidae in our sample tend to have a relatively slender humeral diaphysis, as compared to extant forms. This rules out the eventual occurrence of pachyostosis in the humerus of *N. vitulinoides*.

Bulkiness index values indicate that the femoral diaphysis of ~~*Nanophoca*~~ *N. vitulinoides* (0.200, 0.207, and 0.208) and other extinct Phocidae (0.173 – 0.240) is overall relatively thick, as compared to extant Phocidae (0.158 – 0.187) (~~Tab.~~Table 2). This contrasts with the measurements of the humeri. As for the humerus, the taxon with the bulkiest femur is *Pachyphoca*, returning a value of 0.240 for *Pachyphoca~~P.~~ ukrainica*, based on the average of three specimens presented by Koretsky and Rahmat (2013), and a value of 0.229 for one specimen of *Pachyphoca chapskii*. Given that the femora of the extinct taxa in our sample have consistently higher values, i.e., suggestive of pachyostosis, it remains difficult to find conclusive evidence on the presence or absence of pachyostosis in the femur of *N. vitulinoides* in comparison to contemporaneous taxa.

Formatted: Indent: First line: 0.5"

MICROANATOMY

Vertebrae

[Table 4]

[Figure 4]

Bone compactness in the centra of the two lumbar vertebrae of ~~*Nanophoca*~~ *N. vitulinoides*, ranges from 93.8% for the adult, to 63.6% for the juvenile. (~~Tab.~~Table 4; Fig. 4). These values are much higher than those observed in the other pinnipeds and semi-aquatic mammals included in this study (~~Tab.~~Table 4): compactness values indeed range for these taxa from

22.3% (hooded seal, *Cystophora cristata*) to 44.3% (sea otter, *Enhydra lutris*). Apart from *N. vitulinoides*, the compactness values for the vertebrae of the Phocinae (22.3% for *C. cristata* and 29.3% for the harp seal, *Pagophilus groenlandicus*) are lower than the values calculated for Monachinae and Otariidae.

Rib

[Table 5]

[Figure 5]

With an overall compactness of 99.8%, the rib of ~~*Nanophoca*~~ *N. vitulinoides* is almost completely ossified, and much more compact than that of other semi-aquatic mammals (~~Tab.~~Table 5; Fig. 5). The Cape fur seal *Arctocephalus pusillus* and the Californian sea lion *Zalophus californianus* have the second and third most compact ribs in the biological sample, with compactnesses of 78.4% and 78.2%, respectively. While there is no differentiated medullary cavity in the rib of *N. vitulinoides* (Fig. 5A), the medullary cavity in the ribs of other taxa in the biological sample is occupied by loose spongiosa and surrounded by a compact cortex (Fig. 5B, C).

Humerus

[Table 6]

[Figure 6]

[Figure 7]

With an overall compactness of 99.7% for one specimen and 99.9% for the other, the humerus of ~~*Nanophoca*~~ *N. vitulinoides* is almost completely solid (~~Tab.~~Table 6; Fig. 6). Only the humerus of *Phocanella pumil~~l~~a* has a comparably (though somewhat lesser) high compactness (95.9%); but unlike *Phocanella~~P.~~ pumil~~l~~a*, there is no discernable medullary cavity in the two specimens of *N. vitulinoides* (Fig. 6A, B versus Fig. 6C). Given the poor density differentiation between the mineralized bone tissue and the sediment infill in *Batavipusa neerlandica* and *Praepusa boeska*, quantitative microanatomical analysis using BONE PROFILER was precluded. A qualitative analysis reveals the presence of a porous medullary cavity framed by compact cortices in both taxa (Fig. 7A, B).

Femur

[Table 7]

[Figure 8]

Compactness values for the two femora of ~~*Nanophoca*~~ *N. vitulinoides*, i.e., 97.1% and 99.4%, are much higher than those of all extant and most extinct semi-aquatic taxa considered in this study (~~Tab.~~Table 7; Fig. 8A, B versus Fig. 8C, D, F-I). Only the femur of *Phocanella pumila* shows a compactness approaching the condition in *N. vitulinoides* (~~Tab.~~Table 7; Fig. 8A, B versus Fig. 8E).

Other bones

[Table 8]

[Figure 9]

Other long bones of *N~~anophoc~~.~~a~~ vitulinoides*, i.e., the radius and the tibia, have been studied as well and show very high compactness ratios, similar to the condition observed in the rib, humerus, and femur (~~Tab.~~ Table 8; Fig. 9). There is no discernable medullary cavity present, unlike, for example, the extant *Phoca vitulina* (~~Tab.~~Table 8; Fig. 9A, C versus Fig. 9B, D).

BONE HISTOLOGY

In cross and sagittal sections, all bones of ~~*Nanophoca*~~ *N. vitulinoides* ~~bones~~ examined in this study share the same basic histological features (in addition to their microanatomical similarity), with only few differences most likely related to ontogenetic age. In most of the bones, except one of the radii (Histos 2142) and one of the vertebral centra (Histos 2150), Haversian remodeling is mild in the cortex; the characteristics of primary periosteal deposits thus remain visible (Fig.10A, B). They consist in layers of woven-parallel tissue (according to Prondvai et al.'s 2014 terminology) with longitudinal primary osteons, separated by very birefringent annuli made of parallel-fibered or lamellar bone (Fig.10C). Short Sharpey's fibers (60-80 µm long) colonize the basal parts of the woven-parallel layers (Fig.10C). The annuli are wide (up to 180 µm) in the cortical depth, and thinner (some 60-70 µm) towards the cortical periphery. The bone displaying the greatest number of visible growth marks is the humerus, with five sharp annuli (Fig.10A) associated with lines of arrested growth. Of course, in this specimen, several annuli were erased by remodeling in the depth of the cortex. In the long bones where they occur, the annuli tend to be more tightly spaced towards the cortical periphery, but they nevertheless maintain a significant spacing, e.g. 320 µm between the fourth and fifth annuli in the humerus (Fig.10A). In the femur and the humerus, in which cortical structure is perfectly preserved up to the outer margin of the diaphysis, the last growth mark is an annulus (Fig.10A). The nature of the last growth mark is less evident in the other long bones, due to the impregnation of superficial layers by a dark substance during

Formatted: Space After: 0 pt

Formatted: Font: Not Italic

Formatted: Font: Not Italic

Formatted: Font: Not Italic

Formatted: Font: Not Italic

Formatted: Font: Not Italic

Formatted: Font: Not Italic

fossilization. However, there is no clear indication of the presence of an external fundamental system (EFS) that could have shown that the growth of the bones, at least in diameter, had dropped to a very low level and that skeletal growth was ending by the time the animals died. In the two specimens (radius Histos 2142 and centrum of the vertebra Histos 2150) where the structure of primary periosteal deposits is no longer visible, bone cortices are entirely occupied by a particularly dense Haversian tissue (Fig.10E) that extends continuously towards the central (medullary) region of the bones.

The medullary territory of all bones is entirely compact, with the exception of some scarce, vaguely circular cavities measuring generally less than 300-400 µm in diameter. The dense Haversian tissue occupying this region (Fig.10F) has three basic characteristics: A) Its secondary osteons are roughly longitudinal, but their orientation can be locally variable; moreover, their central canals (Havers' canals) develop numerous transversal anastomoses (Wolkman's canals), suggesting high BMU (Bone Multicellular Units, i.e., the populations of cells responsible for the formation of secondary osteons; Frost 1969) activation frequency, i.e., parameter *Ac.f* in classical histomorphometric nomenclature (cf. Dempster 2013). B) Most of the secondary osteons show evidence of particularly intense remodeling (Fig.10G, H), with the presence of two~~2~~ to four~~4~~ cycles of resorption and reconstruction centered on the Haversian canal. By this process, several generations of osteons with decreasing diameters were formed inside ontogenetically older secondary osteons. This situation is general in ~~*Nanophoca*~~ *N. vitulinoides*; it occurs in all secondary bone deposits, be they localized in the medullary or cortical regions of the bones. C) Such a process resulted in extreme thinning of the lumens of Havers' canals, which are very seldom wider than 10 µm, and most often less than 5 µm. Havers' canals in numerous osteons are so drastically reduced that they seem to be completely occluded (Fig.10H).

Formatted: Indent: First line: 0.5", Space After: 0 pt

This special Haversian tissue, characteristic of the medullary (and occasionally cortical) region, can be observed in all parts of the long bones: in the mid-diaphyseal region as well as in metaphyses, from which it extends continuously into the whole epiphyseal regions, up to the proximal and distal extremities of the bones, where it merges into the thin layers of calcified cartilage covering articular surfaces (Fig.11A-C). None of the longitudinal sections (which were made in all specimens) reveal the presence of a functional growth plate or a lack of fusion of primary and secondary centers of ossification (Fig.11A, B). We thus conclude that the growth in length of long bone specimens in our sample was complete.

With the exception of the vertebral centra (considered below), there is only one variation to this general pattern. In the radius Histos 2174, the medullary territory (51% of the total area in cross section) is occupied by a compacted spongiosa whose former trabeculae, still clearly distinguishable, show numerous reversion lines (created by a strong resorption – reconstruction activity), but no secondary osteons (Fig.11D, E). Conversely, inter-trabecular spaces are entirely filled by endosteal lamellar tissue showing evidence of intense Haversian substitution. This process resulted in several generations of concentric secondary osteons (Fig.10E). Such a detailed topographical difference in remodeling patterns, through which the initial architecture of the medullary spongiosa was preserved, is unknown in all other specimens studied here.

The femur, humerus, and ulna examined here display a strong off-centering of growth (Fig.11F) that provoked, on the one hand, the development of a thick primary cortex on the lateral side of these bones and, on the other hand, the superficial outcropping of remodeled medullary regions, due to extensive resorption on their medial side. The result of this double process was a lateral drift of growth. Moreover, several of the long bones show, on cross sections, variably oriented fissures 120 to 200 µm long (Fig.11E). These cracks are observed only in deep cortical regions and in the medullary territory; they never reach the peripheral

margins of the bones. Their possible nature and the causes of their occurrence are discussed below (see Discussion).

The trabeculae occupying the centrum of the largest vertebra (specimen IRSNB prov. 16), as well as the lamellar bone that partly fills inter-trabecular spaces, have a histological structure similar to that observed in the medullary region of long bones: they are formed of intensively-remodeled tissue (Fig.11G). Remodeling is less intensive in the smaller vertebra; therefore, the growth pattern of this bone remains legible. It was a normal endochondral osteogenesis, with complete resorption of epiphyseal calcified cartilages~~,~~ and active remodeling of primary trabeculae, at a small distance away from the zone of cartilage hypertrophy. In general, none of the bones examined in this study displays the slightest residue of calcified cartilage outside a narrow band (200 to 400 µm) localized just under the epiphyseal surface (Fig.11C). The largest centrum retains only a thin layer of primary periosteal bone tissue spared by remodeling on the walls of the neural arch (Fig.11I). Six tightly spaced growth marks (mean spacing < 50 µm) forming an external fundamental system are visible in this layer: the bone was thus reaching the end of its growth.

Comparative data

The vertebrae of pinniped taxa other than ~~*Nanophoca*~~ *N. vitulinoides* show relatively little microanatomical or histological differences from other mammals. Moreover, the diaphyses of their long bones, though presenting some few, slender medullary trabeculae, do not display typical microanatomical or histological peculiarities (very high or very low global compactness, lack of a medullary cavity, cortical hyperplasy, diaphyseal persistence of calcified cartilage, etc.) likely to distinguish these taxa unambiguously from other mammals (see also the Introduction). The only exception is the small development of the medullary cavity in the femur of *Phocanella pumila* (Fig.12A). When primary periosteal cortices in long

Formatted: Indent: First line: 0.5"

bones, are partly spared by Haversian substitution (as observed in the femur of ~~*P.*~~*Phocanella pumila* and a rib from *Monachus monachus*), they are composed, like those of *N. vitulinoides*, of a woven-parallel complex containing longitudinal primary osteons, annuli and lines of arrested growth (Fig.12B–D). Otherwise, remodeling is intense and spreads to the totality of bone cortices; however, extreme remodeling resulting in the closure of vascular canals does not occur (Fig.12D, E). In all taxa, except *Phocanella*~~*P.*~~ *pumila*, the thin trabeculae occurring in the medullary cavity are made of remodeled lamellar bone, framing wide inter-trabecular spaces (Fig.12E, F). In *Phocanella*~~.~~ *pumila*, medullary trabeculae are also intensely remodeled, but they are much thicker than in other pinnipeds (compare Fig.12A and 12F). As a consequence, they divide the medullary cavity into small lacunae and strongly increase its compactness (on cross sections).

DISCUSSION

MORPHOMETRICS AND MICROANATOMY

Based on the sample of specimens used for the morphometric analysis, the diaphysis of the humerus of extinct Phocidae is generally more slender than in extant specimens, apart from the late Miocene *Pachyphoca ukrainica*, which shows pachyostotic 'swelling' of the humeral diaphysis. However, the femoral diaphysis of the sampled extinct Phocidae is generally a little thicker than that of extant Phocidae. The femoral diaphysis in *Pachyphoca* and, to a lesser extent, *N. vitulinoides* is also relatively bulky, without appearing swollen. Thus, we detected no clear pachyostotic trend in our sample.

Despite the absence of pachyostosis in the humerus and the femur of ~~*Nanophoca*~~ *N. vitulinoides*, osteosclerosis appears to be extreme in this taxon, and occurs also in *Phocanella pumila*. For the studied specimens of *N. vitulinoides*, namely one rib, two humeri, one radius,

Formatted: Font: Not Italic

Formatted: Space After: 0 pt

Formatted: Indent: First line: 0.5", Space After: 0 pt

two femora, and one tibia, actual bone compactness (0.971 – 0.999) approaches 1 (100%). Similarly, although slightly lower (0.959 – 0.977), compactness values in the humerus and femur of *P. hocanella pumila* are much above the common situation of other specimens. The relatively high compactness of the lumbar vertebrae of both the juvenile and the adult specimens of *N. vitulinoides* shows that osteosclerosis in the taxon extends to the entire postcranial skeleton. Moreover, differences in compactness between the adult (93.8%) and the juvenile (63.6%) suggest that the increase in compactness is an ongoing process during the growth of the animal. In addition to that, it is noteworthy that the compactness observed in the vertebrae of Phocinae (excluding *N. vitulinoides*) is noticeably lower than the compactness observed in Monachinae and Otariidae. This may hypothetically be related to differences in locomotion (Pierce et al. 2011; Kühn and Prey 2012) or differences in maternal care (Boness and Bowen 1996). However, this is beyond the scope of the current study and should be treated in a future studies.

Considering the entire set of microanatomical observations made on the bones of *Nanophoca* bones, it seems obvious that osteosclerosis touches most (and perhaps all) of the appendicular elements. This contrasts with the situation prevailing in the sirenian *Dugong dugon*, in which there is a gradual decrease in compactness from the more proximal portion of the forelimb towards its distal portion (Buffrénil and Schoevaert 1989). A similar condition has been described in the marine sloth *Thalassocnus* (Amson et al. 2014) in which the radius is noticeably less compact than the humerus.

GROWTH PATTERN OF THE BONES AND MECHANISM OF THEIR COMPACTION

***Growth pattern of bone cortices*.** According to the experimental data presently available about the relationship between the structure of periosteal bone deposits and their accretion rate, the so-called Amprino's (1947) rule, the growth in thickness of *Nanophoca N.*

Formatted: Space After: 0 pt

vitulinoides bone cortices proceeded at relatively moderate speed. The woven-parallel bone with longitudinal primary osteons that compose them is generally associated, in extant mammals and birds, ~~to~~ with apposition rates ranging between 4 and 8 µm per day (Castanet et al. 1996, 2000). All other forms of woven-parallel bone, i.e., reticular, plexiform, laminar, or radial tissues, correspond to higher growth rates. This question is nevertheless complex; it remains incompletely settled and contrasting results have been presented by Margerie et al. (2002). To our knowledge, there are neither experimental data on bone apposition rate in pinnipeds~~,~~ nor precise histological descriptions of the structure of periosteal cortices in their bones. The comparative observations made in the present study suggest that, despite its modest size, *N. vitulinoides* did not grow at a rate very different from that of larger species.

The growth of primary bone cortices was cyclic in *Nanophoca* with, as in most mammals for which accurate data exist, the yearly alternation of a fast growth phase (accretion of the woven-parallel layers) when food was abundant, and a slow growth phase, corresponding to unfavorable environmental conditions, during which the annuli were formed. In one specimen at least, the humerus Histos 2139, a total arrest of growth occurred each year, resulting in the formation of lines of arrested growth. The comparative sample reveals that *Nanophoca* did not differ from other pinnipeds for these characteristics. More generally, several recent studies (e.g., Castanet 2006; Köhler et al. 2012) show that the presence of growth cycles of annual periodicity (supposed so in fossils) is a general, plesiomorphic feature in vertebrates (it primarily depends on endogenous rhythms), whatever their phylogenetic position, physiological characteristics, or ecological adaptations, as shown by the occurrence of cyclic growth marks in Silurian placoderms (Giles et al. 2013).

The ontogenetic transformation of primary cortices in *Nanophoca* was basically due to intense Haversian remodeling, a situation also observed in other pinnipeds and otherwise common to most mammals. Cortical remodeling presented some delay as compared to that

Formatted: Indent: First line: 0.5", Space After: 0 pt

Formatted: Font: Not Italic

occurring in the medullary region, which explains that non-remodeled primary cortices co-existed with a densely remodeled medulla in most bones.

***Mechanism of medullary compaction*.** Our histological observations suggest that the fundamental process of endochondral osteogenesis was not significantly modified in ~~*Nanophoca*~~ *N. vitulinoides*. Contrary to the situation prevailing in numerous secondarily aquatic tetrapods (reviewed in e.g., Ricqlès and Buffrénil 2001), the calcified cartilage formed in growth plates was entirely eroded and the formation of primary trabeculae was apparently normal. Compaction of the medullary region basically resulted from the mode of remodeling of these trabeculae. The erosion and reconstruction process involved in bone remodeling is generally balanced, the amount of bone resorbed by osteoclasts being approximately compensated by an equivalent amount of reconstructive (secondary) osseous tissue (Parfitt 1981, 1982). In *N. vitulinoides*, imbalance visibly existed in favor of the reconstructive stage: the amount of secondary deposits produced by endosteal osteoblasts exceeded the volume of tissue previously eroded by the osteoclasts. The detailed histogenetical mechanism controlling this peculiar functioning of the osteoblasts is, of course, beyond reach of this study. The regulation of osteoblast activity during Haversian remodeling is a complex, still poorly elucidated question (e.g., Martin 2000; Burr and Allen 2014). It nevertheless remains that the cause responsible for osteosclerosis in *N. vitulinoides* obviously resided in a modification of this regulation mechanism. Occlusion of intra-osseous cavities due to this process was extremely pronounced because several, successive peri-vascular remodeling cycles occurred locally (over-remodeling), up to a quasi-total closure of vascular canals. Vascular canals reduced to diameters less than 10 µm, and a fortiori the thinner capillaries housed in them, are unlikely to have remained functional, ~~since~~ as the mean diameter of mammalian erythrocytes (not to speak of other blood cells) is 7 to 8 µm (e.g., Fawcett and Jensh 1997). In humans, the lumen of the Haversian canal of a normal, fully developed, secondary osteon is 20 – 50 µm in

Formatted: Space After: 0 pt

Formatted: Font: Not Italic

diameter (Jaworski 1993; Fiala 1980; see also Polig and Jee 1990). For example, in the ribs of male humans aged 20 – 25 years, mean Haversian canal perimeter (variable *Hc.Pm* in classical nomenclature) is 0.165 mm, and Haversian canal area (*Hc.Ar*) is 0.002 mm² (Qiu et al. 2003); these parameters indeed correspond to a diameter of some 50 µm.

The compaction process described here in ~~*Nanophoca*~~ *N. vitulinoides* is known also from other marine tetrapods; it was observed in the femur and humerus of *Clausiosaurus germaini* (Buffrénil and Mazin~~,~~ 1989), the rostral region of the skull of several ziphiid whales (Buffrénil and Casinos~~,~~ 1995; Zylberberg et al. 1998; Lambert et al. 2011; Dumont et al. 2016), and the five species of the xenarthran genus *Thalassocnus* (Amson et al. 2014). Conversely, it was not observed in other pinnipeds, albeit our data suggest that *Phocanella pumila* might have displayed a similar specialization, though far less pronounced than in *N. vitulinoides*.

Remark on the timing of somatic growth in Nanophoca vitulinoides—The results of the present study reveal a paradoxical situation in which two conditions, which can be considered contradictory, coexist. A) In several long bones (humerus, femur, ulna), primary periosteal cortices display rather broadly spaced annuli up to bone periphery and, although the outer margins of the bones are bordered by an annulus, there is no clearly characterized external fundamental system. This situation should normally indicate that, on the one hand, the growth of the bones was still actively progressing when the animals died and that, on the other hand, death occurred during the unfavorable season, when annuli were formed. B) However, in all long bones, growth plates are entirely erased by remodeling; therefore, no further growth in length could occur. A possible explanation for these contrasted data is that the growth in diameter of the bones remained active by the time their growth in length was already stopped. This hypothesis is not convincing because such a process would have created a great diversity in the shape of the bones of ~~*Nanophoca*~~ *N. vitulinoides* ~~bones~~, a situation that does not exist

Formatted: Indent: First line: 0.5"

Formatted: Space After: 0 pt

Formatted: Font: Not Italic

Formatted: Font: Not Italic

Formatted: Font: Not Italic

(see Dewaele et al. 2017a). Another hypothesis is to consider that growth ceased abruptly, with both the destruction of growth plates and a sudden stop in periosteal apposition, when a certain size was reached. In this situation, peripheral annuli should be viewed as functional equivalents of EFS. For each individual, this double process of growth cessation is likely to have occurred during the unfavorable season, when annuli were deposited. Depending on the age when this process normally occurred (this age cannot be determined because early growth marks were erased by remodeling) it could explain the small size of *N. vitulinoides*. This issue requires the examination of a larger sample of *Nanophoca* bones and cannot be settled for the present. Moreover, slight local differences in the timing of the growth dynamics are not to be excluded, as suggested by the occurrence of an EFS in the largest vertebra.

Possible consequence of compaction on bone biomechanics—The unusual frequency of the short fissures observed in several specimens of ~~*Nanophoca*~~ *N. vitulinoides* ~~specimens~~ cannot be readily explained by the effect of taphonomic constraints ~~since~~ because *N. vitulinoides* fossils do not show traces of crushing or deformation (although they can be broken). Moreover, the cracks are restricted to the central region of the bones, and never extend towards their peripheral margins; such extensions should nevertheless have occurred if an external constraint had been exerted on the bones. The aspect of the fissures observed here is strongly reminiscent of the fatigue micro-fractures, as they are classically described and illustrated in the skeleton of *Homo* (e.g., Schaffer et al. 1995; Lee et al. 2003; Landrigan et al. 2011) and numerous domestic and wild animals ~~like~~such as, e.g., dogs (Burr et al. 1985), rats (Voide et al. 2011), sheep (Mohsin et al. 2006), etc. In the absence of another plausible interpretation, the fissures observed in bones of *N. vitulinoides* ~~bones~~ are considered as genuine fatigue micro-fractures. The accumulation and coalescence of these small lesions, caused by long-lasting, repetitive mechanical stress, constitute the major processes responsible for the degradation of bone mechanical properties (Danova et al. 2003). Their

Formatted: Font: Not Italic

relative abundance in *N. vitulinoides* could have been indirectly induced by the compaction of bone tissue that occurred in this taxon. It is indeed possible that the pronounced reduction, or even the total occlusion, of the lumen of vascular canals by excessive secondary deposits resulted in a local cessation of Haversian remodeling, ~~since~~ as the precursors of the osteoclasts (monocytes), cells of the blood lineage, arrive in situ via vascular networks (syntheses in Marks and Popoff 1988; Charles and Aliprantis 2014; see also Lafage-Proust et al. 2015). It is therefore likely that the extreme and imbalanced remodeling in bones of *N. vitulinoides* ~~bones~~ was a self-blocking process, a hypothesis that could additionally explain why open resorption cavities are so scarce in the bones of *N. vitulinoides* ~~bones~~ observed in this study. One of the functions most commonly attributed to remodeling, be it of the Haversian type or not, is precisely to operate a local replacement of the osseous tissue damaged by the proliferation of fatigue micro-fractures (Burr 1993; Burr et al. 1995; Lieberman et al. 2003). In *N. vitulinoides*, this process might have been hampered by local restriction to blood supply. If a strong increase in bone compactness in this taxon was positively selected for the functional benefit that it could provide, the "price to pay" was a decrease in the mechanical resistance of the bones. This result is maladaptive because a total closure of vascular canals actually provided negligible gain in mass (which was not the case for the closure of larger bone cavities). This situation suggests that such an extreme degree of bone compaction might have resulted from developmental constraints that could have prevented compaction of the skeleton to be optimal throughout. Several, relatively common, disorders of the skeleton likely to have a genetic origin provoke increased and imbalanced remodeling, e.g., Paget's disease, osseous mastocytosis, etc. (Ralston 2008; Michou and Brown 2011; see also Evans et al. ~~,~~ 1983), and can produce symptoms reminiscent of, though not strictly identical to, the situation observed in *N. vitulinoides*. It seems possible that the peculiarities of bone structure in *Nanophoca* ~~.~~ could have initially resulted from a process akin

Formatted: Font: Not Italic

to such pathological processes. Pending an actual genetic causality, the latter could have been selected and subsequently increased during evolution for its adaptive consequences, if the resulting general compactness increase of the skeleton of *N. vitulinoides* ~~skeleton~~ was advantageous. Such a process might have occurred also in other aquatic tetrapods showing the same bone structural peculiarities as *Nanophoca*. Future studies should address this issue and point out the frequency of this putative process.

FUNCTIONAL CONSIDERATIONS

One of the obvious consequences of the osteosclerotic-like process described here was to increase the overall mass of the ~~*Nanophoca*~~ *N. vitulinoides* skeleton. In the absence of pachyostosis, this increase was relatively moderate, as compared to the extreme situations encountered in the Sirenia (Kaiser 1974; Buffrénil et al. 2010) or the marine squamates (the so-called limbed snakes) from the Cenomanian of Europe and North Africa (Buffrénil and Rage 1993; Houssaye, 2013). Nevertheless, it necessarily provoked an increase in the density and inertia of the body, and proportionally reduced its buoyancy and maneuverability in the water as well as on land (Taylor 2009; Domning and Buffrénil 1991). It is thus likely that, as compared to the other pinnipeds devoid of osteosclerosis, (e.g., *Arctocephalus*, *Phocarctos*, and *Zalophus*: Godfrey 1985; Beentjes 1990; Fish et al. 2003), the locomotor capabilities of *N. vitulinoides* were characterized by a lower swimming speed and a poor aptitude for steep accelerations or sudden direction changes (maneuverability). Until now, no skull of this taxon has been discovered; thus, its feeding strategy and food preferences cannot be determined. The extreme compactness of postcranial elements strongly suggests that *N. vitulinoides* was not adapted to the capture of fast and mobile prey in open seas. Rather, it must have fed upon benthic or fixed animals in coastal shallow waters. One well-known extant benthic feeder is the walrus, *Odobenus rosmarus* (e.g., Fay 1982; Gjertz and Wiig 1992; Dehn et al. 2006).

Formatted: Font: Not Italic

However, bone densification in the walrus is limited to pachyostosis in certain cranial regions (Kaiser 1967), while the postcranial skeleton is largely untouched by pachyosteosclerosis (e.g., Canoville et al. 2016: fig. 7O). In addition, Deméré (1994a, b) showed that the skeleton of the extinct walrus *Valenictus* was pachyosteosclerotic and that this taxon most likely had an even more pronounced benthic foraging lifestyle than the extant *Odobenus*. Moreover, the interpretation of *N. vitulinoides* as a benthic feeder closely fits the conclusions drawn by Dewaele et al. (2017a) from extensive anatomical clues and reconstructions of the appendicular musculature: pectoral and pelvic girdles were used by *N. vitulinoides* in a different way than in other Phocidae, "presumably for grasping and crawling on the substrate." For instance, the strong development of the greater tubercle of the humerus, the weak development of the lesser tubercle of the latter, and the strong development of the olecranon process on the ulna point toward powerful extension and abduction of the foreflippers, contrasting with the conditions displayed by extant phocids. In this functional context, even a limited buoyancy decrease (as compared to other taxa such as the sirenians or some Cenomanian aquatic squamates; the bone ballast of *Nanophoca* is moderate) must have facilitated a passive control, with little energy expense, of body position and trim in the water column. The same may apply to the contemporaneous late Miocene–early Pliocene *Phocanella pumila*, given the similar trend toward density increase in the humerus and femur. Hence, a comparable feeding pattern might have existed in these two taxa. Unfortunately, no dental remains are known from *Pp. hocanella pumila*, which precludes elucidating the feeding habits of this species and, indirectly, that of *N. vitulinoides*. Both are nevertheless found in the same geological context, and might therefore have shared close ecological adaptations. Although our analysis includes only two specimens of the latter taxon (the extent of bone compaction in the rest of the skeleton cannot be assessed), a similar ecology to that of *N. vitulinoides* can be expected. The presence of a (thick) spongy trabecular network in the

medullary cavity of *Batavipusa neerlandica* and *Praepusa boeska*, two small, roughly contemporaneous (late Miocene–early Pliocene) species from the southern margin of the North Sea Bbasin, shows that the extreme compactness of the long bones of *N. vitulinoides* long bones is not strictly correlated withto the small body size of the taxon.

CONCLUSIONS

Nanophoca vitulinoides from the middle Miocene of the North Sea Basin is the first extinct phocid taxon to undergo a detailed microanatomical and osteohistological description. Its long bones are extremely compact, lacking a differentiated medullary cavity and exhibiting compactness values close to 100%. Apart from the extinct phocine seal *Phocanella pumila*, such structural peculiarities are unknown among pinnipeds. The spine of *Nanophoca* was also touched by this process, which is a unique case among mammals. The high compactness is not observed in any other semi-aquatic mammal. The high compactness observed in the skeleton of *Nanophoca* skeleton visibly resulted from an imbalanced remodeling process located in the medullary region. Positively selected during evolution, this process might have been rooted in an initial genetic condition akin to one form of the so-called "metabolic bone diseases." It increased body density, thus reducing buoyancy and facilitating long-lasting underwater stays. Conversely, it limited speed and maneuverability. Although more complete fossils, and especially cranial remains, are needed to draw definite conclusions on *Nanophoca* ecology, the results of this study strongly suggest that *N. vitulinoides* was a bottom-dwelling seal, living in shallow waters close to the shore in the Miocene North Sea Basin, and feeding on benthic prey.

ACKNOWLEDGEMENTS

The research presented in this study is in partial fulfillment of the PhD research of LD, conducted at Ghent University, Ghent, Belgium, and in collaboration with the Royal Belgian Institute of Natural Sciences, Brussels, Belgium. This PhD research is funded by the Research Foundation – Flanders (FWO) through an FWO PhD Fellowship to LD. This research is also partly funded by the Society of Vertebrate Paleontology's 2016 Steven Cohen Award for Excellent Student Research, awarded to LD. TDK holds a postdoctoral Fellowship at the FWO.

We also want to thank S Bruaux, C Cousin, and A Folie from the RBINS for providing access to the collections. We thank R Fraaije and N Peters from the Oertijdmuseum Groene Poort, Boxtel, Netherlands, ~~to allow~~for allowing access to the holotypes of *Batavipusa neerlandica* and *Praepusa boeska*. We are grateful to M Bosselaers for donating specimens from his private collection for the elaboration of thin sections. Special thanks to JR~~J~~ Wible (editor-in-chief ~~of *Journal of Mammalian Evolution*~~), A Houssaye (reviewer), and a second anonymous reviewer for helpful comments that improved the quality of this work.

REFERENCES CITED

Amprino R (1947) La structure du tissu osseux envisagée comme expression de différences dans la vitesse de l'accroissement. Arch Biol 58:315–330~~.~~

Amson E, Muizon C de (2014) A new durophagous phocid (Mammalia: Carnivora) from the late Neogene of Peru and considerations on monachine seal phylogeny. J Syst Paleontol 12:523–548. doi: 10.1080/14772019.2013.799610

Amson E, Muizon C de, Laurin M, Argot C, Buffrénil V de (2014) Gradual adaptation of bone structure to aquatic lifestyle in extinct sloths from Peru. Proc Biol Soc 281:20140192. doi: 10.1098/rspb.2014.0192

Beentjes MP (1990) Comparative terrestrial locomotion of the Hooker's sea lion (*Phocarctos hookeri*) and the New Zealand fur seal (*Arctocephalus forsteri*): evolutionary and ecological implications. Zool J Linn Soc 98:307–325. doi: 10.1111/j.1096-3642.1990.tb01204.x

Berta A, Kienle S, Bianucci G, Sorbi S (2015) A reevaluation of *Pliphoca etrusca* (Pinnipedia, Phocidae) from the Pliocene of Italy: phylogenetic and biogeographic implications. J Vertebr Paleontol 35:e88944. doi: 10.1080/02724634.2014.889144.

Bininda-Emonds ORP, Russell AP (1996) A morphological perspective on the phylogenetic relationships of the extant phocid seals (Mammalia: Carnivora: Phocidae). Bonn Zool Monogr~~aph~~ 41:1–256.

Boness DJ, Bowen WD (1996) The evolution of maternal care in pinnipeds. ~~Biosci~~ Bioscience 46:645–654.

Buffrénil V de, Canoville A, D'Anastasio R, Domning DP (2010) Evolution of sirenian pachyosteosclerosis, a model-case for the study of bone structure in aquatic tetrapods. J ~~Mamm~~ Mammal Evol 17:101–120.doi: 10.1007/s10914-010-9130-1

Buffrénil V de, Casinos A (1995) Observations histologiques sur le rostre de *Mesoplodon densirostris* (Mammalia, Cetacea, Ziphiidae): le tissu osseux le plus dense connu. Ann Sci Nat Zool 13ème Ser 16:21–32.

Buffrénil~~,~~ V de, Mazin~~,~~ J-M (1989) Bone histology of *Claudiosaurus germaini* (Reptilia, Claudiosauridae) and the problem of pachyostosis in aquatic tetrapods. Hist Biol 2:311–322.doi: 10/1080/08912968909386509

Buffrénil V de, Rage J-C (1993) La 'pachyostose' vertébrale de *Simoliophis* (Reptilia, Squamata): données comparatives et considérations fonctionnelles. Ann Paleontol (Vertebr) 79:315–335.

Buffrénil V de, Ricqlès A de, Ray CE, Domning, DP (1990) Bone histology of the ribs of the aArchaeocetes (Mammalia: Cetacea). J Vertebr Paleontol 10:455–466.doi: 10/1080/02724634.1990.10011828

Buffrénil V de, Schoevaert D (1989) Données quantitatives et observations histologiques sur la pachyostose du squelette du dugong, *Dugong dugon* (Müller) (Sirenia, Dugongidae). Can J Zool 67:2107-2119. doi: 10.1139/z89-300

Burr DB (1993) Remodeling and the repair of fatigue damage. Calcif Tissue Internatl 53 (suppl. –1):S75–S81. doi: 10.1007/BF01673407

Burr DB, Allen MR. (eds.) (2014) Basic and Aapplied Bbone Bbiology. Elsevier/Academic Press, London.

Burr DB, Martin RB, Schaffler MB, Radin EL (1985) Bone remodeling in response to *in vivo* fatigue microdamage. J Biomech 18:189–200. doi:10.1016/0021-9290(85)90204-0

Canoville A, Buffrénil V de, Laurin M (2016) Microanatomical diversity of amniote ribs: an exploratory quantitative study. Biol J Linn Soc 118:706–733. doi: 10.1111/bij.12779

Canoville A, Laurin M (2010) Evolution of humeral microanatomy and lifestyle in amniotes, and some comments on palaeobiological inferences. Biol J Linn Soc 100:384–406. doi: 10.1111/j.1095-8312.2010.01431.x

~~Canoville A, Buffrénil V de, Laurin M (2016) Microanatomical diversity of amniote ribs: an exploratory quantitative study. Biol J Linn Soc 118:706–733. doi: 10.1111/bij.12779~~

Castanet J (2006) Time recording in bone microstructures of endothermic animals; functional relationships. CR Palevol 5:629–636. doi: 10.1016/j.crpv.2005.10.006

Castanet J, Grandin A, Abourachid A, Ricqlès A de (1996) Expression de la dynamique de croissance dans la structure de l'os périostique chez *Anas platyrhynchos*. CR Acad Sci Paris, Sci Vie 319:301–308.

Castanet J, Curry Rogers C, Cubo J, Boisard J (2000) Periosteal bone growth rates in extant ratites (ostrich and emu). Implications for assessing growth in dinosaurs. CR Acad Sci Paris, Sci Vie 323:543–550. doi: 10.1016/S0764-4469(00)00181-5

Charles JF, Aliprantis AO (2014) Osteoclasts: more than 'bone eaters'. Trends Mol Med 20:449–459. doi: 10.1016/j.molmed.2014.06.001

Cozzuol MA (2001) A "northern" seal from the Miocene of Argentina: implications for phocid phylogeny and biogeography. J Vertebr Paleontol 21:415–421. doi: 10.1671/0272-4634(2001)021[0415:ANSFTM]2.0.CO;2

Danova NA, Colopy SA, Radtke CL, Kalscheur VL, Markel MD, Vanderby R Jr, McCabe RP, Escarcega AJ, Muir P (2003) Degradation of bone structural properties by accumulation and coalescence of microcracks. Bone 33:197–205. doi: 10.1016/S8756-3282(03)00155-8

Dehn L-A, Sheffield GG, Follmann EH, Duffy LK, Thomas DL, O'Hara TM (2006) Feeding ecology of phocid seals and some walrus in the Alaskan and Canadian Arctic as determined by stomach contents and stable isotope analysis. Polar Biol 30:167–181. doi: 10.1007/s00300-006-0171-0

Deméré TA (1994a) Two new species of fossil walruses (Pinnipedia: Odobenidae) from the upper Pliocene San Diego Formation. Proc SSan Diego Soc Nat Hist 29:77–98.

Deméré TA (1994b) The family Odobenidae: aA phylogenetic analysis of fossil and living taxa. Proc SanS Diego Soc Nat Hist 29:99–123.

Dempster, DW, Compston JE, Drezner MK, Glorieux FH, Kanis JA, Malluche H, Meunier PJ, Ott SM, Recker RR, Parfitt AM (2013) Standardized nomenclature, symbols, and units for bone histomorphometry: aA 2012 update of the report of the ASBMR

Histomorphometry Nomenclature Committee. J Bone Miner Res 28:1–16. doi: 10.1002/jbmr.1805

Dewaele L, Amson E, Lambert O, Louwye S (2017a) Reappraisal of the extinct seal "*Phoca*" *vitulinoides* from the Neogene of the North Sea Basin, with bearing on its geological age, phylogenetic affinities, and locomotion. PeerJ 5:e3316. doi: 10.7717/peerj.3316

Dewaele L, Lambert O, Louwye S (2017b) On *Prophoca* and *Leptophoca* (Pinnipedia, Phocidae) from the Miocene of the North Atlantic realm: redescription, phylogenetic affinities and paleobiogeographic implications. PeerJ 5:e3024. doi: 10.7717/peerj.3024

Domning D, Buffrénil V de (1991) Hydrostasis in the Sirenia: quantitative data and functional interpretation. Mar Mammal Sci 7:331–368. doi: 10.1111/j.1748-7692.1991.tb00111.x

Dumont M, Buffrénil V de, Mijan I, Lambert O (2016) Structure and growth pattern of the bizarre hemispheric prominence of the rostrum of the fossil beaked whale *Globicetus huberus* (Mammalia, Cetacea, Ziphiidae). J Morphol 277:1292–1308. doi: 10.1002/jmor.20575

Dumont M, Laurin M, Jacques F, Pellé E, Dabin W, Buffrénil V de (2013) Inner architecture of vertebral centra in terrestrial and aquatic mammals: a two-dimensional comparative study. J Morphol 274:570–584. doi: 10.1002/jmor.20122

Evans RA, Hughes WG, Dunstan CR, Lennon WP, Kohan L, Hills E, Wong SYP(1983) Adult osteosclerosis. Metab Bone Dis Relat 5:111–117. doi: 10.1016/0221-8747(83)90011-5

Fawcett DW, Jensh RP (1997) Bloom and Fawcett: Ceoncise Hhistology. Chapman and Hall, New York.

Fay FH (1982) Ecology and bBiology of the Pacific wWalrus, *Odobenus rosmarus divergens* Illiger. N Am Fauna 74:1–279. doi: 10.3996/nafa.74.0001

Fiala P (1980) Structure of the long limb bones and its significance in determining age in man. Folia Morphol 28:259–263.

Fish FE, Stein BR (1991) Functional correlates of differences in bone density among terrestrial and aquatic genera in the family Mustelidae (Mammalia). ~~Zoomorphol~~ Zoomorphology 110:339–345. doi: 10.1007/BF01668024

Fish FE, Hurley J, Costa DP (2003) Maneuverability by the sea lion *Zalophus californianus*: turning performance of an unstable body design. J Exp Biol 206:667–674. doi: 10.1242/jeb.00144

Francillon-Vieillot H, de Buffrénil V, Castanet J, Geraudie J, Meunier JF, Sire JY, Zylberberg L, Ricqlès A de (1990) Microstructure and mineralization of vertebrate skeletal tissues.In: Carter JG (ed) Skeletal Biomineralizations: Patterns, Processes and Evolutionary Trends, Vol. 1. Van Nostrand Reinhold, New York, pp 471–530.

Frost HM (1969) Tetracycline-based histological analysis of bone remodeling. Calc Tiss Res 33:211–237. doi: 10.1007/BF02058664

Fulton TL, Strobeck C (2010) Multiple markers and multiple individuals refine true seal phylogeny and bring molecules and morphology back in line. Proc~~P~~ Roy Soc B–Biol Sci 277:1065–1070. doi: 10.1098/rspb.2009.1783.

Germain D, Laurin M (2005). Microanatomy of the radius and lifestyle in amniotes (Vertebrata, Tetrapoda). Zool Scr 34:335–350. doi: 10.1111/j.1463-6409.2005.00198.x

Giles S, Rücklin M, Donoghue PCJ (2013) Histology of "p~~P~~lacoderm" dermal skeletons: implications for the nature of the ancestral gnathostomes. J Morphol 274:627–644. doi: 10.1002/jmor.20119

Girondot M, Laurin M (2003) Bone Profiler: a tool to quantify, model and statistically compare bone section compactness profiles. J Vertebr Paleontol 23:458-461. doi: 10.1671/0272-4634(2003)023[0458:BPATTQ]2.0.CO;2

Gjertz I, Wiig Ø (1992) Feeding of walrus *Odobenus rosmarus* in Svalbard. Polar Record~~Rec~~ 28:57–59. doi: 10.1017/S0032247400020283

Godfrey SJ (1985) Additional observations of subaqueous locomotion in the California Sea Lion (*Zalophus californianus*). Aquat ~~Mamm~~ Mammal 11:53–57~~.~~

Gray N-M, Kainec K, Madar SI, Tomko L, Wolfe S (2007) Sink or swim? Bone density as a mechanism for buoyancy control in early cetaceans. Anat Rec 290:638–653. doi: 10.1002/ar.20533

Higdon JW, Bininda-Emonds ORP, Beck RMD, Ferguson SH (2007) Phylogeny and divergence of the pinnipeds (Carnivora: Mammalia) assessed using a multigene dataset. BMC Evol Biol 7 :216. doi: 10.1186/1471-2148-7-216.

Houssaye A (2009) "Pachyostosis" in aquatic amniotes: a review. Integr Zool 4:325–340. doi: 10.1111/j.1749-4877.2009.00146.x

Houssaye A (2013) Palaeoecological and morphofunctional interpretation of bone mass increase: an example in Late Cretaceous shallow marine squamates. Biol Rev 88:117–139.

Houssaye A, Fish FE (2016) Functional (secondary) adaptation to an aquatic life in vVertebrates: an introduction to the symposium. Integr Comp Biol 56:1266–1270. doi: 10.1093/icb.icw129

Houssaye A, Lindgren J, Pellegrini R, Lee AH, Germain D, Polcyn MJ (2013) Microanatomical and histological features in the long bones of mosasaurine mosasaurs (Reptilia, Squamata)–iImplications for aquatic adaptation and growth rates. PLoS One 8:e76741. doi: 10.1371/journal.pone.0076741

Houssaye A, Sander PM, Klein N (2016) Adaptive patterns in aquatic amniote bone microanatomy—more complex than previously thought. Integr Comp Biol 56:1349–1369. doi: 10.1093/icb/icw120

Houssaye A, Tafforeau P, Muizon C de, Gingerich PD (2015). Transition of Eocene wWhales from lLand to sSea: eEvidence from bBone mMicrostructure. PLoS One 10:e0118409. doi: 10.1371/journal.pone.0118409

Jaworski ZFG (1992) Haversian system and Haversian bone. In: Hall BK (ed) Bone Mmetabolism and Mmineralization., CRC Press, Boca Raton, pp 21–45.

Jefferson TA, Webber MA, Pitman RL (2008) Marine Mammals of the World: A Comprehensive Guide to their Identification. Elsevier/Academic Press, Amsterdam

Kaiser HE (1974) Morphology of the Sirenians. A Mmacroscopic X-Ray Aatlas of the Mmorphology of Rrecent Sspecies. S. Karger, Basel.

Köhler M, Marin-Moratalla N, Jordana X, Aanes R (2012) Seasonal bone growth and physiology in endotherms shed light on dinosaur physiology. Nature 487:358–361. doi: 10.1038/nature11264

Koretsky IA (2001) Morphology and systematics of the Miocene Phocinae (Mammalia: Carnivora) from Paratethys and the North Atlantic Region. Geol Hung Ser Palaeontol 54:1–109.

Koretsky IA, Grigorescu D (2002) The fossil monk seal *Pontophoca sarmatica* (Alekseev) (Mammalia: Phocidae: Monachinae) from the Miocene of eastern Europe. Smithson Contrib Paleobiol 93:149–162.

Koretsky IA, Peters N (2008) *Batavipusa* (Carnivora, Phocidae, Phocinae): a new genus from the eastern shore of the North Atlantic Ocean (Miocene seals of the Netherlands, part II). Deinsea 12:53–62.

Koretsky IA, Peters N, Rahmat SJ (2015) New species of *Praepusa* (Carnivora, Phocidae, Phocinae) from the Netherlands supports east to west Neogene dispersal of true seals. Vestn Zool 49:57–66.

Koretsky IA, Rahmat SJ (2013) First record of fossil Cystophorinae (Carnivora, Phocidae): middle Miocene seals from the northern Paratethys. Riv Ital Paleontol S 119:325–350. doi: 10.13130/2039-4942/6043

Koretsky IA, Rahmat SJ (2017). Preliminary rReport of pPachyosteosclerotic bBones in sSeals. Open Acc Res Anat 1:1–3.

Koretsky IA, Ray CE (2008) Phocidae of the Pliocene of Eastern North America. Virginia Mus Nat Hist, Spec Pub 14:81–140.

Kriloff A, Germain D, Canoville A, Vincent P, Sache M, Laurin M (2008) Evolution of bone microanatomy of the tetrapod tibia and its use in palaeobiological inference. J Evol Biol 21:807–826. doi: 10.1111/j.1420-9101.2008.01512.x

Kühn C, Frey E (2012) Walking like caterpillars, flying like bats—pinniped locomotion.

Palaeobio Palaeoenv 92:197–210. doi: 10.1007/s12549-012-0077-5

Lafage-Proust M-H, Roche B, Langer M, Cleret D, Vanden Bossche A, Olivier T, Vico L (2015) Assessment of bone vascularization and its role in bone remodeling. BoneKEy Rep 4, art. no. 662:1–8. doi: 10.1038/bonekey.2015.29

Lambert O, Muizon C de, Buffrénil V de (2011) Hyperdense rostral bones of ziphiid whales: diverse processes for a similar pattern. CR Palevol 10:453–468. doi: 10.1016/j.crpv.2011.03.012

Lamm ET (2013) Preparation and sectioning of specimens. In: Padian K, Lamm ET (eds) Bone Hh~~i~~stology of Ff~~f~~ossil Tt~~t~~etrapods: Aa~~a~~dvancing Mm~~m~~ethods, Aa~~a~~nalysis, and Ii~~i~~nterpretation. University of California Press, Berkeley, pp 55–160

Landrigan MD, Li J, Turnbull TL, Burr DB, Niebur GL, Roeder RK (2011) Contrast-enhanced micro-computed tomography of fatigue microdamage accumulation in human cortical bone. Bone 48:443–450. doi: 10.1016/j.bone.2010.10.160

Laurin M, Canoville A, Germain D (2011) Bone microanatomy and lifestyle: a~~A~~ descriptive approach. CR Palevol 10:381–402. doi: 10.1016/j.crpv.2011.02.003

Laurin M, Girondot M, Loth M-M (2004) The evolution of long bone microanatomy and lifestyle in lissamphibians. Paleobiology 30:589–613. doi: 10.1666/0094-8373(2004)030<0589:TEOLBM>2.0.CO;2

Lee TC, Mohsin S, Taylor D, Parkesh R, Gunnlaugsson T, O'Brien FJ, Giehl M, Gowin W (2003) Detecting microdamage in bone. J Anat 203:161–172. doi: 10.1046/j.1469-7580.2003.00211.x

Lieberman DE, Pearson OM, Polk JD, Demes B, Crompton AW (2003) Optimization of bone growth and remodeling in response to loading in tapered mammalian limbs. J Exp Biol 206:3125–3138. doi: 10.1242/jeb.00514

Liu XS, Bevill G, Keaveny TM, Sajda P, Guo XE (2009) Micromechanical analyses of vertebral trabecular bone based on individual trabeculae segmentation of plates and rods. J Biomech 42:249–256. doi: 10.1016/j.biomech.2008.10.035

Margerie E de, Cubo J, Castanet J (2002) Bone typology and growth rate: testing and quantifying "Amprino's rule" in the mallard (*Anas platyrhynchos*). CR Biol 325:221–230. doi: 10.1016/S1631-0691(02)01429-4

Marks SC, Popoff SN (1988) Bone cell biology: the regulation of development, structure and function of the skeleton. Am J Anat 183:1–44. doi: 10.1002/aja.1001830102

Martin RB (2000) Toward a unifying theory of bone remodeling. Bone 26:1–6. doi: 10.1016/S8756-3282(99)00241-0

Masschaele B, Dierick M, Loo DV, Boone MN, Brabant L, Pauwels E, Cnudde V, Hoorebeke LV (2013) HECTOR: A 240kV micro-CT setup optimized for research. J Phys Conf Ser 463:012012. doi: 10.1088/1742-6596/463/1/012012.

Michou L, Brown JP (2011) Genetics of bone diseases: Paget's disease, fibrous dysplasia, osteopetrosis and osteogenesis imperfecta. Joint Bone Spine 78: 252–258. doi: 10.1016/j.bspin.2010.07.010

Mohsin S, O'Brien FJ, Lee TC (2006) Osteonal crack barriers in ovine compact bone. J Anat 208: 81-89.

Muizon C de (1981) Les vertébrés fossiles de la Formation Pisco (Pérou). Première partie: deux nouveaux Monachinae du Pliocène de Sud Sacaco. Inst Franc Etud Andines Mem 6 20–161.

Nakajima Y, Endo H (2013). Comparative humeral microanatomy of terrestrial, semiaquatic, and aquatic carnivorans using micro-focus CT scan. Mammal Study 38:1–8.

Parfitt AM (1981) Bone effect of spaceflight: analysis by quantum concept of bone remodeling. Acta Astronaut 8:1083–1090. doi: 10.1016/0094-5765(81)90082-5

Parfitt AM (1982) The coupling of bone formation to bone resorption: a critical analysis of the concept and of its relevance to the pathogenesis of osteoporosis. Metab Bone Dis Relat 4:1–6. doi: 10.1016/022-8747(82)90002-9

Pierce SE, Clack JA, Hutchinson JR (2011) Comparative axial morphology in pinnipeds and its correlation with aquatic locomotory behaviour. J Anat 219:502–514. doi: 10.1111/j.1469-7580.2011.01406.x

Polig E, Jee WSS (1990) A model of osteon closure in cortical bone. Calcif Tissue Int~~Int~~ernatl 47:261–269. doi: 10.1007/BF02555907

Prondvai E, Stein KHW, Ricqlès A de, Cubo J (2014) Development-based revision of bone tissue classification: the importance of semantics for science. Biol J Linn Soc 112:799–816. doi: 10.1111/bio.12323

Pyenson, ND, Kelley NP, Parham JF (2014) Marine tetrapod macroevolution: p~~P~~hysical and biological drivers on 250 Ma of invasions and evolution in ocean ecosystems. Palaeogeogr Palaeoclimatol Palaeoecol 400:1–8. doi:10.1016/j.palaeo.2014.02.18

Qiu S, Fyhrie DP, Palnitkar S, Sudhaker Rao D (2003) Histomorphometric assessment of Haversian canal and osteocyte lacunae in different-sized osteons in human ribs. Anat Rec 272A:520–525. doi: 10.1002/ar.a.10058

Quemeneur S, Buffrénil V de, Laurin M (2013) Microanatomy of the amniote femur and inference of lifestyle in limbed vertebrates. Biol J Linn Soc 109:644–655. doi: 10.1111/bij.12066

Ralston SH (2008) Pathogenesis of Paget's disease of Bone. Bone 43: 819–825.doi: 10.1016/j.bone.2008.06.015

Ricqlès A de (1989). Les mécanismes hétérochroniques dans le retour des tétrapodes au milieu aquatique. Geobios Mem Spec 12:337–348. doi: 10.1016/S0016-6995(89)80034-8

Ricqlès A de, Buffrénil V de (1995) Sur la présence de pachyostéosclérose chez la rhytine de Steller [*Rhytina (Hydrodamalis) gigas*], sirénien récent éteint. Ann Sci Nat Zool Paris, 13e Ser 16:47–53.

Ricqlès A de, Buffrénil V de (2001) Bone histology, heterochronies and the return of Tetrapods to life in water: w[h]ere are we? In: Mazin J-M, Buffrénil V de (eds)Secondary Aadaptation of Ttetrapods to Llife in Wwater. Verlag Dr. Friedrich Pfeil, München, pp 289–310

Schaffler MB, Choi K, Milgrom C (1995) Aging and matrix microdamage accumulation in human compact bone. Bone 17:521–527. doi: 10.1016/8756-3282(95)00370-3

Stein BR (1989) Bone density and adaptation in semiaquatic mammals. J Mammal 70:467–476. doi: 10.2307/1381418

Storå J (2000) Skeletal development in the Grey seal *Halichoerus grypus*, the Ringed seal *Phoca hispida botnica*, the Harbour seal *Phoca vitulina vitulina* and the Harp seal *Phoca groenlandica*. Epiphyseal fusion and life History. ~~Archaeozoolog~~ Archaeozoologia 11:199–222.

Taylor MA (2009) Functional significance of bone ballast in the evolution of buoyancy control strategies by aquatic tetrapods. Hist Biol 14:15–31. doi: 10.1080/10292380009380550

Thompson DW (1961) On Ggrowth and Fform. Cambridge University Press, Cambridge

Turner CH (1998) Three rules for bone adaptation to mechanical stimuli. Bone 23:399–407. doi: 10.1016/S8756-3282(98)00118-5

Uhen MD (2007) Evolution of mMarine mMammals: bBack to the sSea aAfter 300 mMillion yYears. Anat Rec 290:514–522. doi:10.1002/ar.20545

Van Beneden P-J (1871) Les phoques de la mer scaldisienne. Bul Acad R Sci Let b-Arts Belg 2ième Ser 32:5–19.

Van Beneden P-J (1877) Description des ossements fossiles des environs d'Anvers, première partie. Pinnipèdes ou amphithériens. Ann Mus R Hist Nat Belg 1:1–88.

Voide R, Schneider P, Stauber M, van Lenthe GH, Stampanoni M, Müller R (2011) The importance of murine cortical bone microstructure for microcrack initiation and propagation. Bone 49:1186–1193. doi: 10.1016/j.bone.2011.08.011

Wall WP (1983) The correlation between high limb-bone density and aquatic habits in recent mammals. J Paleontol 57:197–207.

Webb P, Buffrénil V de (1990) Locomotion in the biology of large aquatic vertebrates. TransT Am Fish Soc 119:629–641. doi: 10.1577/1548-8659(1990)119<0629:LITBOL>2.3.CO;2

Zylberberg L, Traub W, Buffrénil V de, Alizard F, Arad T, Weiner S (1998) Rostrum of a toothed whale: ultrastructural study of a very dense bone. Bone 23:241–247. doi: 10.1016/S8756-3282(98)00101-X

LEGENDS OF THE FIGURES

Fig. 1 – Reconstruction of the skeleton of the phocid *Nanophoca vitulinoides* from the middle Miocene of the southern North Sea, with the partial skeleton of specimen IRSNB M2276 superimposed. Light gray indicates bone types that have been subjected to micro-CT scanning exclusively; dark gray indicates bone types that have been subjected to thin sectioning exclusively; and intermediate gray indicates bones that have been subjected to both micro-CT scanning and thin sectioning. Thin sectioning includes transverse sections and longitudinal sections. Note: thin sectioning has been performed on other specimens than IRSNB M2276. Modified from Dewaele et al. (2017a: fig. 1).

Fig. 2 – Line drawing of a humerus and femur of the *Nanophoca vitulinoides* neotype specimen IRSNB M2276 showing the measurements taken for the basic morphometric analysis. Gray lines on the humerus show total length of the humerus and least transverse width of the humeral diaphysis. Gray lines on the femur show total length of the femur and least transverse width across the diaphysis. Anteroposterior width is shown as an arrow perpendicular to the field of view (circle with diagonal cross).

Fig. 3 – Phylogeny of *Nanophoca vitulinoides*, as presented by Dewaele et al. (2017a). Both *Leptophoca proxima* and *N. vitulinoides* are ~~returned~~ shown as stem phocines. Based on the literature, the phylogenetic position of *Callophoca obscura* is difficult to ascertain. The phylogenetic position of *Batavipusa neerlandica*, *Phocanella pumila*, and *Praepusa boeska* remains unclear, in part due to the incompleteness of their respective fossil records.

Fig.4 – Microanatomy of the vertebra of *Nanophoca vitulinoides*. Longitudinal microanatomical drawings of an **A**) adult (Histos 2150, thin section) and **B**) juvenile (Histos

Formatted: Font: Bold

Formatted: Font: Bold

2147, thin section) lumbar vertebra. The compactness in the adult specimen is clearly much higher than in the juvenile specimen. Scale bars equal 5 mm.

Fig. 5 – Microanatomy of the rib of *Nanophoca vitulinoides*. Microanatomical drawings of the transverse sections through the ribs of **A**) *N. vitulinoides* (Histos 2152, thin section), **B**) *Callophoca obscura* (Histos 168, thin section), and **C**) *Phoca vitulina* (specimen from Canoville et al. 2016, thin section), and the corresponding compactness profiles. Scale bars equal 5 mm.

Fig.6 – Microanatomy of the humerus of *Nanophoca vitulinoides*. Microanatomical drawings of the transverse sections through the humerus of **A**) *N. vitulinoides* (IRSNB M2276c, micro-CT), **B**) *N. vitulinoides* (Histos 2136, thin section), **C**) *Phocanella pumila* (Histos 163, thin section), **D**) *Phoca vitulina* (IRSNB 1157E, micro-CT), **E**) *Mirounga leonina* (specimen from Canoville and Laurin 2010, thin section), **F**) *Otaria byronia* (specimen from Canoville and Laurin 2010, thin section), and **G**) *Lutra lutra* (specimen from Canoville and Laurin 2010, thin section), and the corresponding compactness profiles. Scale bars equal 5 mm.

Fig.7 – Micro-CT scans of the holotype humeri of *Batavipusa neerlandica* and *Praepusa boeska* from the middle Miocene of the southern North Sea basin. Scans show the diaphyseal cross sections of holotype humeri of **A**) *B. neerlandica* (MAB 3798) and **B**) *P. boeska* (MAB 4686). Anterior end up. White arrows point toward different concentric cortical layers. A spongy medullary region is clearly visible in *B. neerlandica*, but less conspicuous in *P. boeska*. Scale bars equal 5 mm.

Fig.8 – Microanatomy of the femur of *Nanophoca vitulinoides*. Microanatomical drawings of the transverse sections through the femur of **A**) *N. vitulinoides* (Histos 1935, thin section), **B**) *N. vitulinoides* (IRSNB M2276d, micro-CT), **C**) *Leptophoca proxima* (Histos 166, thin

Formatted: Font: Bold
Formatted: Font: Bold
Formatted: Font: Bold
Formatted: Font: Bold
Formatted: Font: Bold
Formatted: Font: Bold
Formatted: Font: Bold
Formatted: Font: Bold
Formatted: Font: Bold
Formatted: Font: Bold
Formatted: Font: Bold
Formatted: Font: Bold
Formatted: Font: Bold

section), **D**) *Callophoca obscura* (Histos 170, thin section), **E**) *Phocanella pumila* (Histos 160, thin section), **F**) *Phoca vitulina* (IRSNB 1157E, micro-CT), **G**) *Otaria byronia* (specimen from Quemeneur et al. 2013, thin section), and **H**) and **I**) *Lutra lutra* (specimen from Quemeneur et al. 2013, thin section), and the corresponding compactness profiles. Scale bars equal 5 mm.

Fig.9 – Microanatomy of the radius and tibia of *Nanophoca vitulinoides*. Microanatomical drawings of the transverse sections through the radius of **A**) *N. vitulinoides* (Histos 2142, thin section), and **B**) *Phoca vitulina* (IRSNB 1157E, micro-CT), and through the tibia **C**) *N. vitulinoides*(IRSNB M2276g, micro-CT), and **DF**) *P. vitulina* (IRSNB 1157E, micro-CT), and the corresponding compactness profiles. Scale bars equal 5 mm.

Fig.10 – Bone structure in the cortex and medulla of *Nanophoca vitulinoides* ~~bones~~. **A**) The cortex of the humeral diaphysis (cross section) is composed of a woven-parallel complex with longitudinal primary osteons and conspicuous, broadly spaced annuli (arrows). Left half: ordinary transmitted light, right half: polarized light. **B**) Longitudinal section in the same bone in the metaphyseal region. The primary osteons appear brightly birefringent. **C**) Closer view at the diaphyseal cortex between annuli 2 and 4. The arrows point to short Sharpey's fibers. **D**) Lines of arrested growth (arrows) in the humeral cortex. **E**) Cross-section in the larger radius (Histos 2174). The whole bone area is occupied by a dense Haversian tissue, and no medullary cavity is visible. **F**) Closer view at the remodeled medullary of the radius shown in Fig.10E. **G**) Detail of the structure of the dense Haversian tissue in the medulla of the radius. Remark that vascular canals are extremely thin or occluded. **H**) Close view at over-remodeled bone in the medulla of the radius. The two arrows point at occluded Haversian canals. Scale bars equal 5 µm, except E) 5 mm, and H) 50 µm.

Formatted: Font: Bold
Formatted: Font: Bold
Formatted: Font: Bold
Formatted: Font: Bold
Formatted: Font: Bold
Formatted: Font: Bold
Formatted: Font: Bold
Formatted: Font: Bold
Formatted: Font: Bold
Formatted: Font: Bold
Formatted: Font: Not Italic
Formatted: Font: Bold
Formatted: Font: Bold
Formatted: Font: Bold
Formatted: Font: Bold
Formatted: Font: Bold
Formatted: Font: Bold

Fig.11 – Inner bone remodeling in long bones and vertebrae. **A**) Longitudinal section in the proximal metaphyseal and epiphyseal regions of the femur. The whole bone is compact and composed of densely remodeled osseous tissue. **B**) Longitudinal section in the proximal metaphysis and epiphysis of a rib. Same comment as for the femur. **C**) Longitudinal section in the epiphysis of the larger radius (Histos 2174). Epiphyseal surface is covered by a thin layer of calcified cartilage. Under it, the metaphyseal medulla is already compact and densely remodeled (right half: polarized light). **D**) Cross section in the diaphysis of the smaller radius (Histos 2142). The architecture of the spongiosa that once occupied the medulla is still visible, though inter-trabecular spaces are filled. **E**) Detail of the medullar of the smaller radius. The endosteal deposits filling inter-trabecular spaces are densely remodeled and vascular canals (arrows) tend to be occluded. The asterisks indicate micro-cracks. **F**) Off-centered growth of Humeral diaphysis. One face of the bone is under resorption (hollow arrow) while accretion occurs on the other (solid arrow). **G**) Cross section in the centrum of the larger vertebra. Polarized light reveals that the thick trabeculae filling the centrum are densely remodeled. **H**) Longitudinal section in the same specimen (polarized light) showing densely remodeled osseous tissue. **I**) External fundamental system on the outer wall of the neural arch (cross section) in polarized light. Scale bars equal 5 mm for A) and B); 1 mm for D), F), G), H), and I); and 500µm for C), and E).

Fig.12 – Comparative data in extant and extinct pinnipeds. **A**) Cross section in the femur of *Phocanella pumila*. Remark the relatively high compactness of this bone, and its non-remodeled cortex. White rectangle: field shown in Fig.11B. **B**) Detail of the cortex showing a woven-parallel tissue with longitudinal primary osteons and annuli. Right half: polarized light. **C**) lines of arrested growth in the femoral cortex of ~~*P.*~~*Phocanella pumila*. **D**) Non-remodeled part of the cortex of a rib in *Monachus monachus* (polarized light). Histology of primary cortices is comparable to that prevailing in ~~*P.*~~*Phocanella pumila* and *Nanophoca*

Formatted: Font: Bold
Formatted: Font: Bold
Formatted: Font: Bold
Formatted: Font: Bold
Formatted: Font: Bold
Formatted: Font: Bold
Formatted: Font: Bold
Formatted: Font: Bold
Formatted: Font: Bold
Formatted: Font: Bold
Formatted: Font: Not Italic
Formatted: Font: Bold
Formatted: Font: Bold

vitulinoides. **E**) Remodeling in the deep femoral cortex of *Callophoca obscura*. Remodeling is intense, but Havers' canals remain widely open. **F)** Normal (most frequent) bone architecture in extant and some extinct pinnipeds (here: femur of ~~*C.*~~*Callophoca obscura*). The medullary region is hollow, and contains only a loose spongiosa with thin trabeculae. Scale bars equal 10 mm for A) and F); 1 mm for the inset of F); and 500 µm for B), C), D), and E).

Formatted: Font: Bold

Formatted: Font: Bold

Figure 1

Click here to download Figure Figure 1.tif

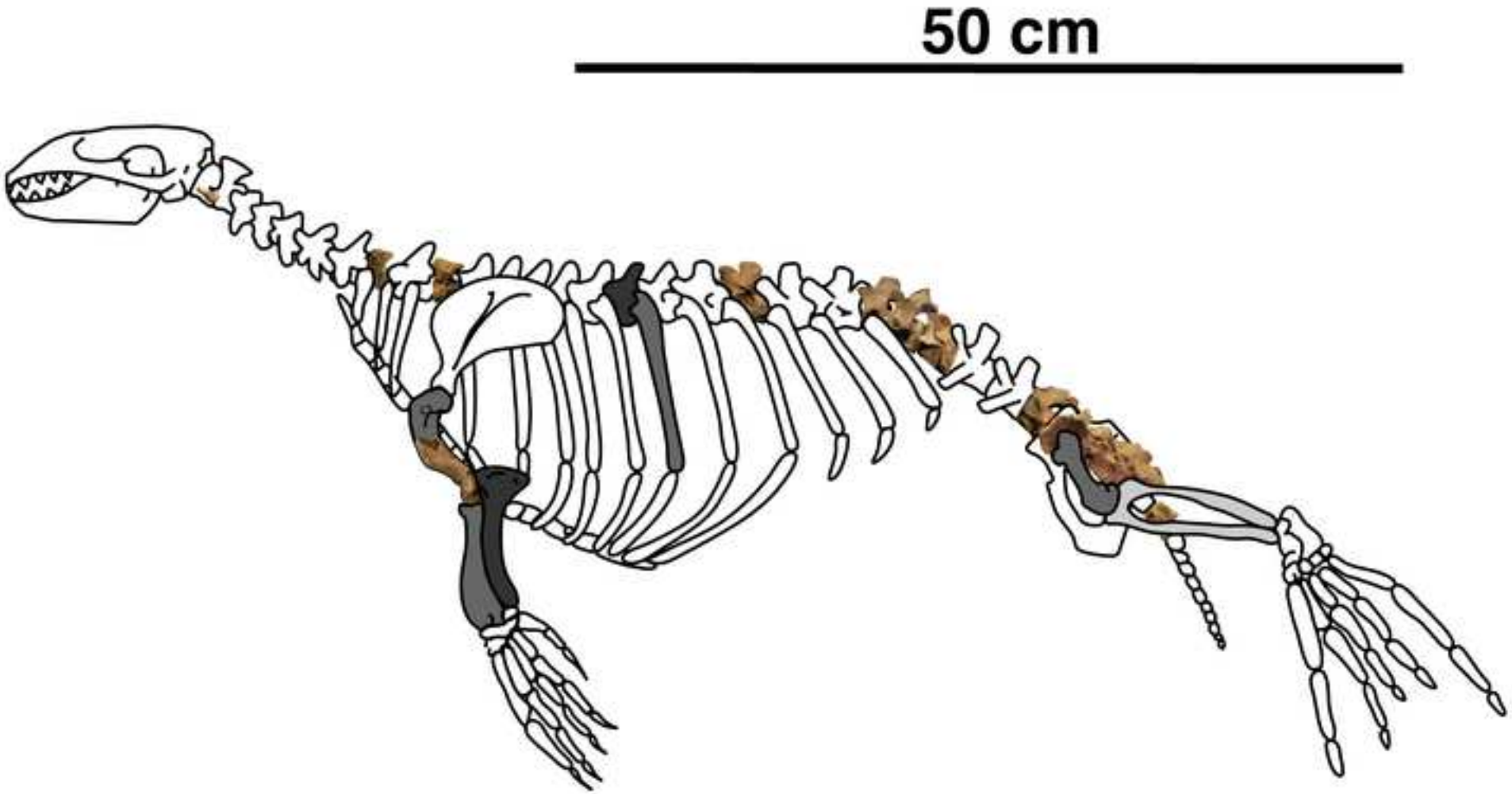

Figure 2

Click here to download Figure Figure 2.tif

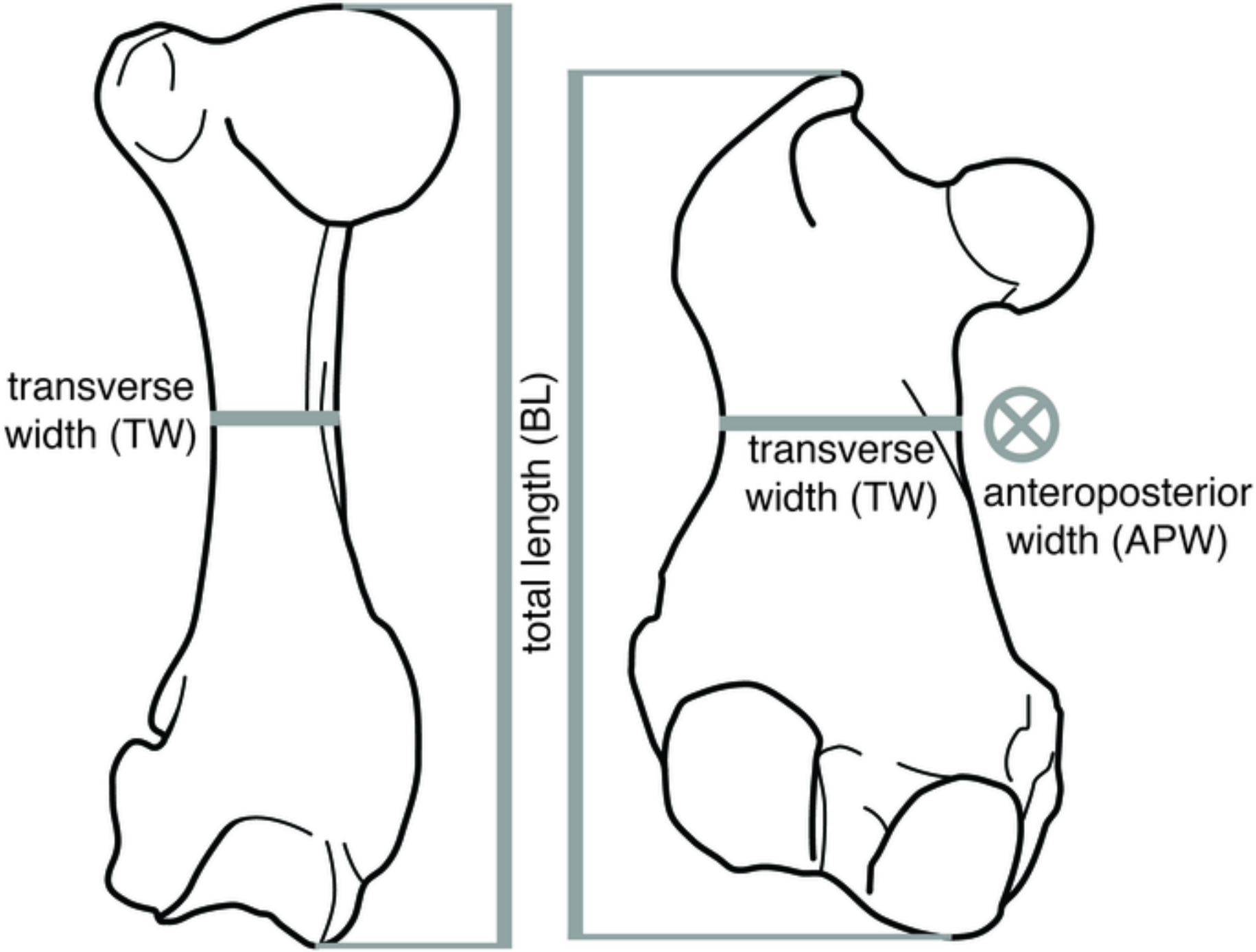

Figure 3

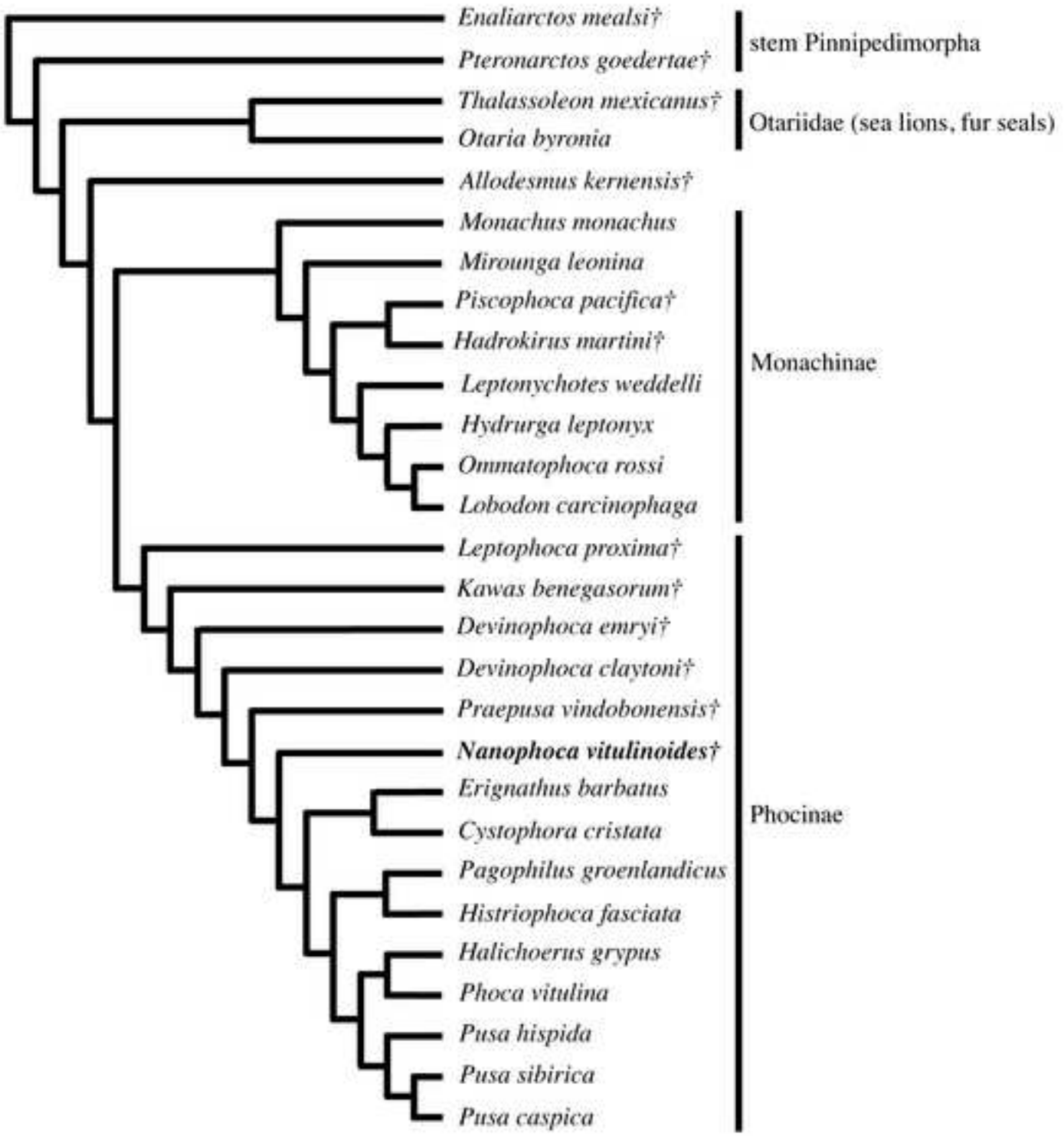

Figure 4

Click here to download Figure Figure 4.tif

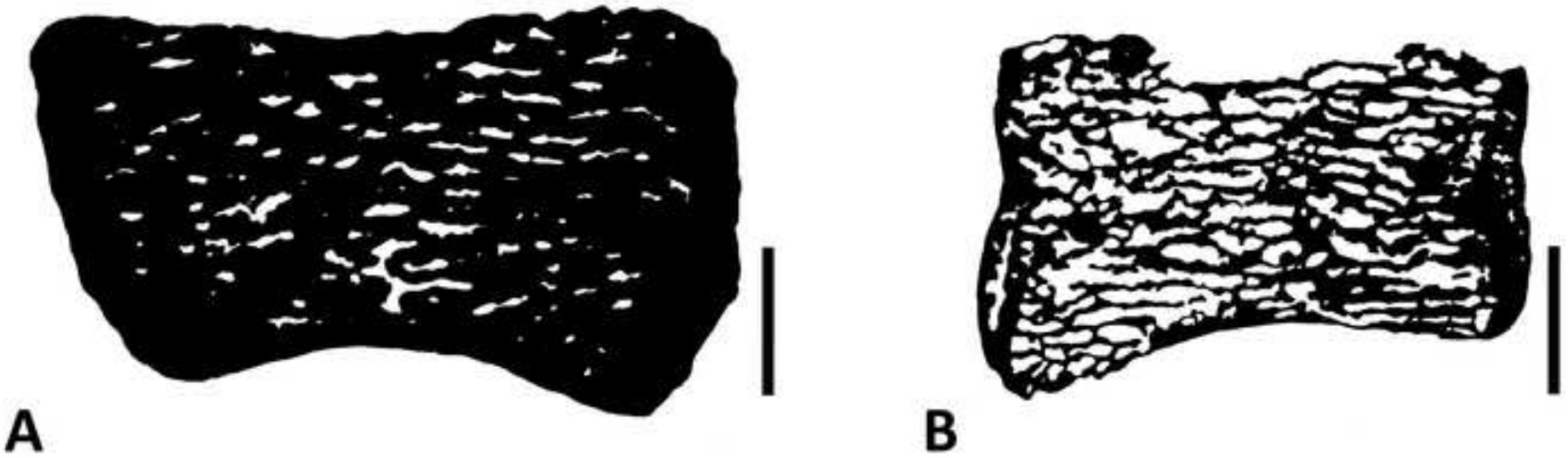

Figure 5

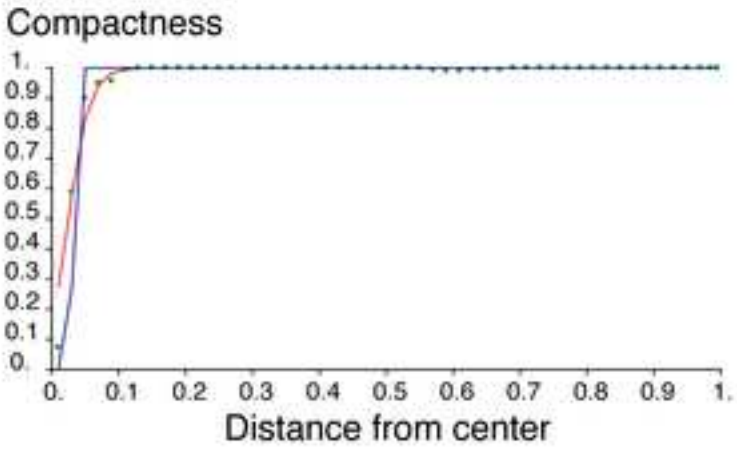

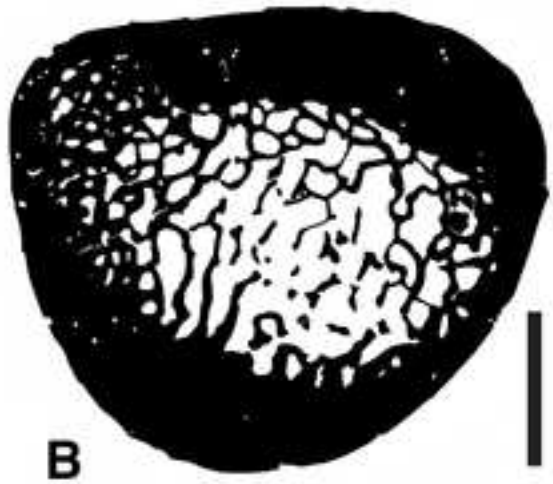

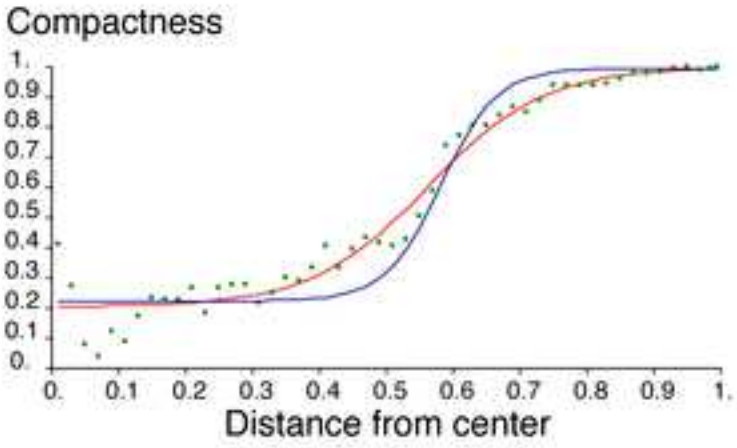

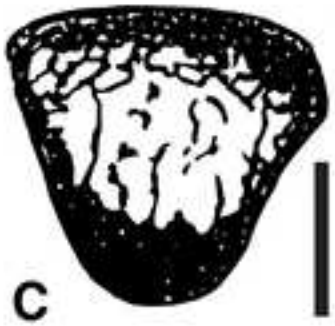

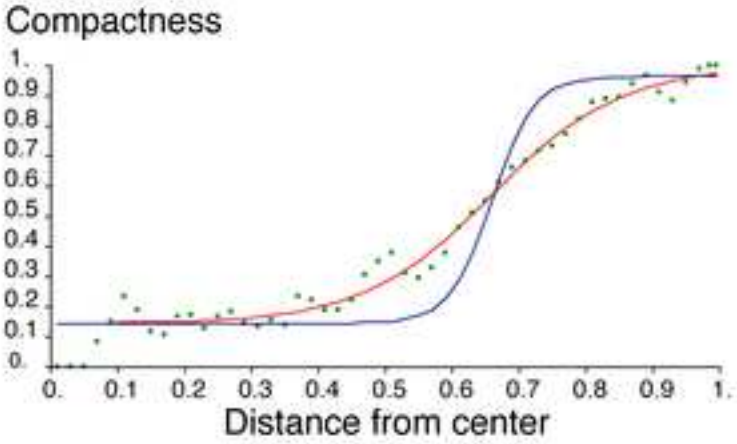

Figure 6

Click here to download Figure Figure 6.tif

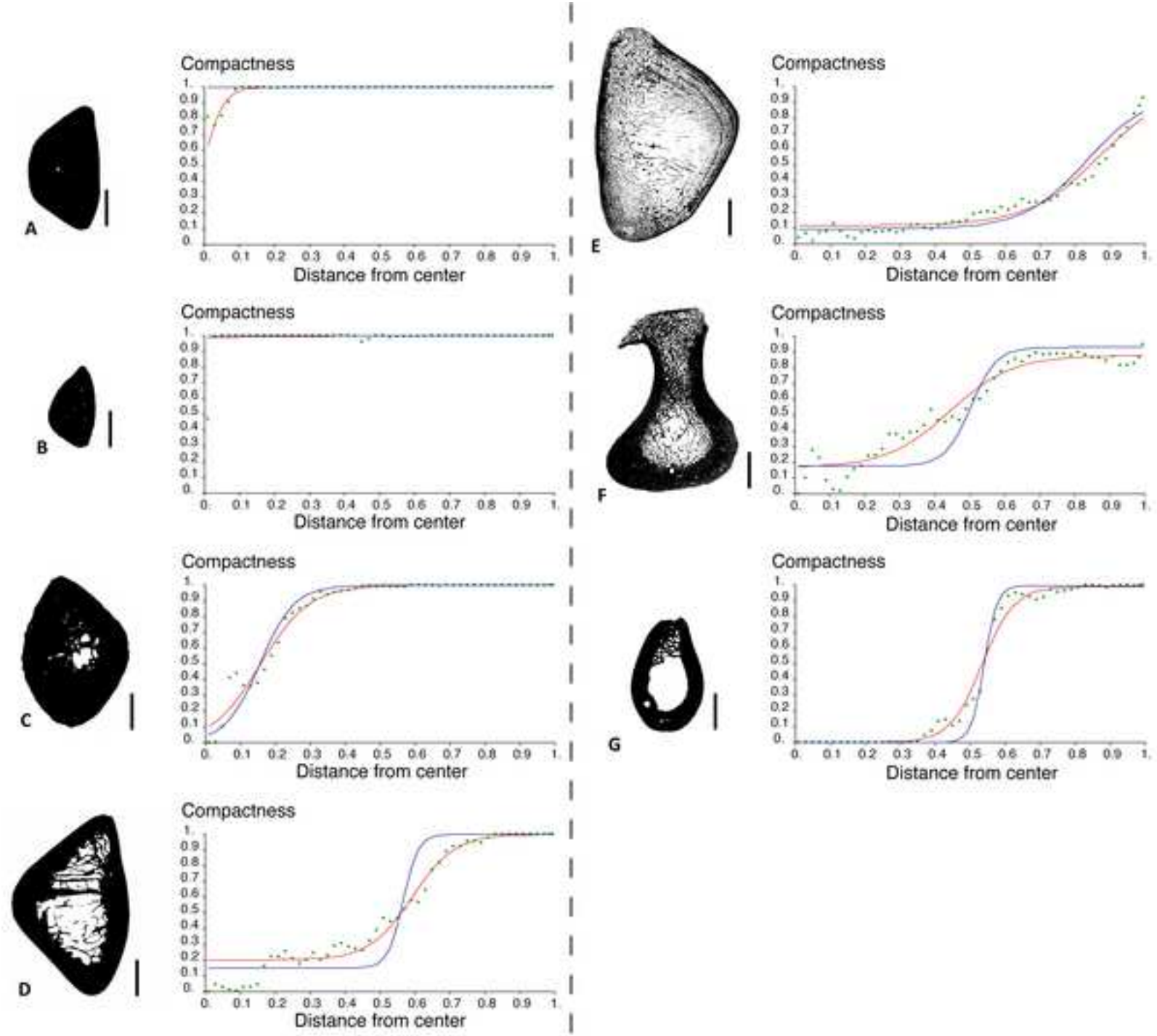

Figure 7

Click here to download Figure Figure 7.tif

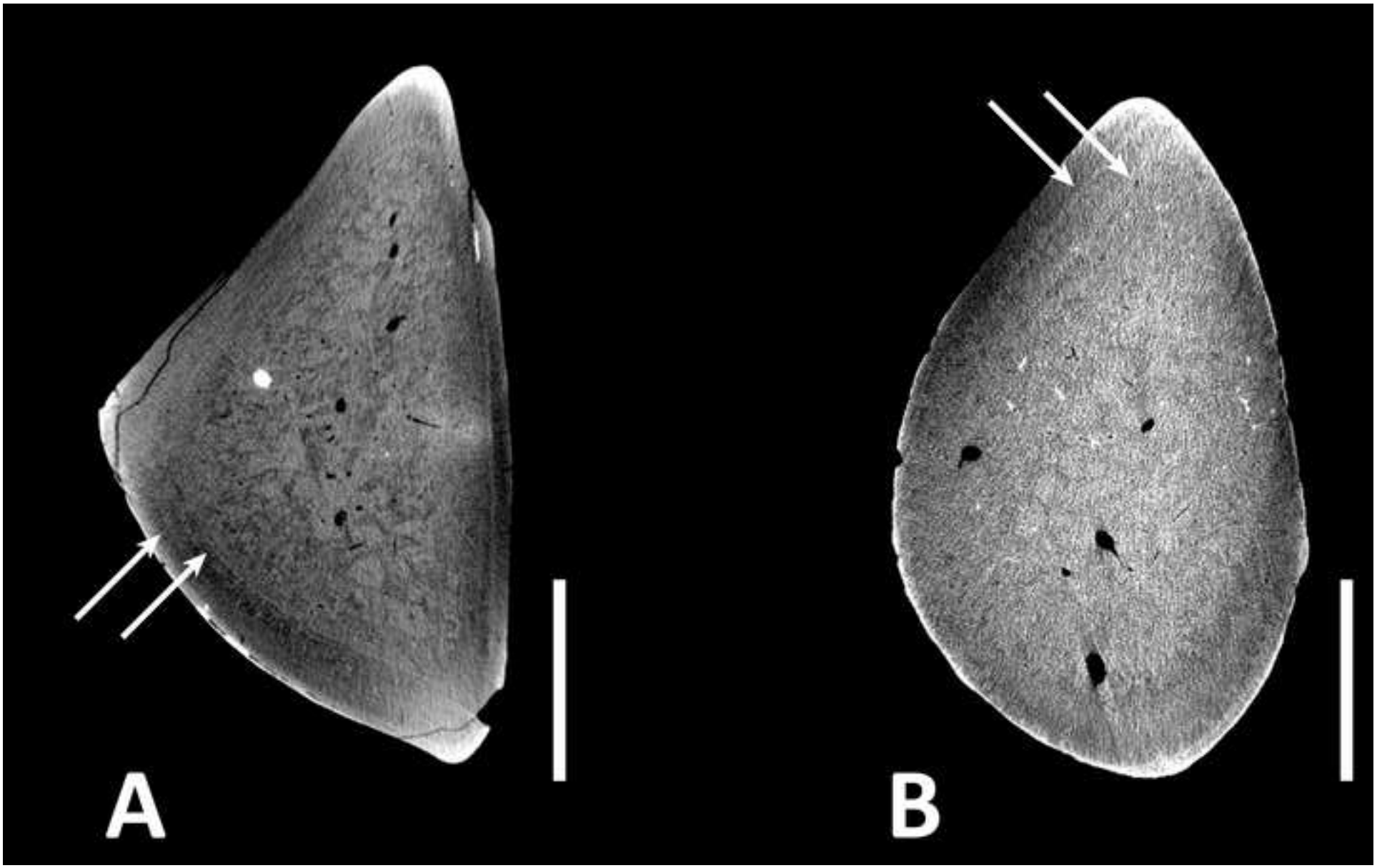

Figure 8

Click here to download Figure Figure 8.tif

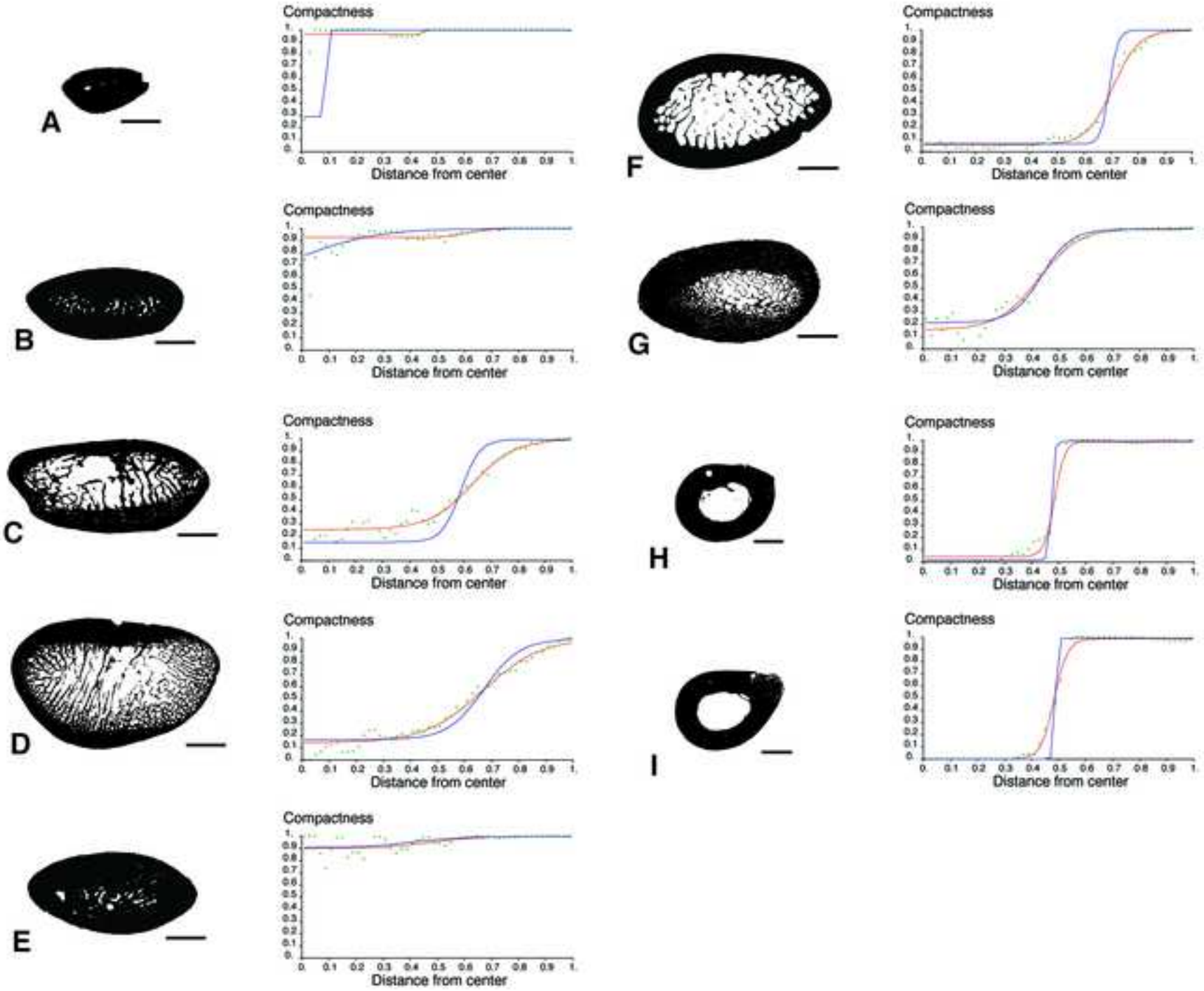

Figure 9

Click here to download Figure Figure 9.tif

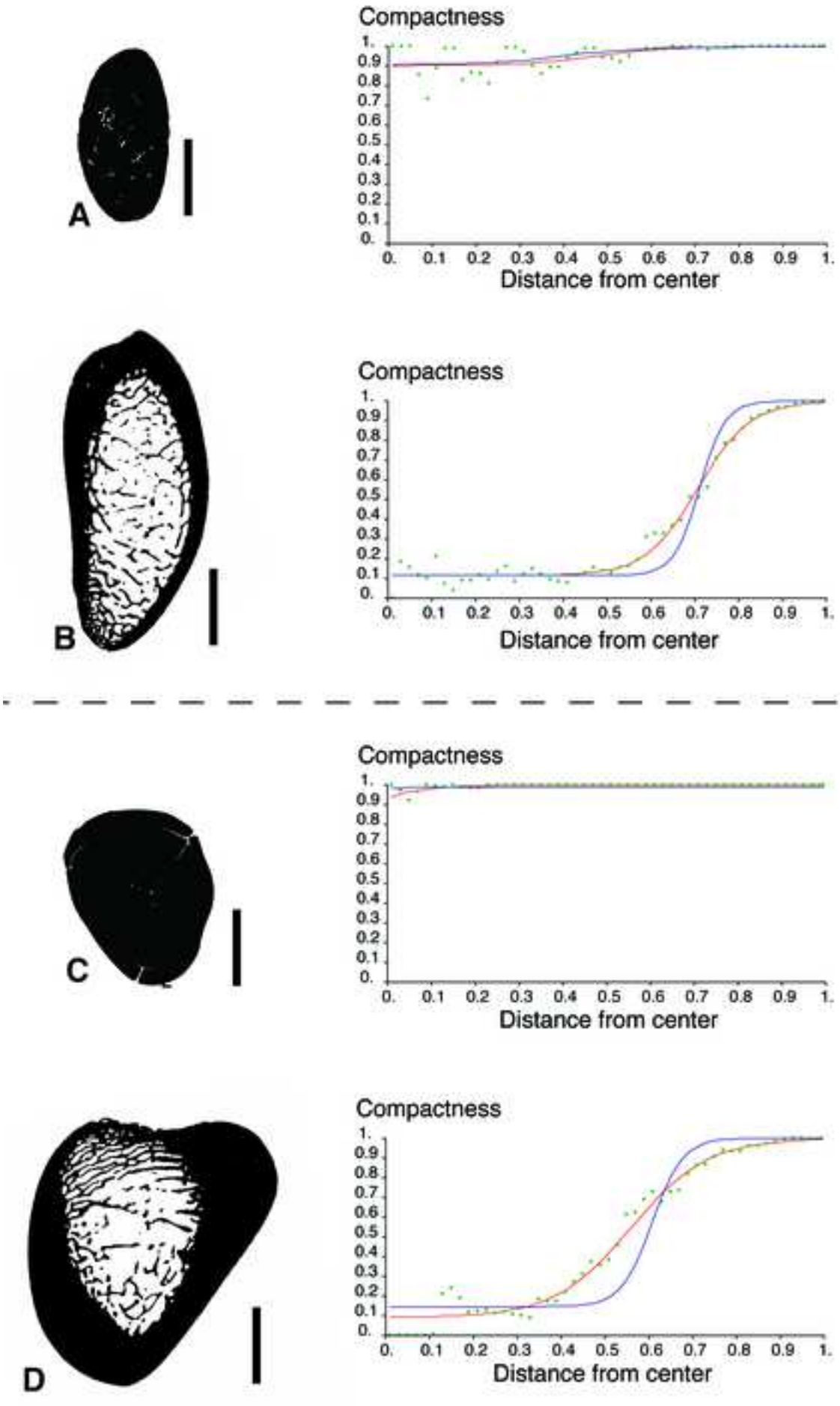

Figure 10

Click here to download Figure Figure 10.tif

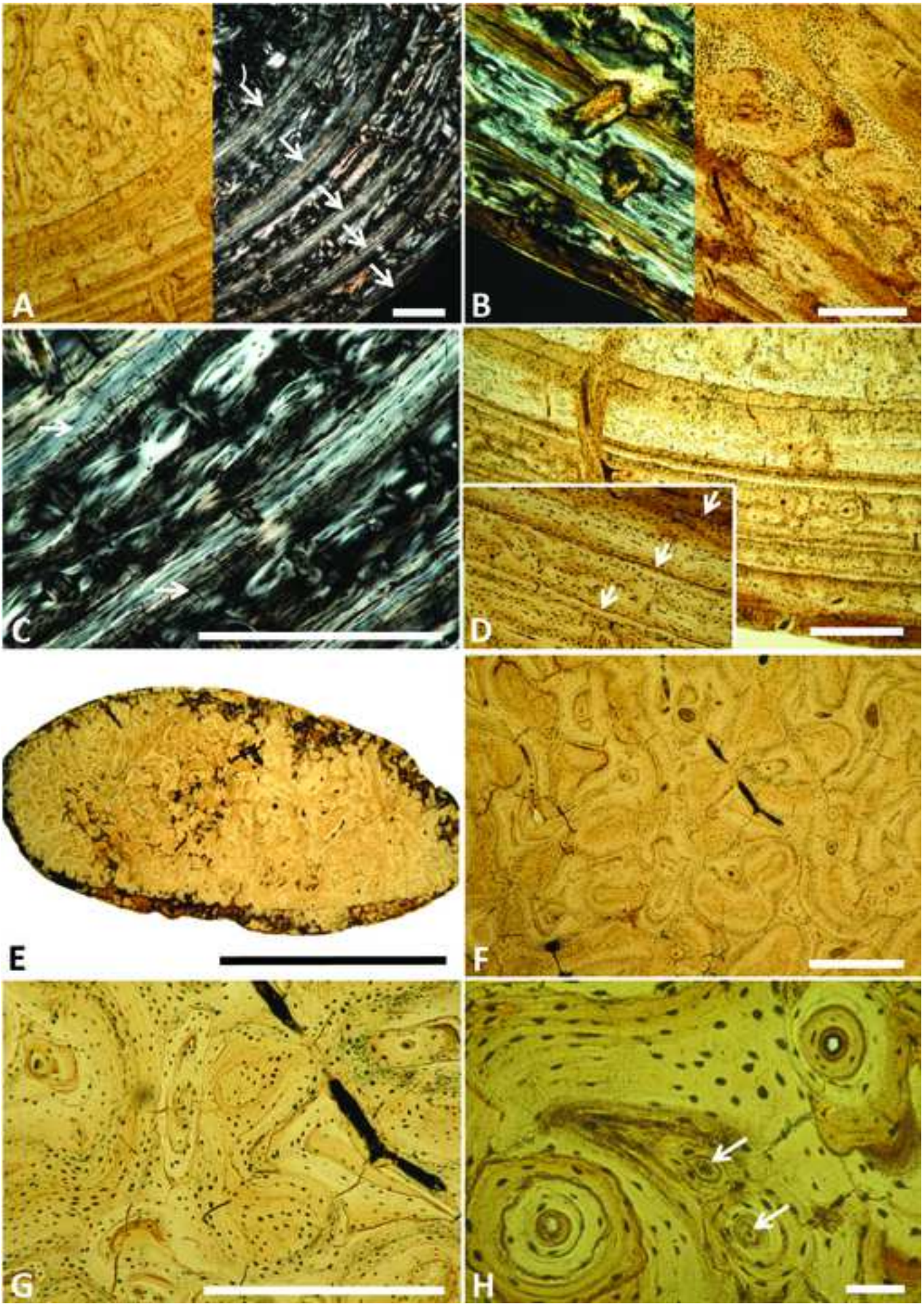

Figure 11

Click here to download Figure Figure 11.tif

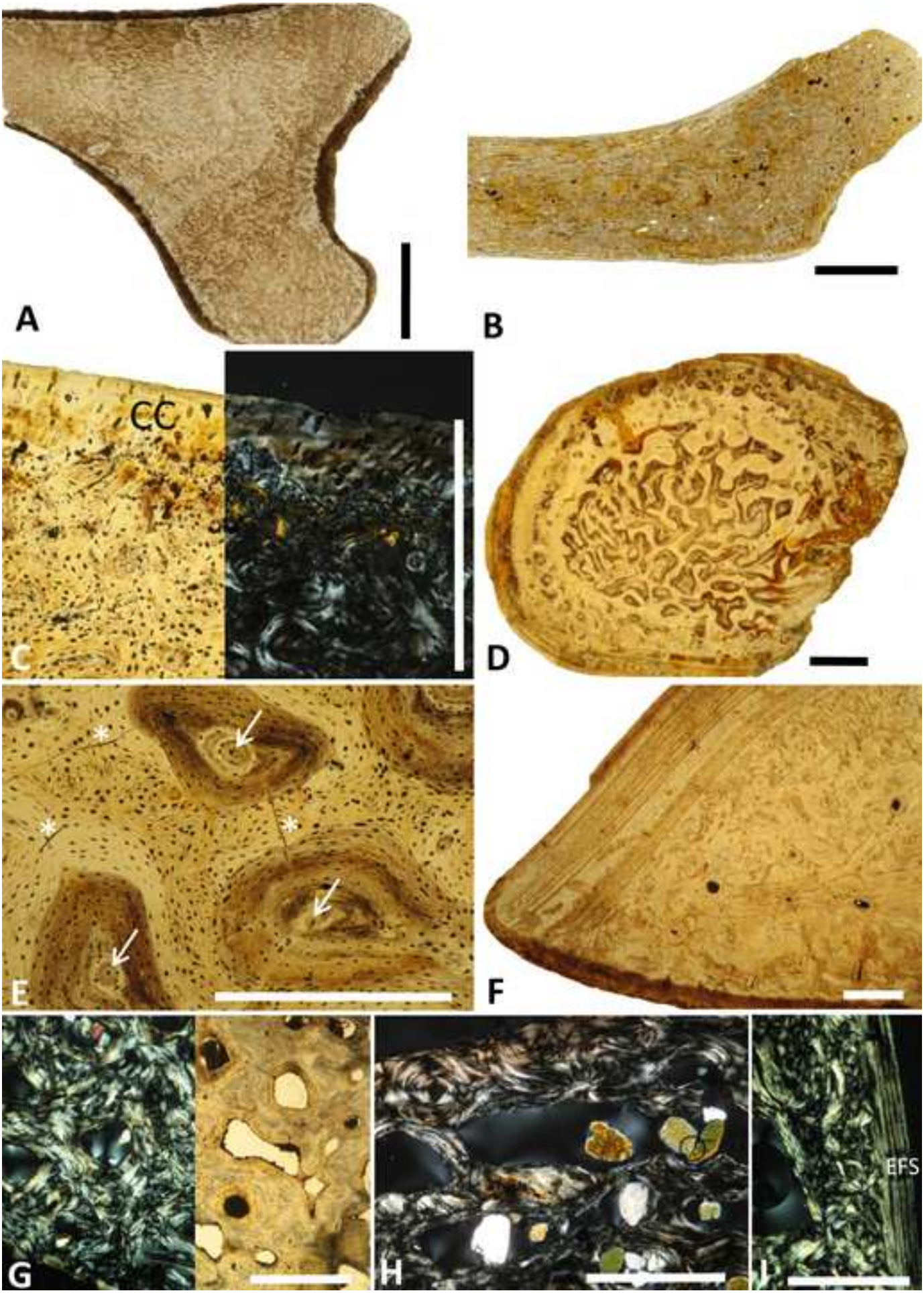

Figure 12

Click here to download Figure Figure 12.tif

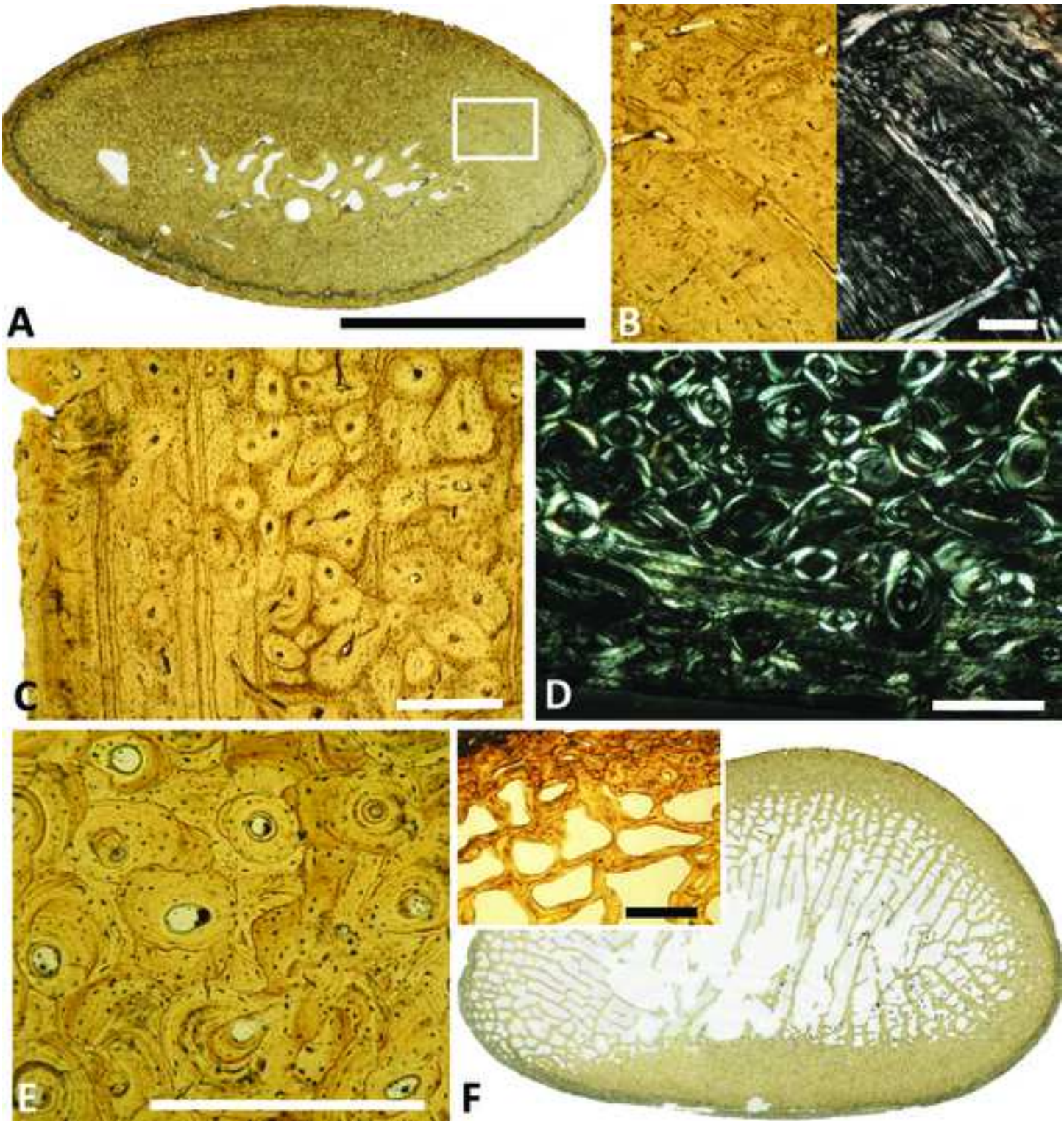

Table 1. Basic morphometric analysis of the humerus. Table showing the specimen numbers of the used specimens, including averages retrieved from the literature. The third and fourth column present the measurements, with the absolute sagittal length (BL) in the third column and the least transverse width of the diaphysis (TW) in the fourth column. The resulting ratio is presented in the final column. Color coding from red (low values, suggesting no pachyostosis) via yellow (medium values) to green (high values, suggesting pachystosis) for easy visual differentiation.

Taxon	Specimen number	Humerus		
		Absolute sagittal length (mm)(BL)	Least transverse width diaphysis (mm)(TW)	Ratio TW/BL
Halichoerus grypus	MSC 1978-48	142.0	24.2	0.170
Pusa sibirica	IRSNB 14210	75.7	10.0	0.132
Pusa sibirica	IRSNB 15264	79.4	11.8	0.149
Pusa sibirica	IRSNB 21170	74.7	10.9	0.146
Pusa sibirica	IRSNB 21171	91.4	12.6	0.138
Pusa sibirica	MSC 504941	85.5	11.6	0.136
Phoca vitulina	IRSNB 1165S	109.6	16.2	0.148
Phoca vitulina	IRSNB 1157C	111.0	16.8	0.151
Phoca vitulina	IRSNB 7605	110.4	18.0	0.163
Phoca vitulina	IRSNB 35247	110.0	15.2	0.138
Phoca vitulina	IRSNB 36548	122.9	18.8	0.153
Leptophoca proxima	USNM 5359	124.5	14.9	0.120

Leptophoca proxima	USNM 23450	113.4	13.5	0.119
Leptophoca proxima	USNM 284721	126.2	15.0	0.119
Leptophoca proxima	USNM 412115	131.7	14.4	0.109
Cryptophoca maeotica	Average Koretsky (2001)	107.1	14.5	0.135
Praepusa vindobonensis	Average Koretsky (2001)	86.3	10.6	0.123
Pachyphoca ukrainica	Average Koretsky & Rahmat (2013)	87.0	18.3	0.210
Sarmatonectes sintsovi	USNM unspecified cast	90.4	13.9	0.154
Monachopsis pontica	Average Koretsky (2001)	80.5	13.6	0.169
Praepusa boeska	MAB 4686 (holotype)	81.1	11.3	0.139
Batavipusa neerlandica	MAB 3798	64.9	11.8	0.182
Phocanella pumilla	USNM 171151	128.8	15.8	0.123
Phocanella pumilla	USNM 305304	131.9	15.4	0.117
Phocanella pumilla	USNM 329059	127.8	15.8	0.124
Phocanella pumilla	USNM 421544	124.6	16.6	0.133
Phocanella pumilla	USNM 437762	125.1	13.9	0.111
Nanophoca vitulinoides	IRSNB 1063-M242	78.2	9.5	0.121
Nanophoca vitulinoides	IRSNB M2276c	72.4	9.8	0.135

Table 2. Basic morphometric analysis of the femur. Table showing the specimen numbers of the used specimens, including averages retrieved from the literature. The third, fourth, and fifth column present the measurements, with the absolute sagittal length (BL) in the third column, the least transverse width of the diaphysis (TW) in the fourth column, and the anteroposterior width of the diaphysis (APW) in the fifth column. The resulting ratio is presented in the final column. Color coding from red (low values, suggesting no pachyostosis) via yellow (medium values) to green (high values, suggesting pachystosis) for easy visual differentiation.

Taxon	Specimen number	Femur			
		Absolute sagittal length (mm)(BL)	Least transverse width diaphysis (mm)(TW)	Anteroposterior width diaphysis (mm)(APW)	Ratio [0.5(TW+APW)] /BL
Halichoerus grypus	MSC 1978-48	120.4	30.7	14.4	0.187
Pusa sibirica	IRSNB 14210	68.5	14.7	7.0	0.158
Pusa sibirica	IRSNB 15264	72.4	15.1	8.2	0.161
Pusa sibirica	IRSNB 21170	67.8	15.6	6.7	0.164
Pusa sibirica	IRSNB 21171	86.1	17.1	9.9	0.157
Pusa sibirica	MSC 504941	76.7	16.1	8.2	0.158
Phoca vitulina	IRSNB 1157C	99.4	22.6	13.9	0.184
Phoca vitulina	IRSNB 7605	106.4	21.8	14.0	0.168
Phoca vitulina	IRSNB 35247	98.4	18.7	13.7	0.165
Phoca vitulina	IRSNB 36548	109.3	21.5	15.2	0.168
Leptophoca proxima	USNM 263648	107.8	27.0	15.1	0.195

Leptophoca proxima	USNM 347348	118.9	28.9	17.2	0.194
Leptophoca proxima	USNM 559330	115.8	27.6	17.0	0.193
Cryptophoca maeotica	Average from Koretsky (2001)	106.0	27.6	12.4	0.189
Praepusa vindobonensis	Average from Koretsky (2001)	72.8	18.4	10.4	0.198
Pachyphoca ukrainica	Average from Koretsky & Rahmat (2013)	80.3	24.3	14.3	0.240
Pachyphoca chapskii	NMNHU-P 64-706	120.0	33.5	21.5	0.229
Sarmatonectes sintsovi	Specimen Koretsky (2001)	89.5	21.0	13.0	0.190
Sarmatonectes sintsovi	Specimen Koretsky (2001)	94.5	22.5	13.0	0.188
Monachopsis pontica	Average from Koretsky (2001)	68.3	18.1	9.7	0.204
Phocanella pumilla	USNM 181649	124.1	29.5	15.9	0.183
Phocanella pumilla	USNM 481569	115.0	27.4	12.3	0.173
Nanophoca vitulinoides	IRSNB1049-M246	73.6	19.8	9.7	0.200
Nanophoca vitulinoides	IRSNB M2271	71.5	20.3	9.5	0.208
Nanophoca vitulinoides	IRSNB M2276d	69.4	19.6	9.1	0.207

Table 3. Taxa and specimens considered for the micro-anatomic and osteohistological parts of the study. Specimens that have exclusively been considered for microanatomy are indicated by an asterisk (*) and specimens that have exclusively been considered for osteohistology are indicate by a dagger (†) For institutional abbreviations, see 'materials and methods' section. Other abbreviations: Av. = "average of"; Histos = collection of osteohistological sections at the Muséum national d'Histoire naturelle.; Sp. = "specimen from". Note that, for cells containing multiple specimens, asterisks and daggers apply to all specimens in that cell.

Taxon	Rib	Humerus	Radius	Ulna	Femur	Tibia	Vertebra
Arctocephalus pusillus	Sp. Canovile et al. (2016)*						Sp. Dumont et al. (2013)*
Callophoca obscura	Histos 168				Histos 170		
	Histos 169†						
Cystophora cristata	Sp. Canovile et al. (2016)*						Sp. Dumont et al. (2013)*
Enhydra lutris	Sp. Canovile et al. (2016)*						Sp. Dumont et al. (2013)*
Eumetopias jubatus	Sp. Canovile et al. (2016)*						
Halichoerus grypus					Sp. Quemeneur et al (2013)*		
Leptophoca lenis					Histos 166		
Lutra lutra		Sp. Canoville and Laurin (2010)*			Av. 8 sp. Quemeneur et al (2013)*		Sp. Dumont et al. (2013)*
Mirounga leonina		Specimen from Canoville and Laurin (2010)*					Sp. Dumont et al. (2013)*
Monachus monachus	Sp. Canovile et						

	al. (2016)*						
Nanophoca vitulinoides	Histos 2152	Histos 2135, 2137–2140†	Histos 2142	Histos 2143, 2144†	Histos 1934, 1936–1941†	IRSNB M2276g*	Histos 2147, 2150
	Histos 2153–2156†	Histos 2136	Histos 2174†		Histos 1935		Histos 2148, 2149, 2151†
		IRSNB M2276c*			IRSNB M2276d*		
Odobenus rosmarus	Sp. Canovile et al. (2016)*						
Otaria byronia		Sp. Canoville and Laurin (2010)*			Sp. Quemeneur et al (2013) *		Sp. Dumont et al. (2013)*
Pagophilus groenlandicus							Sp. Dumont et al. (2013)*
Phoca vitulina	Sp. Canovile et al. (2016)*	IRSNB 1157E*	IRSNB 1157E*		IRSNB 1157E*	IRSNB 1157E*	
Phocanella pumila		Histos 162, 164†			Histos 159, 161†		
		Histos 163			Histos 160		
Ursus maritimus	Histos 42*						Sp. Dumont et al. (2013)*
Zalophus californianus	Sp. Canovile et al. (2016)*						Sp. Dumont et al. (2013)*

Table 4. Histomorphometry of the vertebrae with BONE PROFILER.

Taxon	Specimen number / Collection	Global compactness
Carnivora		
Ursidae		
Ursus maritimus	Specimen from Dumont et al. (2013)	0.294
Phocidae		
Phocinae		
Cystophora cristata	Specimen from Dumont et al. (2013)	0.223
Nanophoca vitulinoides	**Histos 2150**	**0.938**
Nanophoca vitulinoides	**Histos 2147**	**0.636**
Pagophilus groenlandicus	Specimen from Dumont et al. (2013)	0.293
Monachinae		
Hydrurga leptonyx	Specimen from Dumont et al. (2013)	0.380
Mirounga leonina	Specimen from Dumont et al. (2013)	0.341
Otariidae		
Arctocephalus pusillus	Specimen from Dumont et al. (2013)	0.411
Otaria byronia	Specimen from Dumont et al. (2013)	0.354
Zalophus californianus	Specimen from Dumont et al. (2013)	0.363
Mustelidae		
Enhydra lutris	Specimen from Dumont et al. (2013)	0.443
Lutra lutra	Specimen from Dumont et al. (2013)	0.412

Table 5. Histomorphometry of the ribs with BONE PROFILER. Analyses were conducted on thin sections. Min, Max, S, and P values are global values for each bone. Abbreviation: Comp., global compactness.

Taxon	Specimen number / Collection	Min	Max	S	P	Comp.
Carnivora						
Ursidae						
Ursus maritimus	Histos 42	0.129	1.000	0.049	0.707	0.554
Phocidae						
Phocinae						
Cystophora cristata	Specimen from Canoville et al. (2016)	0.138	1.000	0.037	0.895	0.307
Nanophoca vitulinoides	**Histos 2152**	**0.000**	**0.999**	**0.015**	**0.025**	**0.998**
Phoca vitulina	Specimen from Canoville et al. (2016)	0.000	0.963	0.135	0.624	0.603
Monachinae						
Callophoca obscura	Histos 168	0.205	1.000	0.087	0.562	0.727
Monachus monachus	Specimen from Canoville et al. (2016)	0.017	1.000	0.127	0.517	0.687
Otariidae						
Arctocephalus pusillus	Specimen from Canoville et al. (2016)	0.154	1.000	0.136	0.445	0.784
Eumetopias jubatus	Specimen from Canoville et al. (2016)	0.032	0.942	0.122	0.506	0.666
Zalophus californianus	Specimen from Canoville et al. (2016)	0.000	1.000	0.125	0.410	0.782
Odobenidae						
Odobenus rosmarus	Specimen from Canoville et al. (2016)	0.084	1.000	0.119	0.765	0.449
Mustelidae						
Enhydra lutris	Specimen from Canoville et al. (2016)	0.694	0.957	0.044	0.421	0.908

Table 6. Histomorphometry of the humeri with BONE PROFILER. Min, Max, S, and P values are global values. Abbreviations: TS, Thin section; CT, micro-CT; Comp., global compactness.

Taxon	Specimen number / Collection	TS / CT	Resolution (µm)	Min	Max	S	P	Comp.
Carnivora								
Phocidae								
Phocinae								
Nanophoca vitulinoides	**Histos 2136**	**TS**	**—**	**0.007**	**0.998**	**0.113**	**-0.486**	**0.997**
Nanophoca vitulinoides	**IRSNB M2276c**	**CT**	**45.8**	**0.000**	**1.000**	**0.028**	**-0.005**	**0.999**
Phoca vitulina	IRSNB 1157E	CT	45.7	0.202	1.000	0.061	0.591	0.706
Phocanella pumilla	Histos 162	TS	—	0.000	1.000	0.069	0.158	0.959
Monachinae								
Mirounga leonina	Specimen from Canoville and Laurin (2010)	TS	—	0.118	1.000	0.101	0.870	0.348
Otariidae								
Otaria byronia	Specimen from Canoville and Laurin (2010)	TS	—	0.167	0.879	0.090	0.442	0.720
Mustelidae								
Lutra lutra	Specimen from Canoville and Laurin (2010)	TS	—	0.000	0.990	0.046	0.534	0.697

Table 7. Histomorphometry of the femora with BONE PROFILER. Min, Max, S, and P values are global values. Abbreviations: TS, Thin section; CT, micro-CT; Comp., Global compactness.

Taxon	Specimen number / Collection	TS / CT	Resolution (µm)	*Min*	*Max*	*S*	*P*	*Comp.*
Carnivora								
Phocidae								
Phocinae								
Halichoerus grypus	From Quemeneur et al. (2013)	TS	—	0.109	0.980	0.045	0.638	0.615
Leptophoca proxima	Histos 166	TS	—	0.225	1.000	0.076	0.605	0.700
Nanophoca vitulinoides	**Histos 1935**	**TS**	**—**	**0.969**	**1.000**	**0.002**	**0.451**	**0.994**
Nanophoca vitulinoides	**IRSNB M2276d**	**CT**	**45.8**	**0.574**	**1.000**	**0.207**	**0.001**	**0.971**
Phoca vitulina	IRSNB 1157E	CT	45.7	0.061	1.000	0.048	0.706	0.520
Phocanella pumilla	Histos 170	TS	—	0.902	1.000	0.083	0.476	0.977
Monachinae								
Callophoca obscura	Histos 170	TS	—	0.143	1.000	0.106	0.667	0.591
Otariidae								
Otaria byronia	From Quemeneur et al. (2013)	TS	—	0.159	0.992	0.074	0.426	0.824
Mustelidae								
Lutra lutra	From Quemeneur et al. (2013)	TS	—	0.043	0.991	0.018	0.485	0.764
Lutra lutra	From Quemeneur et al. (2013)	TS	—	0.000	0.988	0.024	0.484	0.751
Lutra lutra	From Quemeneur et al. (2013)	TS	—	0.003	0.995	0.034	0.517	0.722
Lutra lutra	From Quemeneur et al. (2013)	TS	—	0.000	1.000	0.009	0.574	0.666
Lutra lutra	From Quemeneur et al. (2013)	TS	—	0.024	0.994	0.013	0.473	0.773
Lutra lutra	From Quemeneur et al. (2013)	TS	—	0.043	0.991	0.018	0.485	0.764

Lutra lutra	From Quemeneur et al. (2013)	TS	—	0.000	0.998	0.024	0.484	0.751
Lutra lutra	From Quemeneur et al. (2013)	TS	—	0.000	1.000	0.009	0.574	0.666

Table 8. Histomorphometry of the radii and tibiae with BONE PROFILER. Min, Max, S, and P values are global values. Abbreviations: TS, Thin section; CT, micro-CT; Comp., Global compactness.

Taxon	Specimen number / Collection	TS / CT	Resolution (µm)	*Min*	*Max*	*S*	*P*	*Comp.*
Carnivora								
Phocidae								
Phocinae								
Nanophoca vitulinoides	**Histos 2142**	**TS**	**—**	**0.974**	**1.000**	**0.070**	**0.676**	**0.986**
Nanophoca vitulinoides	**IRSNB M2276g**	**CT**	**83.9**	**0.000**	**1.000**	**0.064**	**-0.154**	**0.999**
Phoca vitulina	IRSNB 1157E	CT	45.7	0.115	1.000	0.060	0.707	0.541
Phoca vitulina	IRSNB 1157E	CT	46.3	0.091	1.000	0.087	0.559	0.691